AD-A245 194

NAVAL POSTGRADUATE SCHOOL
Monterey, California

DTIC
S ELECTE
JAN 3 1 1992
D
D

THESIS

METEOROLOGICAL FEATURES DURING PHASE I
OF THE COORDINATED EASTERN ARCTIC
EXPERIMENT (CEAREX) FROM 17 SEPTEMBER
1988 TO 7 JANUARY 1989

by

Stephanie W. Hamilton

March 1991

Co-Advisor	Kenneth L. Davidson
Co-Advisor	Carlyle H. Wash

92-02439

92 1

REPORT DOCUMENTATION PAGE

1a Report Security Classification Unclassified		1b Restrictive Markings		
2a Security Classification Authority		3 Distribution/Availability of Report		
2b Declassification/Downgrading Schedule		Approved for public release; distribution is unlimited.		
4 Performing Organization Report Number(s)		5 Monitoring Organization Report Number(s)		
6a Name of Performing Organization Naval Postgraduate School	6b Office Symbol (if applicable) 35	7a Name of Monitoring Organization Naval Postgraduate School		
6c Address (city, state, and ZIP code) Monterey, CA 93943-5000		7b Address (city, state, and ZIP code) Monterey, CA 93943-5000		
8a Name of Funding/Sponsoring Organization	8b Office Symbol (if applicable)	9 Procurement Instrument Identification Number		
8c Address (city, state, and ZIP code)		10 Source of Funding Numbers		
		Program Element No	Project No	Task No	Work Unit Accession No

11 Title (include security classification) METEOROLOGICAL FEATURES DURING PHASE I OF THE COORDINATED EASTERN ARCTIC EXPERIMENT (CEAREX) FROM 17 SEPTEMBER 1988 TO 7 JANUARY 1989

12 Personal Author(s) Stephanie W. Hamilton

13a Type of Report Master's Thesis	13b Time Covered From To	14 Date of Report (year, month, day) March 1991	15 Page Count 98

16 Supplementary Notation The views expressed in this thesis are those of the author and do not reflect the official policy or position of the Department of Defense or the U.S. Government.

17 Cosati Codes			18 Subject Terms (continue on reverse if necessary and identify by block number)
Field	Group	Subgroup	arctic meteorology, arctic storms, arctic climate, arctic research, boundary layer front, marginal ice zone, CEAREX

19 Abstract (continue on reverse if necessary and identify by block number)

The synoptic and mesoscale meteorological conditions were analyzed for Phase I of the Coordinated Eastern Arctic Experiment (CEAREX) from 17 September 1988 to 7 January 1989. Meteorological observations from a research ship (R/V Polarbjoern), an array of drifting buoys and satellite imagery from DMSP and NOAA satellites were the primary tools for analysis. Several short periods of high cyclone activity followed by long periods of high pressure dominated the weather pattern in the eastern Arctic Ocean from Greenland to Novaya Zemlya for this period. Two case studies are presented. An infrequent cyclogenesis event that formed within a strong baroclinic zone over Arctic pack ice was observed in a "baroclinic leaf" on satellite imagery. Ship and drifting buoy observations provided critical insight to the location and intensity of the "leaf's" subsequent vertical development to the surface. In the second study, a boundary layer front was observed in the East Greenland Sea by satellite imagery. The front then moved northeast into Fram Strait and a polar low formed at the northern end of the front. The event lasted less than 24 h and would not have been observed except through satellite imagery.

20 Distribution/Availability of Abstract ☒ unclassified/unlimited ☐ same as report ☐ DTIC users	21 Abstract Security Classification Unclassified	
22a Name of Responsible Individual Kenneth L. Davidson	22b Telephone (include Area code) (408) 646-2563	22c Office Symbol MR(Ds)

DD FORM 1473,84 MAR   83 APR edition may be used until exhausted   security classification of this page
All other editions are obsolete

Meteorological Features during Phase I of the
Coordinated Eastern Arctic Experiment (CEAREX)
from 17 September 1988 to 7 January 1989

by

Stephanie W. Hamilton
Lieutenant, United States Navy
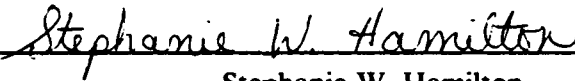B.S., Old Dominion University, 1980

Submitted in partial fulfillment of the
requirements for the degree of

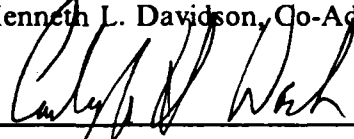MASTER OF SCIENCE IN METEOROLOGY AND PHYSICAL
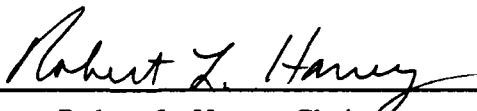OCEANOGRAPHY

from the

NAVAL POSTGRADUATE SCHOOL
March 1991

Author: _____
Stephanie W. Hamilton

Approved by: _____
Kenneth L. Davidson, Co-Advisor

_____
Carlyle H. Wash, Co-Advisor

_____
Robert L. Haney, Chairman,
Department of Meteorology

ABSTRACT

The synoptic and mesoscale meteorological conditions were analyzed for Phase I of the Coordinated Eastern Arctic Experiment (CEAREX) from 17 September 1988 to 7 January 1989. Meteorological observations from a research ship (R/V Polarbjoern), an array of drifting buoys and satellite imagery from DMSP and NOAA satellites were the primary tools for analysis. Several short periods of high cyclone activity followed by long periods of high pressure dominated the weather pattern in the eastern Arctic Ocean from Greenland to Novaya Zemlya for this period. Two case studies are presented. An infrequent cyclogenesis event that formed within a strong baroclinic zone over Arctic pack ice was observed in a "baroclinic leaf" on satellite imagery. Ship and drifting buoy observations provided critical insight to the location and intensity of the "leaf's" subsequent vertical development to the surface. In the second study, a boundary layer front was observed in the East Greenland Sea by satellite imagery. The front then moved northeast into Fram Strait and a polar low formed at the northern end of the front. The event lasted less than 24 h and would not have been observed except through satellite imagery.

TABLE OF CONTENTS

LIST OF TABLES

LIST OF FIGURES

ACKNOWLEDGMENTS

I. INTRODUCTION

The Arctic Ocean is arguably one of the most difficult areas in the world to make an accurate meteorological forecast. This is due to the limited observational data, which is critical to making good analyses. Without a complete understanding of the present state of the atmosphere, it is impossible to consistently produce accurate forecasts. This thesis will provide additional analyses during a meteorological experiment of Arctic weather to gain insight into the unique forecasting problems of the Arctic. The use of satellite imagery will be used extensively in this thesis to enhance the analysis.

United States interest in Arctic research has increased significantly in the past decade. The Arctic Research and Policy Act of 1984 established policy and goals for scientific research in the Arctic. On 28 June 1985, Executive Order 12501 was signed establishing an Arctic Research Committee (National Science Foundation 1987). Following the Arctic Research Plan in 1987, the United States, and the Navy in particular, have participated in several multinational Arctic experiments. The Marginal Ice Zone Experiments (MIZEX-83, MIZEX-84, and MIZEX-87) were studies of the physical processes of the ocean, ice, and the atmosphere. The Coordinated Eastern Arctic Experiment (CEAREX), from September 1988 through May 1989, was a continuation of studies in this area with further U.S. Navy involvement.

The Navy's primary meteorological interest is to learn of the effect of Arctic weather on naval operations and particular areas of study include polar fronts and deep convection. Specific regions of interest for the Navy are the marginal ice zone (MIZ), Fram Strait, Greenland and Norwegian Seas, and the central Arctic basin (National Science Foundation 1988).

This thesis will examine meteorological and oceanographic features in the lower atmosphere during Phase I of CEAREX from 17 September 1988 through 7 January 1989. In Phase I, the U.S. Coast Guard ice breaker, *Northwind*, led the *R/V Polarbjoern* into multiyear pack ice north of Svalbard, Norway. During CEAREX, the *R/V Polarbjoern* was used to gather meteorological information. In addition to the ship's surface and upper air reports, six buoys were deployed and collected surface observations of pressure and temperature. From 17 September to 15 November, the *R/V Polarbjoern* was moored to a large ice floe and drifted slowly southward with the advancing ice pack under the influence of northerly winds. The ice floe was destroyed on 15 November by

a strong northwesterly wind event. The *R/V Polarbjoern* continued to drift slowly south while trapped in the Arctic ice pack. A strong storm with high winds in early January allowed the ship to break free on 7 January.

The major geographic and oceanographic points of interest for this study appear on Fig. 1. The ship was located northeast of Svalbard. Spitzbergen is the largest island to the west. The two smaller islands east of Spitzbergen are Northeast Land and Edge Island, located northeast and southeast, respectively, of Spitzbergen. The *R/V Polarbjoern* passed very close to Kvitoya, the small island located due east of Northeast Land. A branch of the Norway Current runs north along the west coast of Spitzbergen heading into the Arctic basin and is referred to as Fram Strait. The MIZ is located in Fram Strait and East Greenland Sea throughout the year.

This thesis presents a climatological summary along with significant meteorological features indigenous to the region in Chapter II. Chapter III details data sources and then presents an overview of the synoptic situation during Phase I for the region. Two case studies are presented in Chapter IV. One case study involves an infrequent cyclogenesis event that occurred over the *R/V Polarbjoern* on 12 October 1988, located in Arctic pack ice at the time. The second case study pertains to the formation of a boundary layer front in Fram Strait on 10 October 1988 that evolved into a polar low. Summary and recommendations follow in Chapter V.
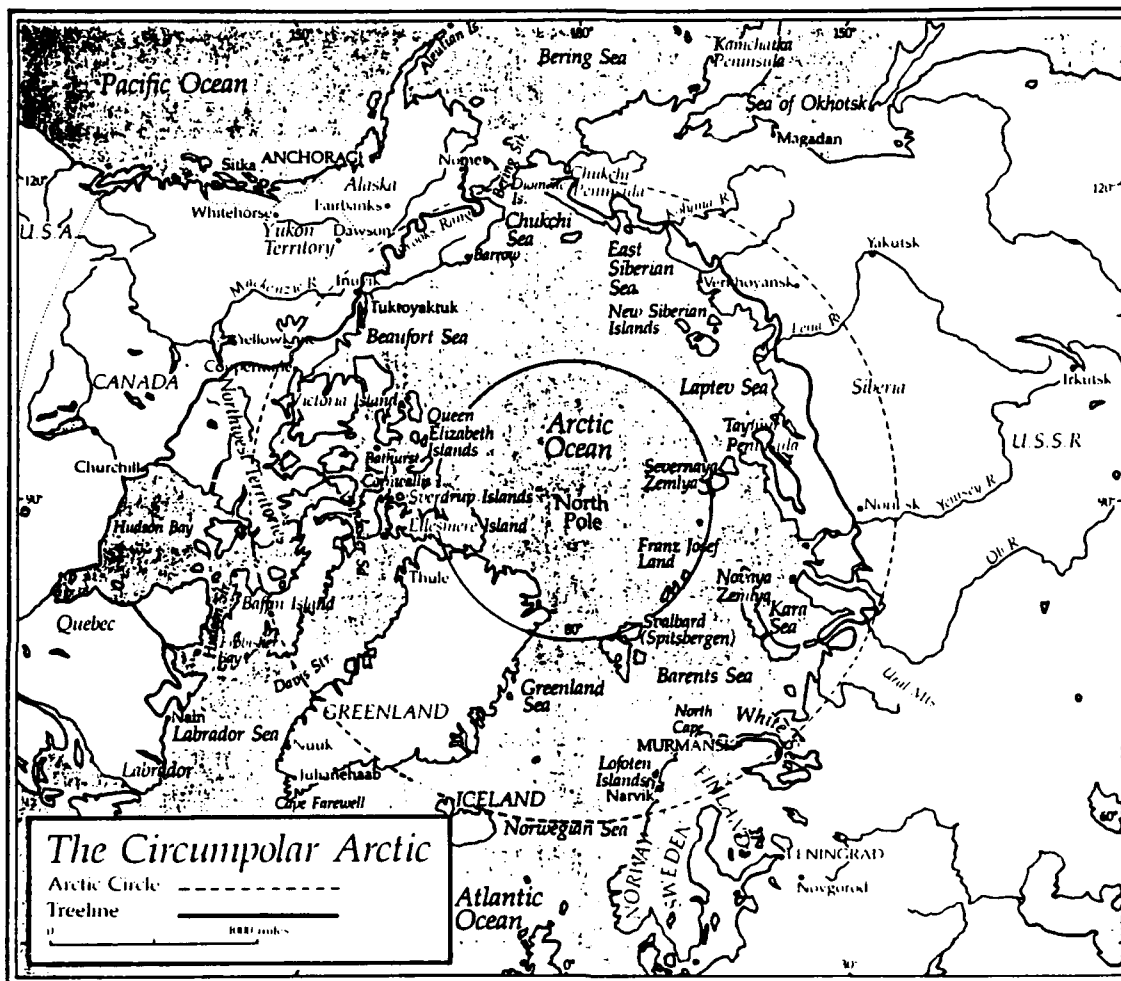
Fig. 1. Key geographic locations of the circumpolar Arctic (from Zumberge 1986)

3

II. BACKGROUND

There are significant climatological aspects that dominate Arctic weather: sunlight, circumpolar vortex, ice cover and temperature inversion. Each can cause great variability in Arctic weather, from month to month and from year to year. The Arctic ocean circulation also plays an important role in the formation of sea ice and temperature gradients. The climatological synoptic patterns for fall and early winter are presented for air temperatures, sea level pressure, 700 mb, and cyclone tracks. Significant atmospheric features seen in the Arctic are defined and their satellite characteristics presented.

A. FACTORS IN ARCTIC CLIMATOLOGY

1. Amount of Daylight and Solar Elevation

Sunlight is one of two prime heat sources for the Arctic. Decreases in the amount of sunlight combined with the low solar elevation at high latitudes cause extended periods of radiational heat loss from the surface. Late September and early October represent the strongest transition period as Arctic daylight each day is 25 minutes less. The amount of sunlight changes from approximately 14 hours of sunlight on 17 September to continuous darkness by approximately 10 October at 80°N. Even with daylight present in late September and early October, the sun has a very low elevation. For example, on 1 October the solar elevation is only 6° 50' above the horizon. North of 80°N. there is complete darkness during Phase I and as a result the visible channels in satellite imagery will have considerable variation in illumination in the areas on the border between daylight, twilight, and darkness.

2. Circumpolar Vortex

The most significant factor in the large scale surface weather patterns is the position of the cold-core circumpolar vortex. The polar vortex is the mid and upper level atmospheric large scale cyclonic circulation centered at the pole. The position and strength of the vortex depends on the degree of the north-south temperature gradient. The vortex is strongest and penetrates further south during the winter months when the differential heating is the greatest. October is a transitional month when the vortex is moving from its maximum northern extent during the summer to its maximum southern extent during the winter. The band of upper level westerlies on the periphery of the vortex steer the surface cyclones into the Arctic. As the planetary wave number increases, the more upper level troughs and ridges are present, which increase the number

4

of surface cyclones in the Arctic. This provides much variability in the Arctic climate as warm air advection from cyclones moving into the central Arctic basin is the second prime heat source for the Arctic (Vowinckel and Orvig 1970).

3. Marginal Ice Zone

The presence of ice is also a major controlling factor in Arctic weather. Average ice conditions are illustrated in Fig. 2. The Naval Polar Oceanography Center (NPOC) prepares operational weekly ice edge analyses which were used in this study. The extent of sea ice is at a minimum in September and October. The ice edge penetrates farther south in late fall and winter, with a maximum extent from March to April (Stringer et al. 1984). The difference between the minimum and maximum extent of sea ice is greater east of Svalbard than west of Svalbard due to the presence of a warm ocean current (a branch of the Norway Current) penetrating northward along the west coast of Spitzbergen throughout the year. The ocean currents play a large role in the extent of sea ice and will be discussed in a subsequent section. As noted in Fig. 2, there is almost always a permanent ice sheet affixed to the east coast of Greenland and the MIZ region is always present in Fram Strait and Greenland Sea. There are sharp temperature and moisture gradients in the vicinity of the MIZ. Also the open water in Fram Strait produces considerable convective cloudiness. Low clouds and fog are the dominant weather features in this region.

4. Temperature Inversion

The fourth aspect of Arctic climate is the temperature inversion that is almost always present in the Arctic as shown in Fig. 3. Long periods of darkness result in the presence of a semi-permanent surface temperature inversion over the ice as a function of radiational cooling. When light surface winds preclude mixing from above and skies are clear, maximum surface temperature inversions occur (Sechrist et al. 1989). Inversions also exist due to subsidence, advection, and mixing. Surface inversions on the average extend up to 2 km and have a temperature increase of 5°C (Shultz 1987). These low-level inversions preclude mixing from above, trap fog and suppress convection. A very cold, relatively moist, and stable surface layer exists over the Arctic ice cap with a relatively warm, dry layer above for the majority of the fall and winter.
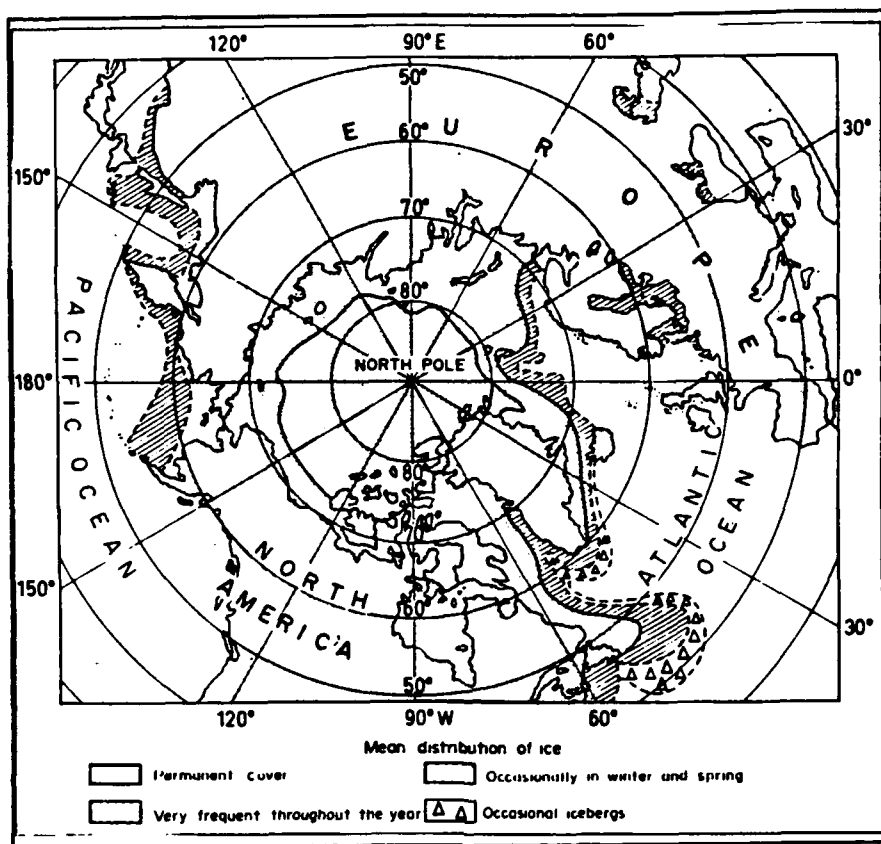
Fig. 2. Average Ice conditions in the Arctic (from Tchernia 1980)
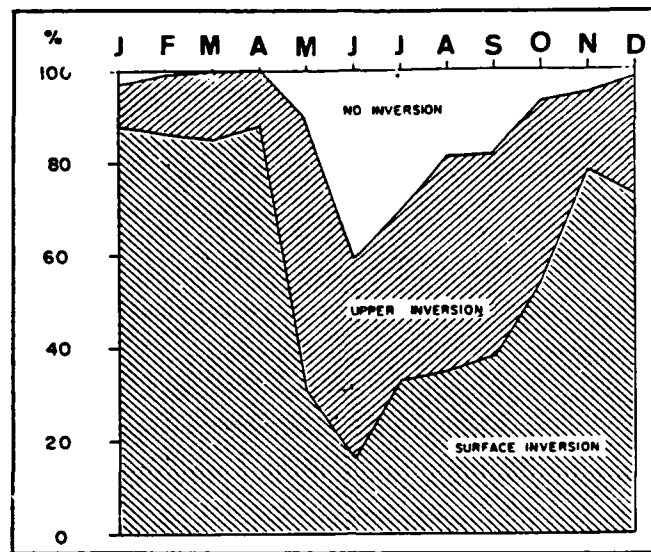
Fig. 3. Frequency of arctic inversion types during the year (from Vowinckel and Orvig 1970)

Elevated inversions occur as frequently as surface inversions during October as seen in Fig. 3. By early winter, surface inversions dominate the central Arctic basin. Elevated inversions can result from warm air advection aloft or by subsidence (sharp decrease of relative humidity with height). These inversions are less intense than surface inversions with a thickness of .5 to .9 km and temperature increase of only 1.2°C (Vowinckel and Orvig 1970).

5. Arctic Ocean Surface Circulation

The general circulation of the Arctic Ocean is depicted in Fig. 4. A branch of the North Atlantic Drift, the Norway Current brings warm and salty water into the Arctic circle north along the west coast of Spitzbergen in Fram Strait as far as 80°N. This warm tongue of water is reflected in the Arctic ice pack formation and in the mean surface air temperature to be discussed in the following section. The East Greenland Current runs south along the east coast of Greenland bringing cold and fresh water from the central Arctic basin to the tip of Greenland. This intrusion of cold water maintains a permanent ice sheet attached to the east coast of Greenland. The northbound Norway Current and the southbound East Greenland Current set up a cyclonic eddy in the Greenland and Norwegian Seas as illustrated in Fig. 4.

7
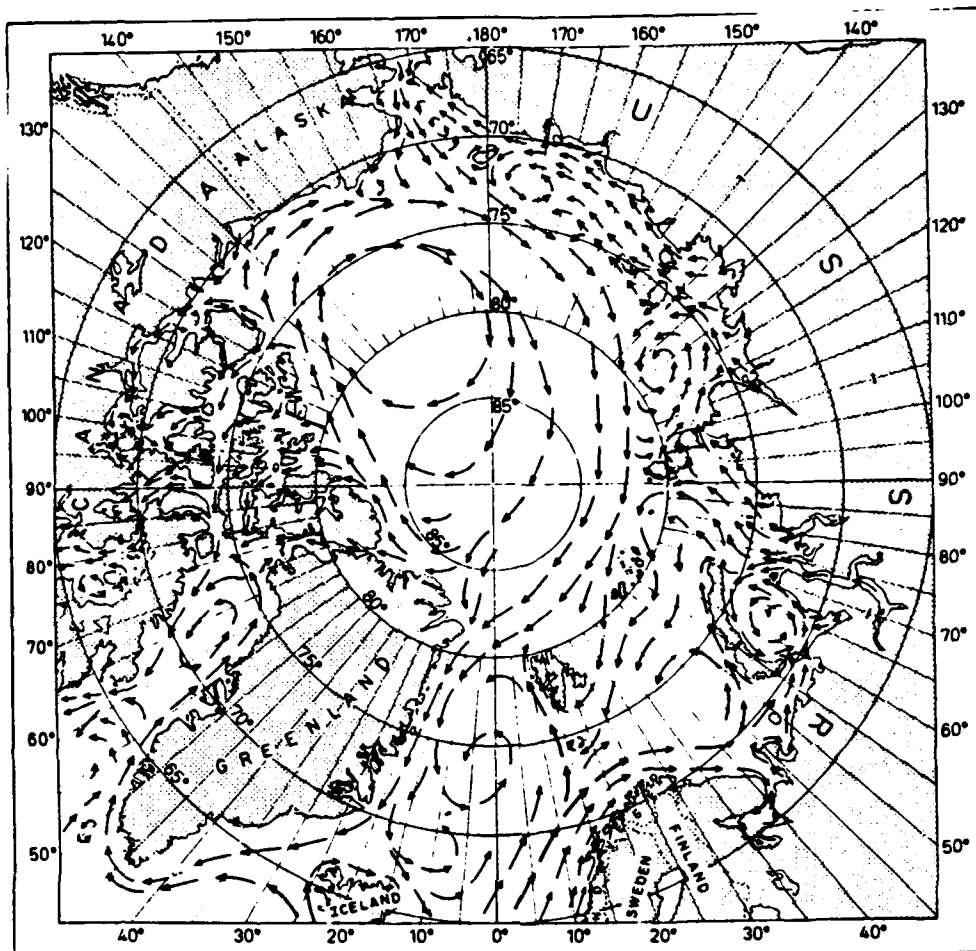
Fig. 4. Ocean circulation of the Arctic (from Tchernia 1980)

B. FALL AND EARLY WINTER SYNOPTIC CLIMATOLOGY

There are many important factors to consider when examining meteorological features in the Arctic as presented above. Fall and early winter are a time of great transition in the Arctic in the amount daylight, the temperature gradient, the strength of the circumpolar vortex, and extent of sea ice. A thorough knowledge of the climate and features indigenous to the Arctic is a crucial factor in the correct analysis of synoptic conditions.

1. Surface Air Temperature Patterns

Temperature changes in the Arctic are small and steady as the temperature of the ice regulates the surface air temperature. Although the amount of sunlight decreases rapidly over the most northern latitudes, the temperature of the ice slowly cools until it reaches its wintertime minimum in February. The central Arctic basin has an average

8

air temperature of 0°C during the summer and slowly cools to an average of -18°C in October and -34°C in January. The Greenland Sea, Fram Strait, and Svalbard region have a weak horizontal temperature contrast of 2-5°C during the summer season which increases to 12-14°C in October. The maximum temperature gradient occurs in the winter which increases to a contrast of 18-20°C from the southern portion of Fram Strait to north of Svalbard. The tight temperature gradients in this region are illustrated in Fig. 5 for October and January.
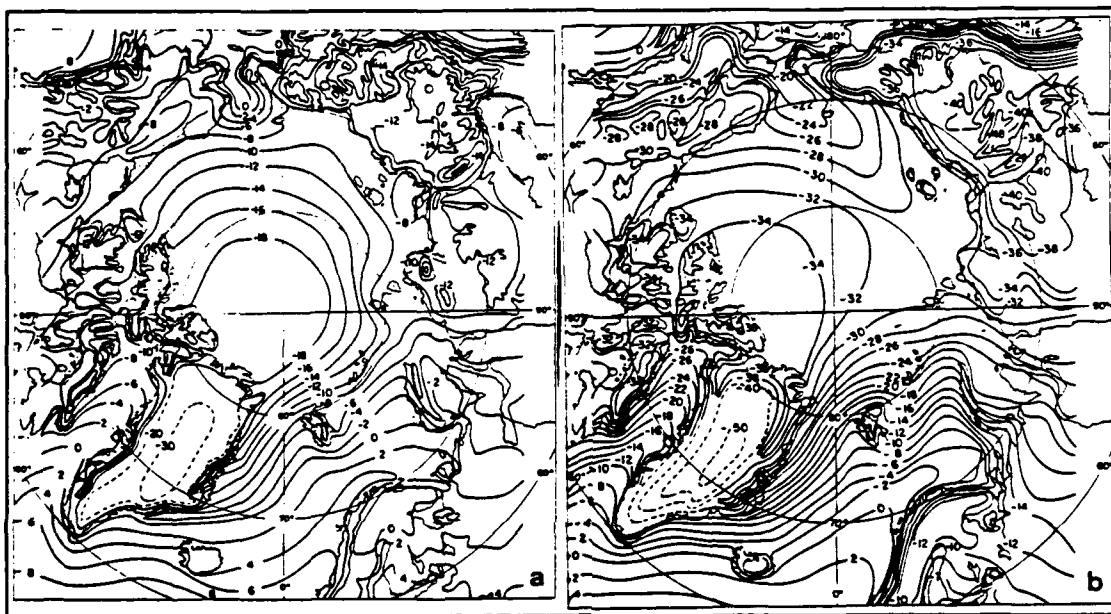
Fig. 5. Mean Surface Air Temperatures (°C) for a) October and b) January (from Sater et al. 1971)

Over the Arctic ice pack warm air advection, usually from North Atlantic cyclones, can increase surface air temperatures. Soon after these events, the surface air rapidly cools to its normal values. The surface air temperature in the MIZ is greatly influenced by the presence of ice or the relatively warm ice-free waters. The effect of the warm Norway Current is readily apparent in the temperature gradient in the MIZ.

Surface air temperature anomalies are persistent in the fall when variations in the ice coverage are the greatest. Temperatures will also vary due to the intrusion of North Atlantic cyclones which can increase surface temperatures by as much as 25°C. Walsh and Chapman (1990) have observed that the North Atlantic MIZ has shown significant warming events over the last twenty years.

2. Surface Pressure Patterns

The monthly mean sea level pressure pattern for October and January are presented by Sechrist et al. (1989) in Fig. 6. The pressure charts were compiled by the Applied Physics Laboratory at the University of Washington. Data obtained from a drifting buoy network in the Arctic from 1979-1985 was used to construct the charts. High pressure and anticyclonic flow dominate the Arctic basin from September through January with a maximum in winter. A high pressure center over Greenland during the summer moves toward the western Arctic during the winter months. A low pressure trough persists from a low pressure center over Iceland northeast through the Norwegian Sea to Novaya Zemlya. In October, the Icelandic low intensifies and reaches a maximum during the winter months. Monthly sea level pressure anomalies are most persistent during the fall east of Greenland. The large variability in this region is associated with the intrusion of North Atlantic cyclones (Walsh and Chapman 1990).
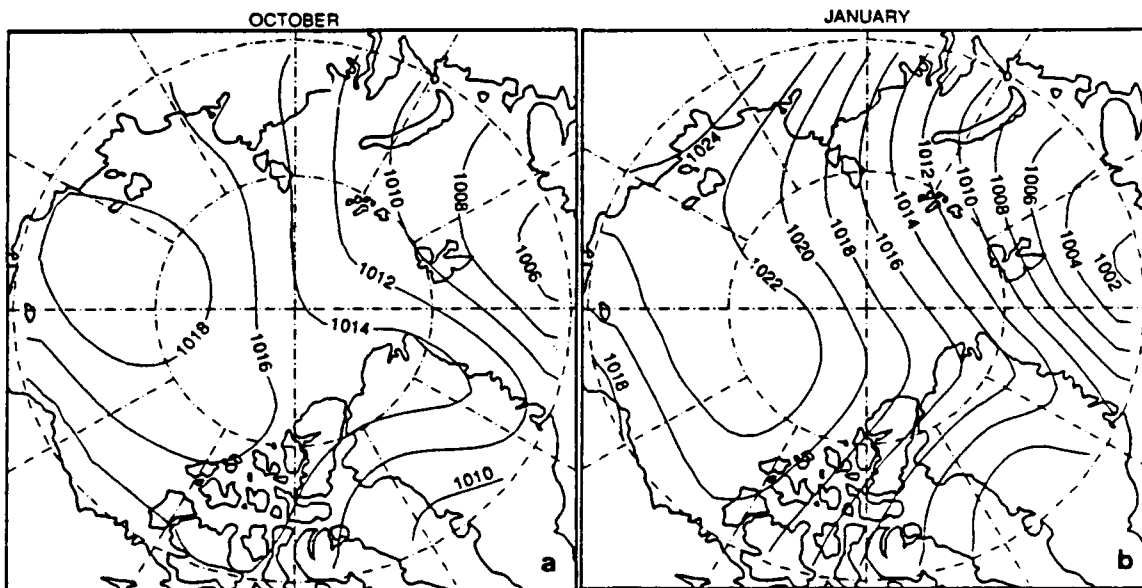
Fig. 6.   Mean Sea Level Pressure (mb) for a) October and b) January (from Sechrist et al. 1989)

Serreze and Barry (1988) used data from a network of drifting buoys to analyze surface pressure patterns in the Arctic. Autumn (September to November) percent frequencies for cyclones and anticyclones are summarized in Fig. 7. Serreze and Barry (1988) counted as cyclones those systems that appeared on at least two consecutive charts, had one closed isobar at 4 mb contour intervals, and reached a minimum pressure

of less than 1012 mb. Anticyclones must have a maximum pressure equal or greater to 1012 mb. There is a cyclone frequency maximum near Svalbard in all seasons except summer where the maximum frequency of cyclones shifts to the central Arctic basin. Autumn is a transition period where the cyclone frequency maximum is shifting from the central Arctic basin to its winter maximum between Svalbard and Novaya Zemlya. Anticyclone frequencies remain the highest in the western Arctic basin in all seasons with the highest frequencies in the spring and fall. Greenland was omitted in Serreze and Barry (1988) frequency studies because of the problem of reducing the pressures over the Greenland ice cap to sea level.
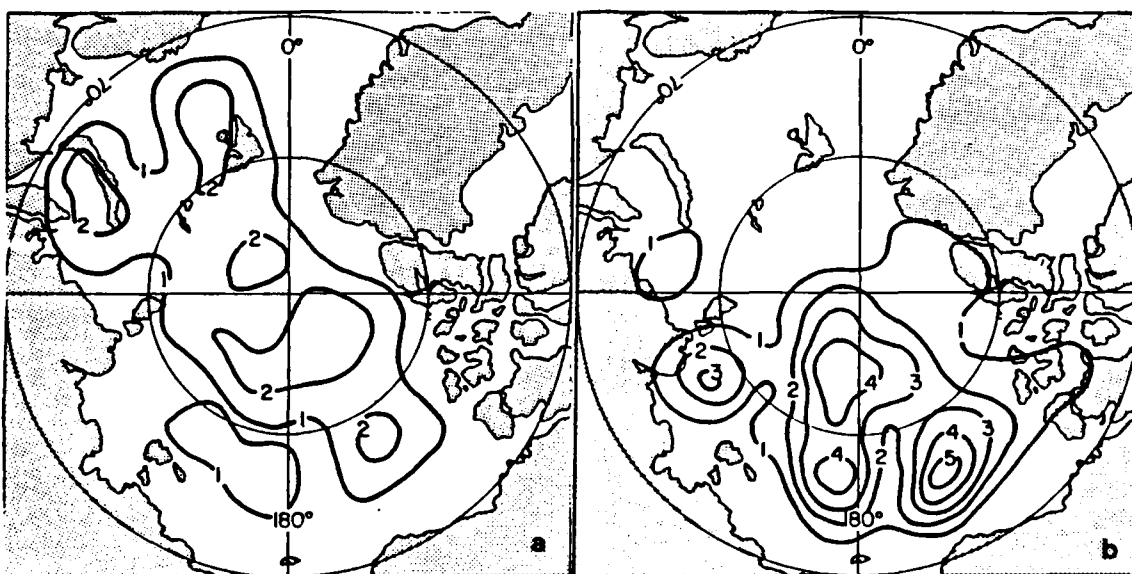
Fig. 7.   Autumn a) cyclone and b) anticyclone percent frequencies (from Serreze and Barry 1988)

3.   700 mb Pattern

The circumpolar vortex can be located using the 700 mb chart. The mean 700 mb heights for October and January presented by Sechrist et al (1989) are depicted in Fig. 8. The band of westerlies around the vortex lies far to the south of the Arctic circle from October through January. There is a deep trough that extends from Greenland south in the North Atlantic in September and October and cyclones tracking into the Arctic from the North Atlantic are steered northeast toward Svalbard. The circumpolar vortex strengthens from October to January as the north to south temperature gradient is maximized and two low height centers establish over the Arctic basin. The southward

11

extent of the circumpolar vortex will dominate the weather near Svalbard in any season. A strong vortex extending south of Svalbard will decrease cyclonic activity in the region. Lows that move northward under the vortex will become occluded and stagnate over the Central Arctic basin.
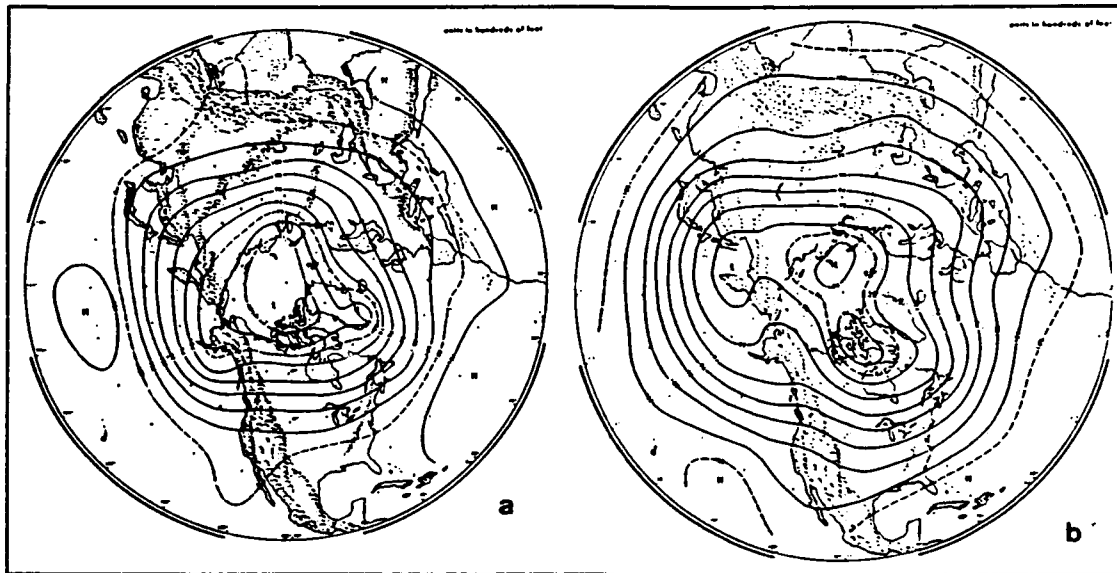
Fig. 8.   700 mb mean height (m) for a) October and b) January (from Sechrist et al. 1989)

4.   Cyclone Tracks

Serreze and Barry (1988) compiled cyclone tracks from 70 to 90 °N for the 1979-85 period. The prevalent cyclone tracks for winter and summer are illustrated in Fig. 9. During the winter three to five cyclones per season entered the Arctic basin from the North Atlantic, which is the most frequent entrance zone. There is a high variability from year to year and in some years the North Atlantic track did not dominate. Serreze and Barry (1988) also found that upper level troughs and lows tracked from Baffin Bay east across Greenland into the Greenland Sea to Svalbard. Summer cyclones from the North Atlantic track north over Svalbard at the rate of 2 to 4 per season but they seldom enter the western Arctic basin.
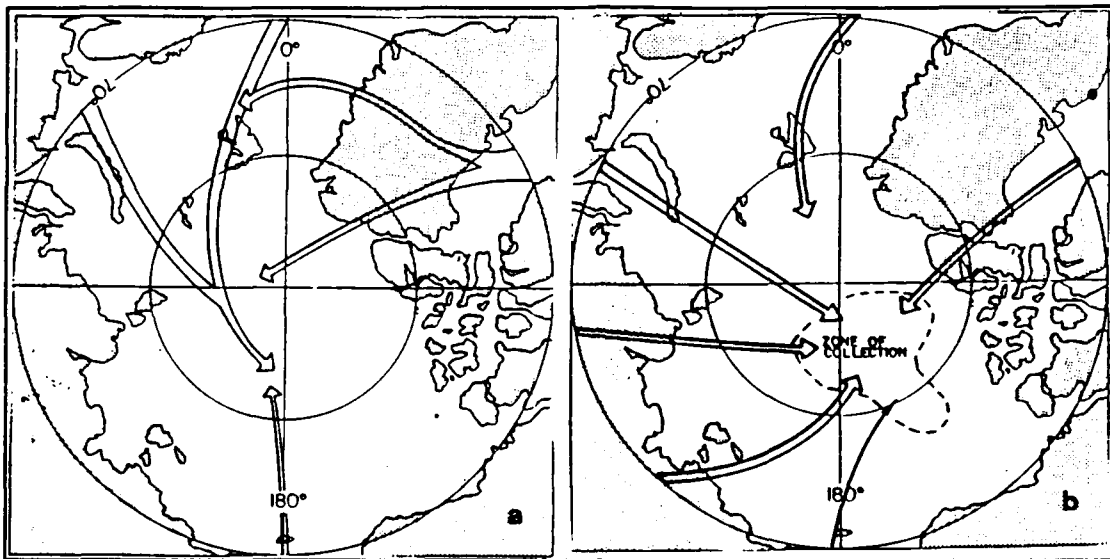
Fig. 9. **a) Winter and b) summer cyclone tracks (from Serreze and Barry 1988):** the width of the arrow indicates the importance of the track.

The comprehensive Atlas of the Arctic Ocean by Gorshkov (1983) depicts the trajectories and frequencies of cyclones and anticyclones in the Arctic for every month. The information was compiled from global synoptic weather charts from 1960 to 1970. Only rapidly moving cyclones and anticyclones were included. The tracks were calculated by averaging the actual path in one direction in groups of 400-500 km wide zones. The frequency of all cyclones and anticyclones (slow and fast moving) were calculated as a percentage of the number of days in a month. The average climatic cyclone tracks for October, December, January and February as compiled by Gorshkov (1983) are presented in Fig. 10. The widest arrows represent a frequency of 4 to 6 days of the month, the hollow arrows 2 to 4 days per month, and the thin solid arrows represent a frequency of less than 2 days per month.

The charts for October and December show the major cyclone track from Iceland northeast through the Norwegian Sea south of Svalbard, then northeast over Franz Joseph Land or southeast to Novaya Zemlya. The cyclone frequency for October is higher than November through January.

13
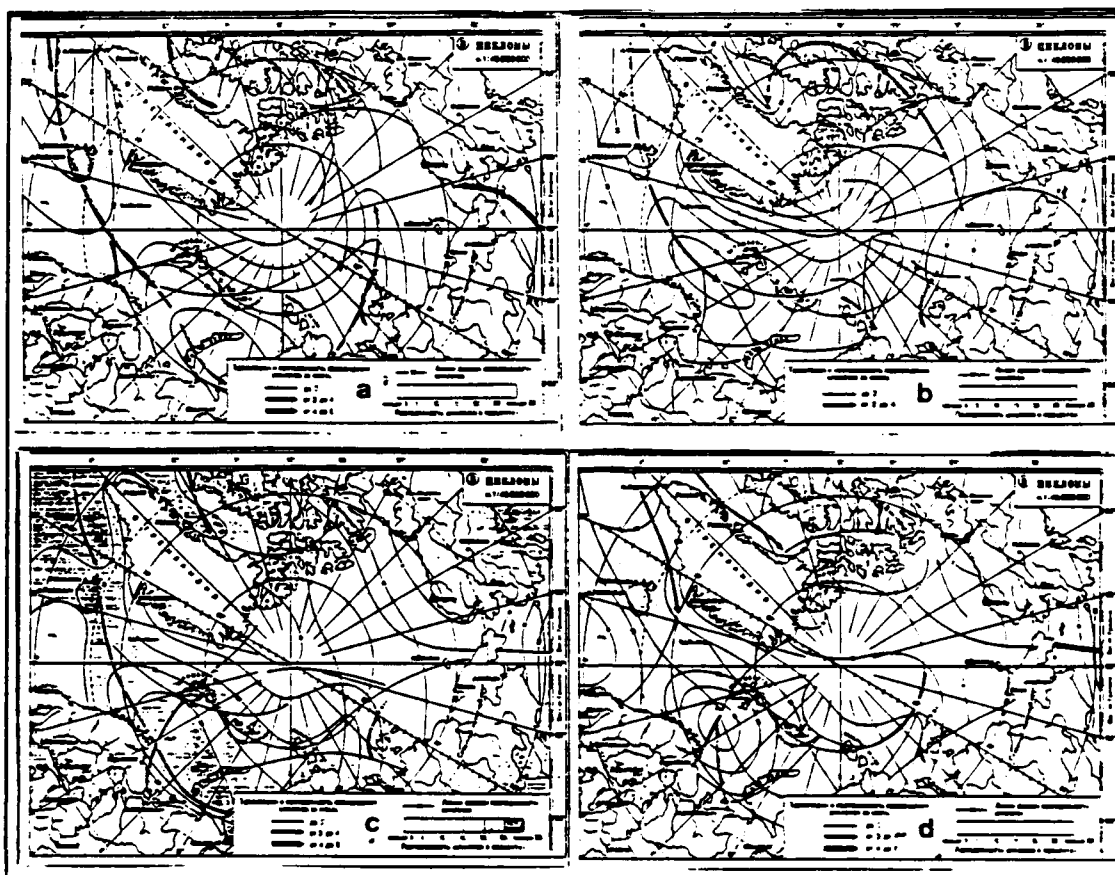
Fig. 10.   Cyclone Tracks for a) October, b) December, c) January and d) February
            (from Gorshkov 1983)

The charts for January and February in Fig. 10 show very different tracks from
the previous three months. January has the major cyclone track east northeast from
Iceland to north of Norway then east along 72°N. A secondary track from north of
Greenland has cyclones moving southeast to Svalbard then a major track resumes
southeast from Svalbard to northwest U.S.S.R.   A secondary track also exists from
Norwegian Sea northeast between Svalbard and Franz Joseph Land. February is in-
cluded because it is the only month that indicates a major region of cyclogenesis inside
the Arctic circle. The maximum frequency of cyclones and the change in the storm paths
from minor to major tracks suggest a major area of cyclogenesis between Svalbard and
Norway. Lows from northern Greenland track southeast to Svalbard and then to
Novaya Zemlya. The major cyclone tracks are from the region of cyclogenesis south and
southeast to northern Europe. These tracks differ sharply from the results compiled by

Serreze and Barry (1988). The major cyclone tracks for their study have all cyclones heading into the central Arctic basin for both winter and summer seasons. Gorshkov (1983) presents much more variability in Arctic cyclone tracks than Serreze and Barry (1988). Gorshkov illustrates many different trajectories between 70 and 90 °N. Serreze and Barry's major cyclone tracks extend south to north into the central Arctic basin. Gorshkov depicts a major cyclone track that extends from Iceland northeast through Barents Sea to Novaya Zemlya. He also has trajectories extending from north of Greenland southeast through the Barents Sea. Serreze and Barry indicate a winter cyclone rate of three to five per season while Gorshkov lists up to four to six in October alone through the major track. The cyclone frequency is significantly higher in Gorshkov's study.

Gorshkov (1983) presents sixteen types of synoptic patterns (called processes in the translation) covering two seasons and lists the frequencies for each type for every month. Gorshkov used the diurnal weather maps for Eurasia and the Northern Hemisphere from 1939-1962 for June to November data. and 1948-1968 maps for compiling the December through May data. All the synoptic type patterns were formed into the groups on the basis of the overall distribution of pressure fields over the Arctic Ocean. The letter 'H' denotes a cyclone and 'B' denotes an anticyclone. The heavy arrows are cyclone tracks and the light arrows are anticyclone tracks.

Six synoptic patterns that cover summer, fall, and winter constructed by Gorshkov (1983) are illustrated in Fig. 11. Autumn-winter climate patterns that have a 30 to 40 percent occurrence in each month from October to January are depicted in Fig. 11a-c. In Fig. 11a, a cyclone lies over the Barents Sea between Svalbard and Franz Joseph Land. A depression over the Barents Sea and a principle cyclone track from Norwegian Sea east to Novaya Zemlya is shown in Fig. 11b. Multiple low pressure centers over Norwegian Sea and northwest of Svalbard are reflected in Fig. 11c.

A summer-autumn situation (Fig. 11d) shows a low over Barents Sea and a principle track southeast to Novaya Zemlya. A summer-autumn process with a low in the Norwegian Sea and a principle cyclone track northwest over Svalbard is depicted in Fig. 11e. Fig. 11f reflects an autumn-winter scenario with an anticyclone over the Arctic basin and a depression over the southern Barents Sea. The principle cyclone track is east through the Norwegian Sea and southern Barents Sea. Fig 11d through f have a 20% frequency in each month from September through December.

The tracks of the North Atlantic cyclones steered by the position of the circumpolar vortex has its greatest effect on the climate of the MIZ in the Greenland

15
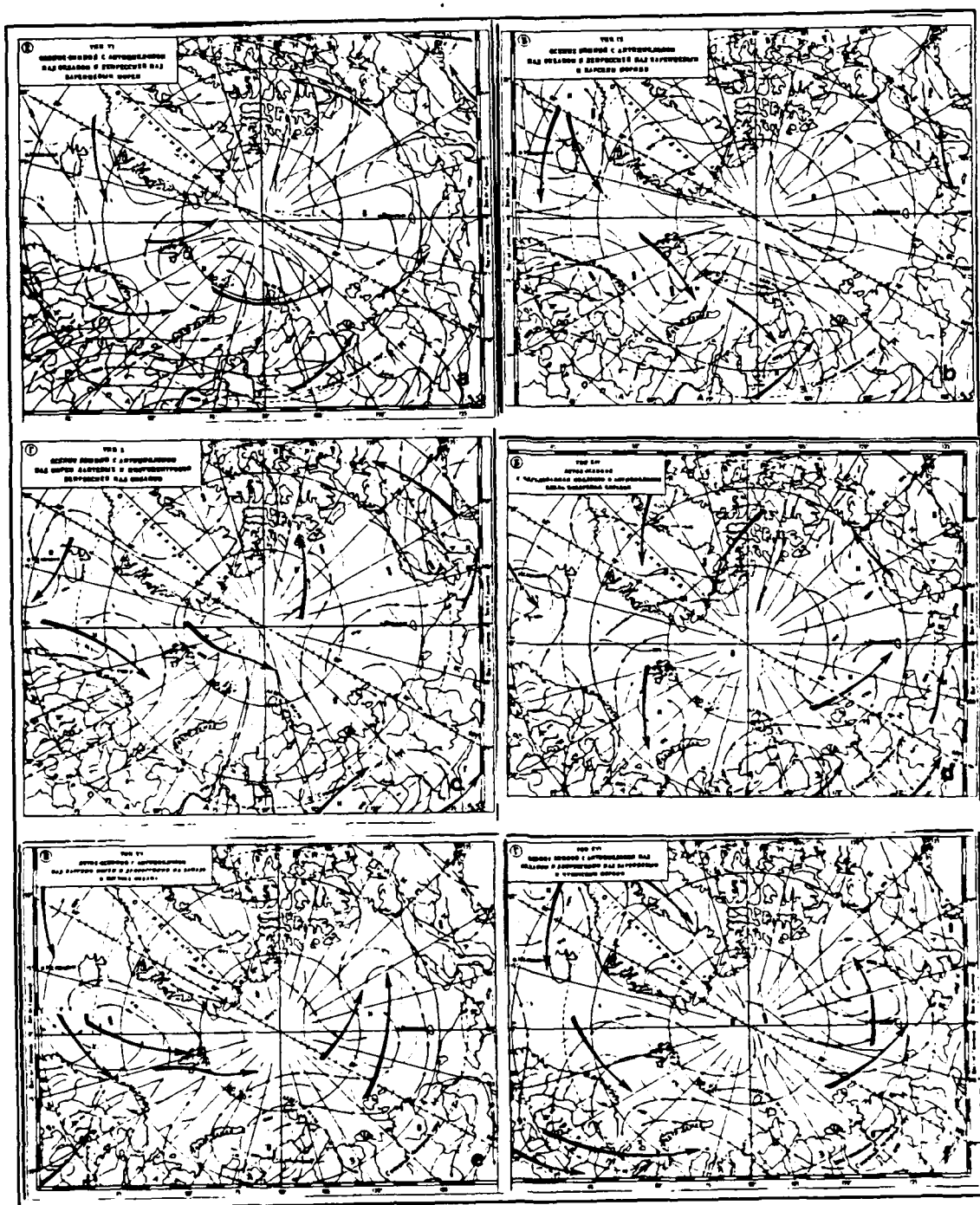
Fig. 11.   Autumn synoptic patterns (from Gorshkov 1983)

and Norwegian Seas, Fram Strait, and vicinity of Svalbard. Low pressure systems can
regenerate in the MIZ as well as off the east coast of Greenland and the vicinity of

Novaya Zemlya. However, North Atlantic cyclones typically stagnate and fill near Novaya Zemlya. The surface low pressure systems tracking from the North Atlantic onto the polar ice cap rise up over the cold layer of Arctic air and become occluded. Once the cyclones move over the ice basin their tracks are slow, erratic, and difficult to predict.

C. SIGNIFICANT ATMOSPHERIC FEATURES

There are many significant features which are common and unique to the Arctic. The first section covers the "baroclinic leaf" which can be seen in satellite imagery during Phase I. The second section covers the importance of polar lows which are very common in the Norwegian and Barents seas. Boundary layer fronts which form in Fram Strait are described in the third section. Several features visible on the Arctic satellite imagery used in this thesis will be discussed in the final section.

1. Baroclinic Leaf

Weldon (1979) defines a "baroclinic leaf" as the elongated cloud pattern that forms prior to the comma shaped cloud pattern. The "leaf" is associated with frontogenesis aloft and usually forms in a westerly wind field. The "baroclinic leaf" cloud pattern delineates a boundary that is being deformed and is a precursor to comma shaped systems. Weldon (1986) states that 75% of the "baroclinic leaf" systems form comma systems with surface cyclogenesis. In the deformation boundary a new baroclinic zone forms downstream from an established baroclinic area. New clouds are forming and precipitation becomes more organized but surface pressures have not lowered and there is no closed surface circulation. There is frequently a surface trough or cyclonic shear zone present. The system usually develops vertically and surface deformation also occurs. Typical shapes for "baroclinic leafs" are illustrated in Fig. 12 from Weldon (1986b).

17
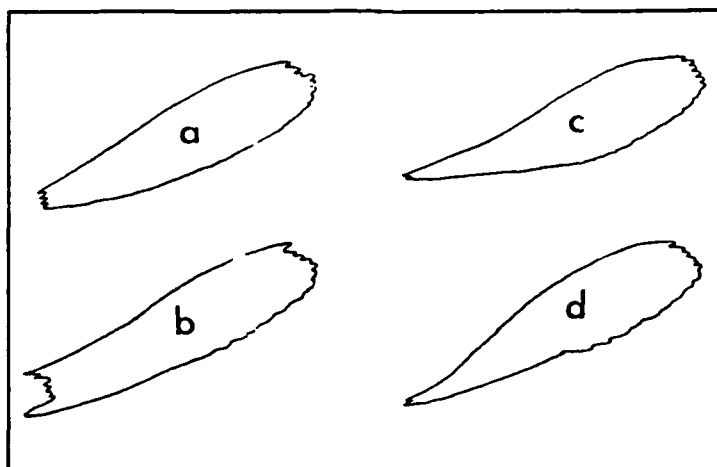
Fig. 12. Baroclinic Leaf Cloud Patterns (from Weldon 1986b)

Upstream of the deformation zone, in the pre-existing baroclinic zone, the upper level winds are increasing and the flow is confluent. Downstream, the wind speeds are decreasing and the flow is difluent. There is cyclonic flow north of the zone and anticyclonic flow south of the deformation area. Fig. 13a shows a "baroclinic leaf" embedded in the upper level flow. Fig. 13b reflects the surface pressure pattern under a "baroclinic leaf" system. The maximum winds at the upper level are upstream from the "leaf" and downstream speeds are lower. The jet stream maximums are south of the sharp northern boundary of the "leaf". This is unlike a cirrus shield where the jet axis lies on the northern edge of the cloud pattern. Significant precipitation will occur on the western or trailing edge of the "leaf". At the surface, under the southern boundary of the "leaf", a surface frontal zone will typically lie parallel to the cloud pattern.
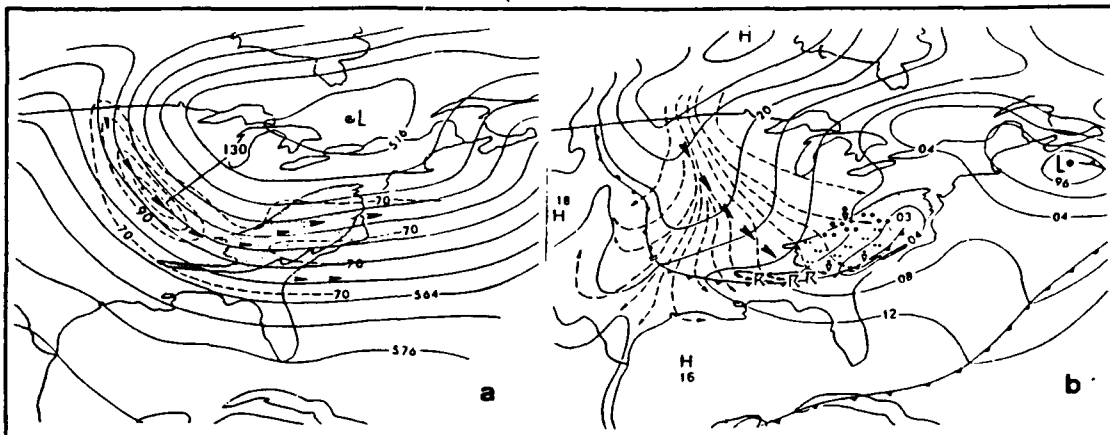
Fig. 13.   a) 500 mb and b) Surface Analysis with a Baroclinic Leaf (from Weldon 1986b)

The "baroclinic leaf" cloud system will not usually move in the direction of the flow, but will rotate slightly counterclockwise. The "leaf" can form on the forward side of an upper level trough. Weldon (1986a) describes formation of a "baroclinic leaf" cloud pattern in a high amplitude upper level trough. Fig. 14 shows a "leaf" forming on the downstream side of a high amplitude upper level trough. High cloudiness is present on the warm side of the jet axis.
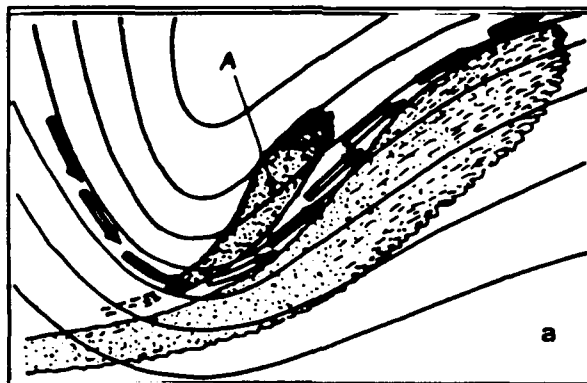
Fig. 14.   Baroclinic Leaf Embedded in Upper Level Trough (from Weldon 1979)

2. Polar Lows

Businger and Reed (1989) define a polar low as a "small synoptic- or subsynoptic-scale cyclone that forms in a cold air mass poleward of major jet streams or frontal zones and whose main cloud mass is largely of convective origin." As cold

19

arctic air flows off the Arctic ice basin or the Greenland ice cap it turns strongly cyclonically over the open ocean wrapping itself around the relatively warmer air over the ice-free water. Hence, polar lows are thought to be warm core and are sometimes compared to tropical cyclones because some form the distinctive clear eye (Rasmussen 1989). Polar lows have weak vertical tilt, experience their strongest circulation at the surface, exhibit low-level cyclonic shear, and the geostrophic wind backs with height. Polar lows form over open oceans and can be seen on satellite imagery as comma or spiral shaped cloud patterns. They range in size from 50 to 1000 km in diameter and can produce strong winds and heavy precipitation. In the seas north and west of Norway, polar lows form most frequently from October through April with a maximum occurrence in January (Businger and Reed 1989).

Of the three types of polar lows defined by Businger and Reed (1989), the Arctic-front type is the most common in the Greenland, Norwegian, and Barents Seas. Arctic-front type polar lows form in the cold air mass behind arctic fronts. Arctic fronts are difficult to detect on weather maps because tight temperature gradients may not be evident. However, Arctic fronts can be seen on satellite imagery as described in Section 1, above. Arctic fronts can be located along the MIZ where relatively warm water meets the polar ice pack. Differential heating of the boundary layer over the warm water and the ice cover causes a strong low-level baroclinic zone. Polar lows form when the cold air from the polar ice pack or Greenland continent flows over the open waters of the Greenland, Norwegian, or Barents Seas. Clouds streets as described in Section 1. indicate the flow of air off the ice pack over the open water.

Arctic-front type polar lows can form in reversed shear situations where the storm motion is in the opposite direction of the thermal wind. In this case, the cloud pattern lies upstream of the trough. Reverse shear polar lows have been observed north and west of Norway (Businger and Reed 1989) and in the warm intrusion of water west of Spitzbergen.

Modeling polar lows and especially Arctic-front polar lows has proven to be an almost impossible task due to their small size. The Arctic-front type polar low is difficult to forecast because of the scarce observations in the regions of formation. The most important tool for detecting and analyzing polar lows are infrared images. The Polar Lows Project (Lystad 1986) identified three criteria for polar low formation: (1) cold air advection at the sea surface; (2) 850-500 mb thickness layer must be less than 3960 m (adjust with sea surface temperature); and (3) 500 and 700 mb levels must have cyclonic or zero curvature.

3. Boundary Layer Fronts

Boundary layer fronts in the Arctic are associated with outbreaks of cold Arctic air and appear as bands of enhanced cumulus activity formed from diabatically forced vertical circulations. Boundary layer fronts typically form when the surface wind flow is parallel to snow or ice covered surfaces and ice free water areas. Ice edge boundary layer fronts can maintain their identities for long distances while being advected by the synoptic flow.

Shapiro and Fedor (1989) studied the case of a stationary boundary layer front that formed on 14 February 1984 from low-level northerly flow from an east-west oriented ice edge west of Spitzbergen and running parallel to the west coast of Spitzbergen and a north-south oriented ice edge at the southern tip of Spitzbergen. The boundary layer front appeared where the northerly air flow from the ice cap modified by the relatively warmer ice free water meets the unmodified cool air flowing from the cold ice/snow covered Spitzbergen and sea ice to the south. The narrow tongue of warm water from the Norway Current that runs in Fram Strait adds to the boundary layer forcing. The frontal structure was determined from dropsonde data (Fig. 15). A low-level jet is clearly depicted in Shapiro and Fedor's cross section of the boundary layer front in Fig. 15. Fett (1989a) proposes that the low-level jet is caused by thermal wind forcing between the surface temperature gradient from the open sea to the ice-covered land. The low-level jet is a result of a secondary thermally direct circulation where the air is being returned toward the land at the upper levels. Shapiro and Fedor (1989) found that the thermal gradient above the low-level jet was in the opposite direction of the horizontal gradient in the boundary layer front. This then supports Fett's hypothesis of a return flow to land or ice covered surfaces at upper levels. The boundary layer front in this case extends to 850 mb. The surface inversion west of the front is deeper due to convective overturning by turbulence in the boundary layer. There is also a strong surface inversion over Spitzbergen and the ice pack due to radiational cooling. Shapiro and Fedor (1986) found large values of relative and potential vorticity along the front.

21
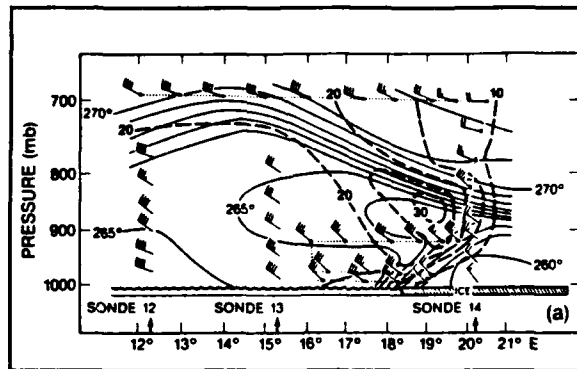
Fig. 15. Vertical cross-section of a boundary layer front (from Shapiro and Fedor 1989)

Fett (1989b) observed a westward propagating boundary layer front that formed in Fram Strait on 25 March 1987. The front was embedded in north-south oriented cloud streets with colder air to the east and relatively warmer air to the west. Along the front multiple vortices were observed with the largest vortices located at the southern end. Unlike Shapiro and Fedor (1986) case, the surface inversion was higher east of the front and extended to 2 km. East of the front the boundary layer was only 1 km.

Vortex generation plays an important role in boundary layer fronts. Fett (1989b) proposes that the vortices that form due to boundary layer fronts can generate into polar lows under certain conditions. The boundary layer front is thought to pre-condition the lower levels for polar low development but other factors must be present. Cold air aloft and upper level support in the form of a 500 mb trough or low is needed. In addition low-level baroclinicity and vorticity is required. Fett (1989b) observed that on 12 December 1982 in the Norwegian Sea a polar low formed at the southern end of a boundary layer front. Shapiro and Fedor (1989) also cited the formation of a polar low on the southern end of boundary layer front on 19 April 1985 south of Spitzbergen.

4. Cloud Features in Satellite Imagery

An extremely useful Navy Tactical Applications Guide for satellite imagery was recently published for the Arctic (Greenland/Norwegian/Barents Seas) by the Naval Environmental Prediction Research Facility (Fett 1989a). This guide uses high resolution satellite data to illustrate significant cloud patterns in the Arctic.

a. Surface Streamlines

Streamline analysis using satellite imagery is a useful tool in the Arctic where surface observations are sparse and satellite imagery may be the primary data

22

source. Identifying troughs and ridges through cloud types is the first step. Overcast stratus, stratocumulus, or fog, are associated with anticyclonic flow. Ridge lines appear in clear or very thin, shallow, fog areas with weak winds. Cyclonic or straight flow is characterized by open cell or stratocumulus clouds. Col areas are regions where the wind curvature changes drastically over a small distance (Fett 1989a). Cloud streets are indicative of off-ice flow and can be used to clearly draw streamlines. Clear conditions in the MIZ also indicates off-ice flow.

b. *Arctic Fronts*

An Arctic front is a disjointed band of low and high level cloudiness that moves southward in association with an outbreak of a cold Arctic air mass. Enhanced satellite imagery and a practiced eye are needed to detect and monitor Arctic fronts. Fig. 10-11a in Fett (1989a) depicts a well defined Arctic front. Cloud plumes form when strong low-level winds encounter elevated terrain. When cyclonically curved cloud streaks or banded cloudiness align with these observed cloud plumes, an Arctic front may be indicated. Mountain waves form when high winds are orographically lifted and this can be another indication of an Arctic front location.

c. *Polar Lows*

Polar lows often develop within open-celled cumulonimbus. The lows have a comma or spiral shaped cloud pattern and some may have a clear eye. Elongated bands of cloud clusters that lead into low pressure centers with strong convective activity are a favorable region for polar low development. Multiple polar lows may form in this type of region. The life span of a polar low may be as short as 6 hours or last 2 to 3 days and therefore satellite imagery must be monitored every 1 to 2 hours for polar low detection and tracking. Two other favorable regions for development are in the cold air masses behind Arctic fronts and in the vortices at the southern end of boundary layer fronts.

III. SYNOPTIC OVERVIEW OF PHASE I

A. DATA SOURCES

Information for describing the synoptic and mesoscale conditions of Phase I were derived from several sources. The R/V *Polarbjoern* provided the most continuous and frequent surface and upper air data. A buoy array deployed in the drift region for the experiment provided reasonably continuous but limited surface data. The synoptic scale fields were based on operational surface and upper air reports and hemispheric prediction models. Meteorological satellite imagery was used to verify the synoptic scale analyses and match them to the in situ measured data.

1. R/V Polarbjoern

Surface layer vector wind, air temperature, humidity, and surface pressure were recorded for 10-minute intervals on the R/V *Polarbjoern*. The system used for the measurement and initial signal processing was the Coastal Climate WeatherPak meteorological weather station. The 10-minute average values, and gust and variance statistics with the periods were calculated with a micro-computer based acquisition system. At least twice daily rawinsondes launched from the ship provided vertical profiles of temperature, humidity, and wind speed and direction at mandatory and significant pressure levels. The R/V *Polarbjoern's* track during the drift phase is depicted in Fig. 16. The position of the ship at the beginning of the experiment and on the 10th and 20th of each month were plotted. The thick black lines represent the position of the ice edge obtained from the NPOC weekly analyses. The analyses are based on data from 21 September, 19 October, 16 November, and 21 December 1988 with the ice edge analyzed further south each month.

2. Surface Buoys

Surface layer temperature and pressure were measured from six buoys that were deployed in an array around the R/V *Polarbjoern*. The initial array pattern appears in Fig. 16. as well as each buoy's position on the 10th and 20th of each month. The measured values as well as position were relayed to a polar orbiting satellite within the Argos network. Argos is a French-designed sensor located on a polar orbiting satellite that collects environmental data. Data is acquired by the satellite as it passes over the buoy. The Argos system has been tested to be locationally accurate to within 50 meters (Rao et al. 1990).

24
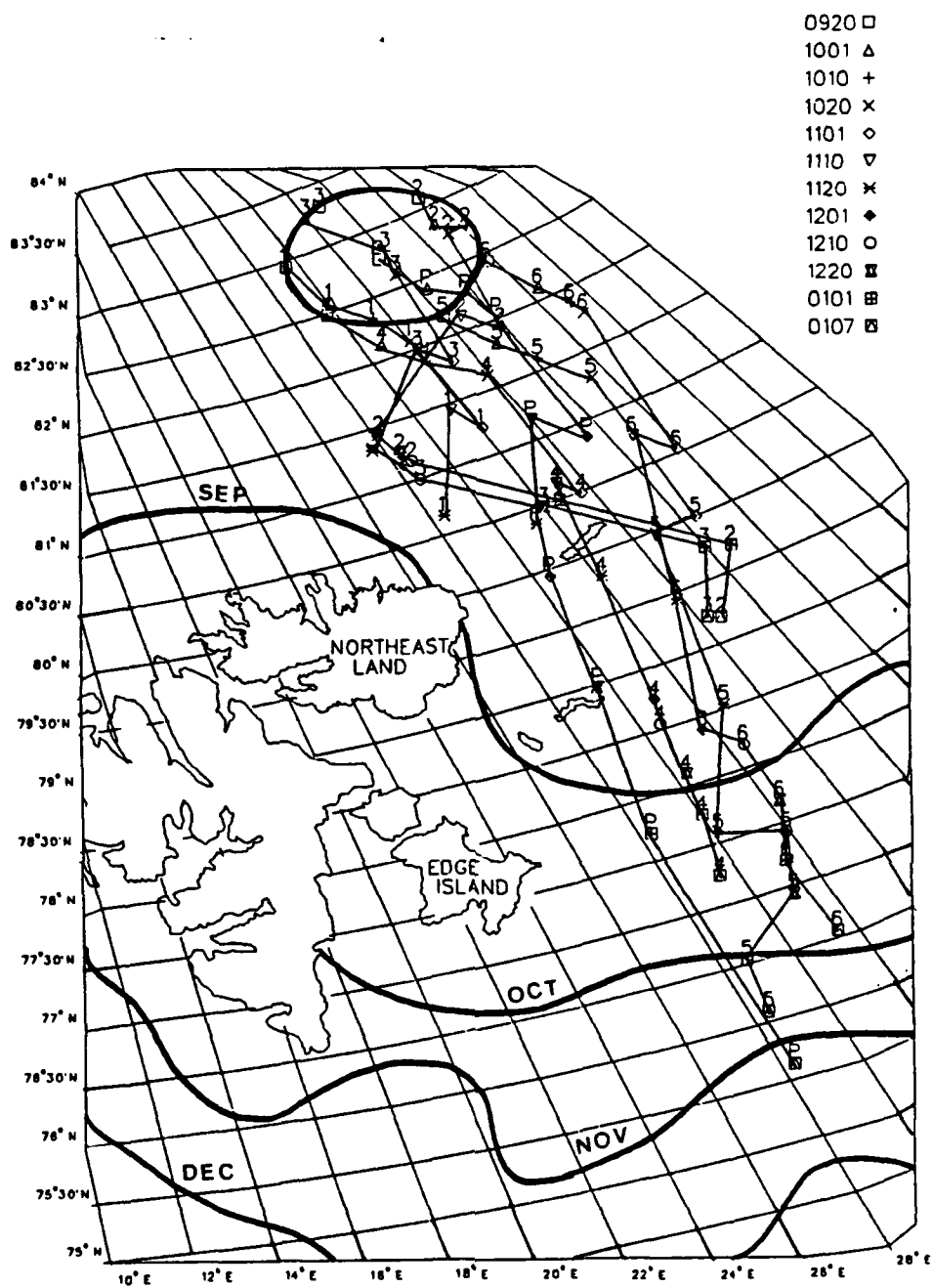
Fig. 16. Buoy array and R/V Polarbjoern positions during drift phase for dates September 20 to January 7: buoys are denoted by numbers 1-6, ship is denoted by a P, and ice edge analyses are represented by thick black lines.

25

The Pacific Marine Environmental Laboratory (PMEL) received the buoy data, processed into pressure and temperature information, and then averaged the data into hourly data sets. There were no gaps greater than three hours. Buoy 1 was deployed on 16 September and transmitted data until 19 November. All the buoys, except buoy 1, transmitted data through Phase I. Buoy 3 was also deployed on 16 September. Buoys 2, 4, 5 and 6 were deployed on 17 September. The buoy array translated and changed it configuration during the drift period as shown in Fig. 16. The lighter lines depict the individual buoy tracks. The symbols represent the buoy positions on the 1st, 10th, and 20th of each month.

3. Surface and Upper Air Reports and Global Analyses

The approach in analyzing meteorological features during Phase I was to use available land and ship observations and satellite imagery. Fewer upper air reports were available in the region, so the emphasis shifted to the upper air analyses from Naval Operational Global Atmospheric Prediction System (NOGAPS) which were used in conjunction with information on the satellite images. Satellite imagery, above all, proved indispensable in the Arctic as the number and frequency of weather reports in the region is sparse.

The number of stations reporting surface and upper air meteorological data for synoptic scale descriptions within the region are few but not as scarce as for an open ocean region. Information form these stations, of course, are used to make the analyzed and predicted fields which were the basis for describing synoptic scale conditions. Fig. 17 depicts the reporting stations on a synoptic map for the eastern part of the Arctic Circle. Table 1 lists the names and locations of some of the stations. The WMO code is the two number country block code and three number station identifier. The station's actual reports, listed in columns five and six, are only for the period covered during Phase I of CEAREX. The Norwegian community on Svalbard reports as station 01008 not 01005 or 01007. The Greenland station 04340 did not report, but another station, 04339, not on the chart, did report. Of the Greenland stations only 04320 and 04339 reported with any regularity, and only one station, 04320, located on the east-northeast Greenland coast, reported upper air observations. Of the Norwegian stations, Bear, Hopen (Hope) Island and Svalbard reported frequent surface observations as well as those located on mainland Norway. Only Jan Mayen and Bjornoya (Bear) Island produced upper air reports. All the U.S.S.R. stations frequently transmitted surface observations, and all but one frequently transmitted upper air observations. There are

many other WMO stations listed on the synoptic map but no data was received from those stations during this period.

Table 1. REPORTING STATIONS, LOCATION, AND DATA REPORTS

Country/Station Name	WMO Code	Latitude	Longi-tude	Surface Reports	UA Re-ports
GREENLAND					
Nord	04310	81.36N	16.40W	X	—
Danmarkshaven	04320	76.46N	18.40W	X	X
Danebord	04330	74.18N	20.13W	X	—
Scoresbysund	04339	70.29N	21.58W	X	—
Kap Tobin	04340	70.25N	21.58W	—	—
NORWAY					
Jan Mayen	01001	70.57N	08.40E	X	X
Isfjord Radio, Svalbard	01005	78.43N	13.38E	—	—
Longyearbyen, Svalbard	01007	78.13N	15.35E	—	—
Svalbard	01008	78.15N	15.28E	X	—
Bjornoya Island	01028	74.31N	19.01E	X	X
Hopen Island	01062	76.30N	25.04E	X	—
Hammerfest Aeradio	01053	70.45N	23.41E	—	—
Fruholmen fyr	01055	71.05N	24.00E	X	—
Sletnes fyr	01078	71.05N	29.14E	—	—
U.S.S.R.					
Kheysa Ostrov, Franz Joseph	20046	80.37N	58.03E	X	X
Vize Ostrov	20069	79.30N	76.59E	X	X
Barencburg, Svalbard	20107	78.04N	14.13E	X	X
Mys Zhelaniya, N. Z.	20353	76.57N	68.35E	X	X
Russkaya Gavan, N. Z.	20357	76.11N	63.34E	X	—

Synoptic scale conditions were interpreted from fields generated at two meteorological centers, the Navy's Fleet Numerical Oceanography Center (FNOC) and the National Meteorological Center (NMC). FNOC's NOGAPS model surface analyses were compared with the National Meteorological Center's (NMC) final hand analyzed
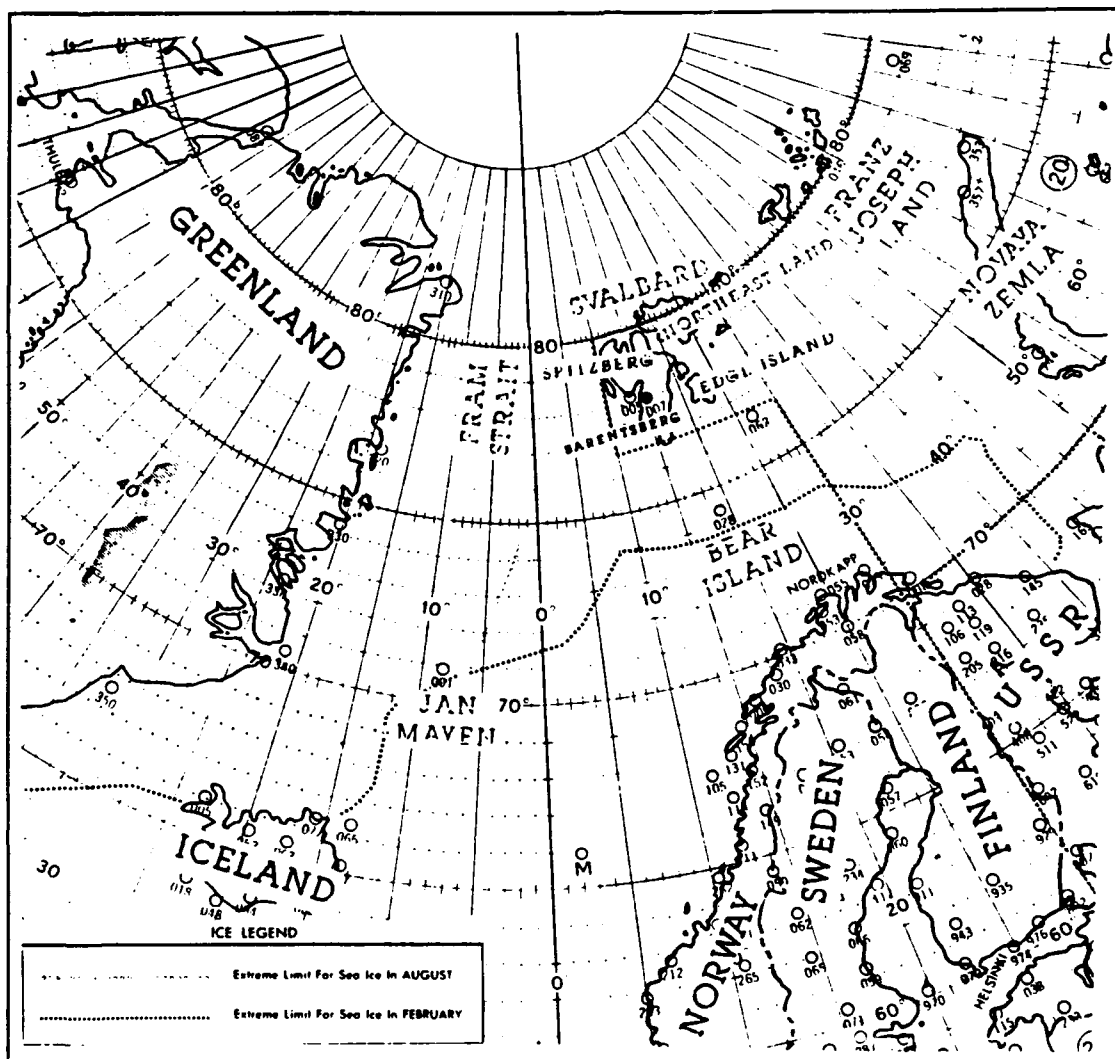
Fig. 17.   Synoptic map of eastern Arctic Circle showing reporting stations.

surface analyses and satellite imagery.   The 700 mb, 850 mb, and 500 mb upper air fields used were available from NOGAPS.

NOGAPS is the Navy's current numerical weather prediction model for use over the Arctic as well as the globe.   NOGAPS version 3.0 was in use during Phase I of CEAREX.   NOGAPS uses a six hour (or twelve if six is not available) forecast for its first guess.   The first guess is used at a grid point where there are no data.   In the Arctic, where there is limited data, the model relies heavily on its six (or twelve) hour forecasts. The six (or twelve) hour forecasts in turn rely heavily on previous forecasts.   This can cause significant problems when unexpected and rapidly developing systems occur.

28

NOGAPS grid resolution is not fine enough to resolve boundary layer fronts and most polar lows.

NMC's Northern Hemisphere surface analyses are subjectively generated four times a day. All available surface reports, satellite imagery, ship reports, buoy reports, and upper air observations are used. Consequently, the NMC hand drawn final analyses depict fronts and other features better than NOGAPs model analyses. NMC analyses showed much greater detail in the Arctic and picked up mesoscale features which are not possible with NOGAPS due to the resolution of the model.

4. Meteorological Satellite Imagery

The meteorological satellite imagery used are from the National Oceanic and Atmospheric Administration (NOAA) 9, 10, and 11 satellites and the Defense Meteorological Satellite Programme (DMSP). The NOAA imagery are from the Advanced Very High Resolution Radiometer (AVHRR) High Resolution Picture Transmission (HRPT) sensors on board the satellite and has a resolution of 1 km by 1 km. Most of the enhancements were done at Tromso, Norway using Channel 4. The remainder of the enhancements were conducted using tapes supplied by Tromso on the computers at the Naval Postgraduate School and Naval Oceanographic and Atmospheric Research Laboratory Administrative Directorate (NOARL-AD), both located in Monterey, California.

Channels 1 (.58 - .68 μm) and 2 (.73 - 1.1 μm) detect visible and near infrared solar radiation and could not be used in this thesis due to insufficient sunlight within the Arctic basin during this time period. Channel 3 (3.55 - 3.93 μm) detects both emitted and reflected solar radiation. If there is an imbalance of sunlight in the satellite pass, channel 3 must be used with care. Channels 4 (10.3 - 11.3 μm) and 5 (11.5 - 12.5 μm) both provide thermal mapping of clouds and surface features with channel 5 accounting for water vapor attenuation. In the Arctic where the atmosphere is very dry, the differences between channels 4 and 5 were not discernable. The DMSP mosaics were compiled by NOARL-AD and used to supplement NOAA satellite imagery. The DMSP infrared mosaics have a resolution of approximately 4.0 km.

The satellite imagery was especially useful in detecting sub-synoptic and short-lived systems which are not resolved or handled well by numerical models and frequently missed by hand analyses. Cyclogenesis in the Arctic was only observed through satellite imagery and land observations. Neither NOGAPS nor NMC detected this event in the Arctic.

B. GENERAL SYNOPTIC FEATURES

The meteorological fields were analyzed for the eastern Arctic Circle from Greenland east through Novaya Zemlya and north of Iceland to the central Arctic Ocean. The Arctic Circle is defined as north of 66°N. The Arctic basin or Arctic Ocean encompasses the area north of 80°N. NOGAPS upper level analyses, NMC surface analyses, satellite imagery, drifting buoy, land and ship observations were used. The mean and anomaly charts referenced in this study for sea level pressure, 500 mb geopotential heights and 1000-500 mb thickness were compiled by the Climate Analysis Center of NOAA. The meteorological conditions at the ship were analyzed using time series of all the surface data collected. Time series of the surface pressure, wind speed and direction, and temperature measured on the R/V Polarbjoern from September 1988 to early January 1989 give a good synopsis of the surface meteorological variability at the *R/V Polarbjoern* during Phase I of CEAREX.

1. September 1988

The mean northern hemisphere sea level pressure analysis for September 1988 (Fig. 18a) shows the dominance of a low pressure center over the central Arctic basin. High pressure exists over the Canadian Archipelago with ridging east across Greenland to Svalbard. The northern hemisphere sea level pressure anomaly chart (Fig. 18b) depicts lower than average sea level pressures for the central Arctic basin. The northern hemisphere 500 mb mean geopotential heights (Fig. 19a) reflect the persistence of a 500 mb low height center over the central Arctic basin throughout September defining the center of the circumpolar vortex. The anomaly chart (Fig. 19b) reflects that the heights are significantly lower than average over the central Arctic and through the Greenland and Norwegian Seas. Higher heights than average exist over Greenland. The northern hemisphere 1000-500 mb anomaly thickness chart (Fig. 20b) shows slightly cooler temperatures over the central Arctic basin but slightly warmer temperatures in the Greenland Sea.
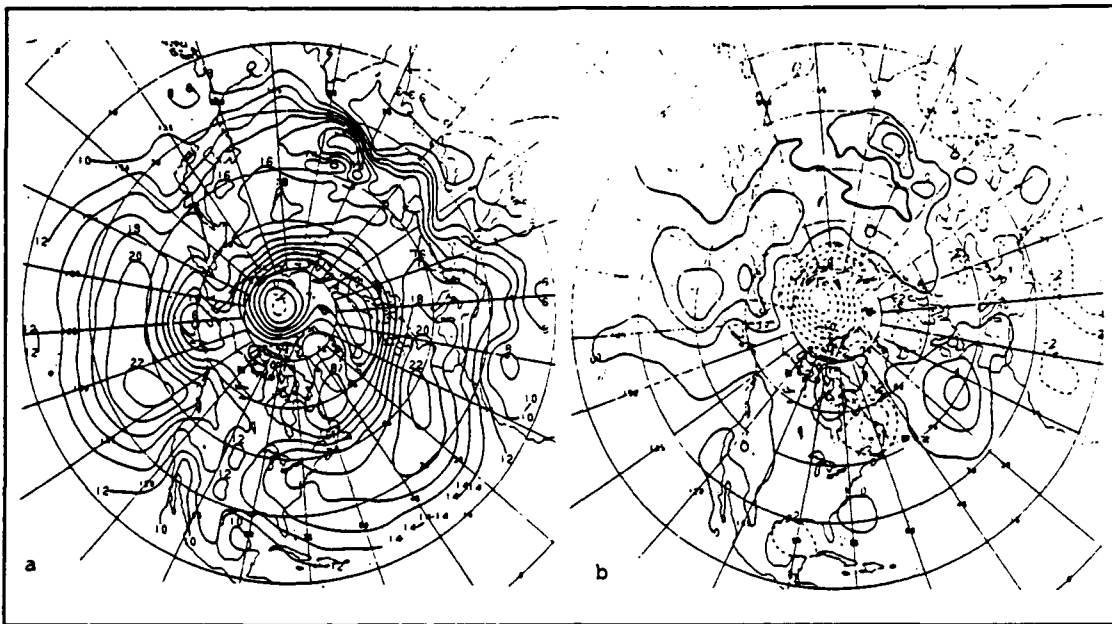
Fig. 18. **a) Mean and b) anomaly sea level pressure for September 1988** (Climate Analysis Center 1988a)
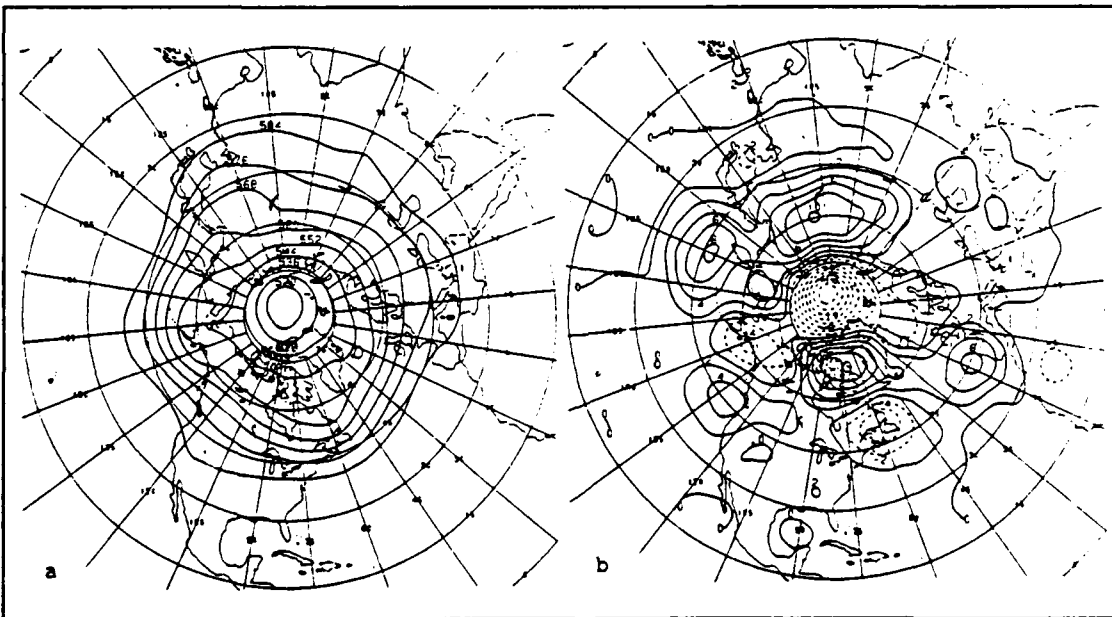
Fig. 19. **a) Mean and b) anomaly 500 mb geopotential heights for September 1988** (Climate Analysis Center 1988a)

Fig. 20.   a) Mean and b) anomaly 1000-500 mb thickness for September 1988 (Climate Analysis Center 1988a)

A 500 mb low height center over the central Arctic basin dominates September weather as reflected in the 500 mb mean geopotential heights chart (Fig. 19a). The key synoptic events of the month are now reviewed. On 17 September, a low height center in the central Arctic basin has a trough extending south, west of Greenland, and a trough extending south, over Franz Joseph Land and Novaya Zemlya. In the next few days, the 500 mb low height center deepens and moves into the eastern Arctic basin with the associated long wave trough moving east across Greenland, Fram Strait, and Svalbard. The 500 mb height center then moves south into northern U.S.S.R. and fills. A second low height center forms over the western Arctic basin and associated troughing extends south over Greenland and Norwegian Seas, and Svalbard the later part of the month.

On 17 September a surface quasi-stationary high pressure center over the Canadian Archipelago ridges east across Greenland to Svalbard. A 984 mb low pressure center is in the western Arctic basin. By the 20th, the surface low pressure center over the Arctic, moves east, north of Svalbard, which decreases the surface pressure in the area, but a weak pressure gradient exists. The low pressure center moves south, then southeast through the Barents Sea. High pressure ridging east over Greenland Sea and

32

Svalbard resumes from the high pressure that remains over Greenland for the remainder of the month. Two low pressure systems move northeast along the coast of Norway, but do not reach farther north than 70°N.

The time series from the *R/V Polarbjoern* for September (Fig. 21) shows relatively steady pressure changes at the ship with no sharp pressure increases or decreases. The only significant drop in pressure occurs when the low pressure system over the central Arctic basin migrates south over Northeast Land then moves southeast to Novaya Zemlya on the 20th. Winds are predominately from the northwest to west in response to the strong ridging over Greenland. The southerly winds from 18 to 20 September occur when the central Arctic low migrates south to the ship's position. By the evening of the 22nd, the low pressure system is east of the ship and west-northwest winds resume. Speeds range from calm to 10 ms^{-1}, but usually are 5 ms^{-1} or less. Air temperatures range from 0 to −20°C with a general cooling trend noted during the month.
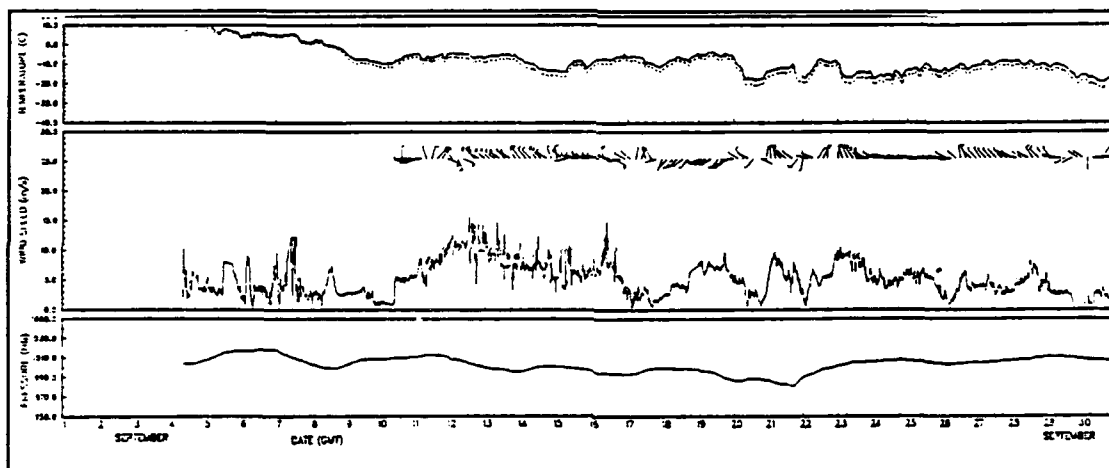
Fig. 21. R/V Polarbjoern time series for September

2. October 1988

The mean northern hemisphere sea level pressure pattern for October 1988 (Fig. 22a) shows low pressure dominating the northern Arctic circle shifting to near the U.S.S.R. and high pressure dominating the Greenland, Norwegian and Greenland Seas, and Svalbard region. The anomaly sea level pressure chart (Fig. 22b) shows pressures lower than average over Severnaya Zemlya and Novaya Zemlya. Higher pressures than average are over the Greenland Sea, Fram Strait, Svalbard and Norwegian Sea. This produces a tight gradient east of Svalbard over the Barents Sea. The mean northern hemisphere 500 mb geopotential heights (Fig. 23a) illustrate the low height center over

the central Arctic which has strengthened from September's analysis. Lower heights over Greenland are evident which produces a tight gradient in the south Greenland Sea. This gradient is much tighter than September. The northern hemisphere 1000-500 mb thickness chart (Fig. 24a) depicts the coldest air over the central Arctic. The anomaly thickness chart (Fig. 24b) shows colder temperatures than the average over Svalbard and Franz Joseph Land. East of Greenland, the layer is much warmer than average, which sets up a stronger temperature gradient than normal in Fram Strait and Norwegian Sea.
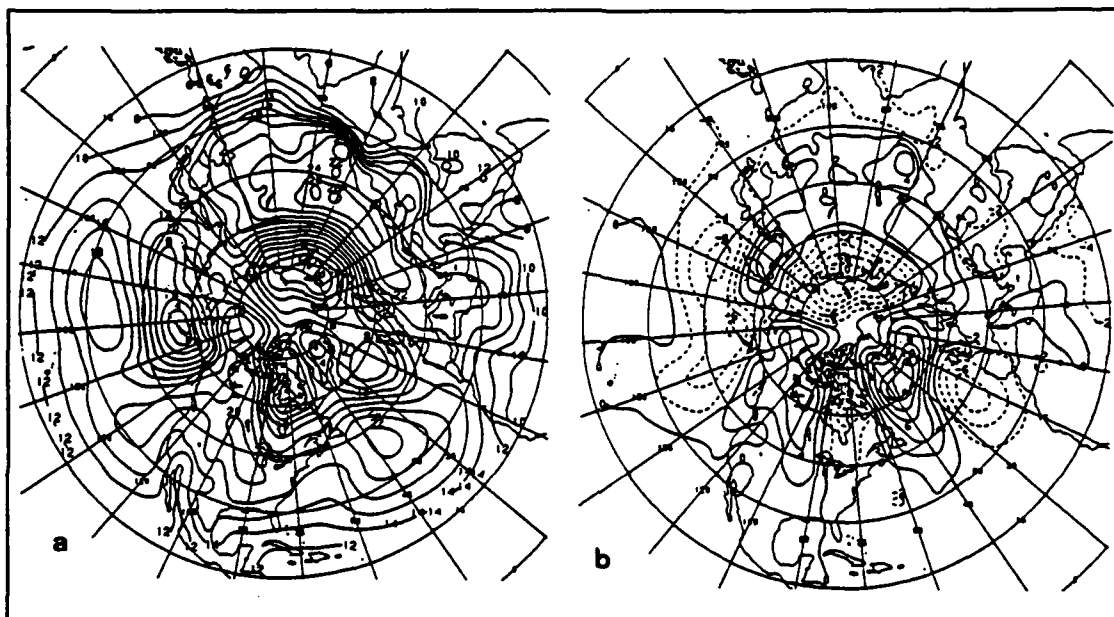
Fig. 22.   a) Mean and b) anomaly sea level pressure for October 1988 (Climate Analysis Center 1988c)
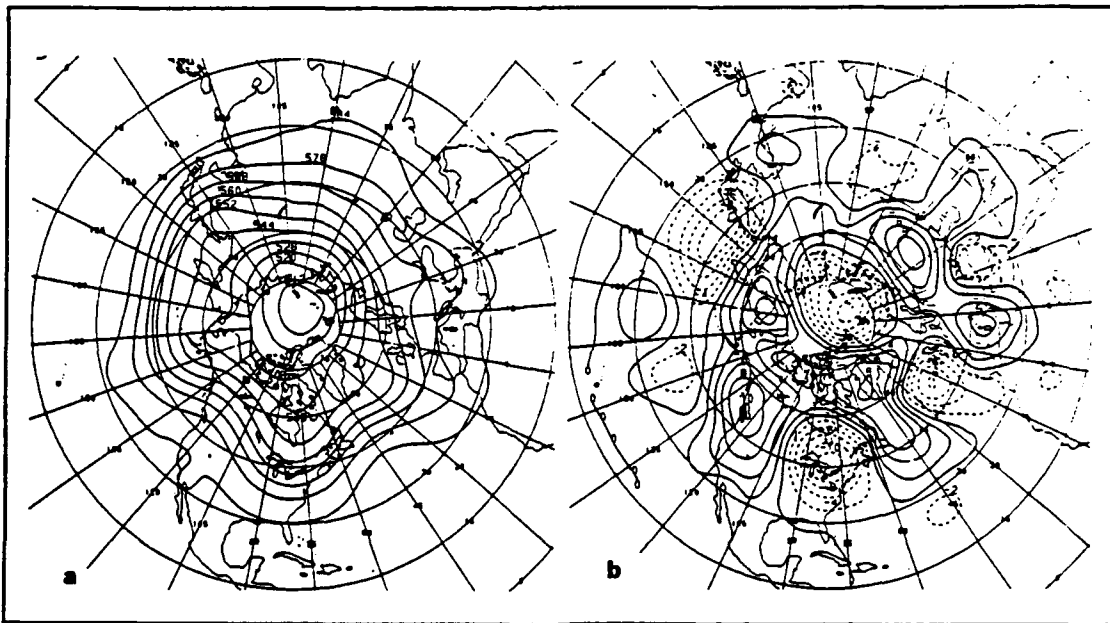
Fig. 23. a) Mean and b) anomaly 500 mb geopotential heights for October 1988 (Climate Analysis Center 1988c)
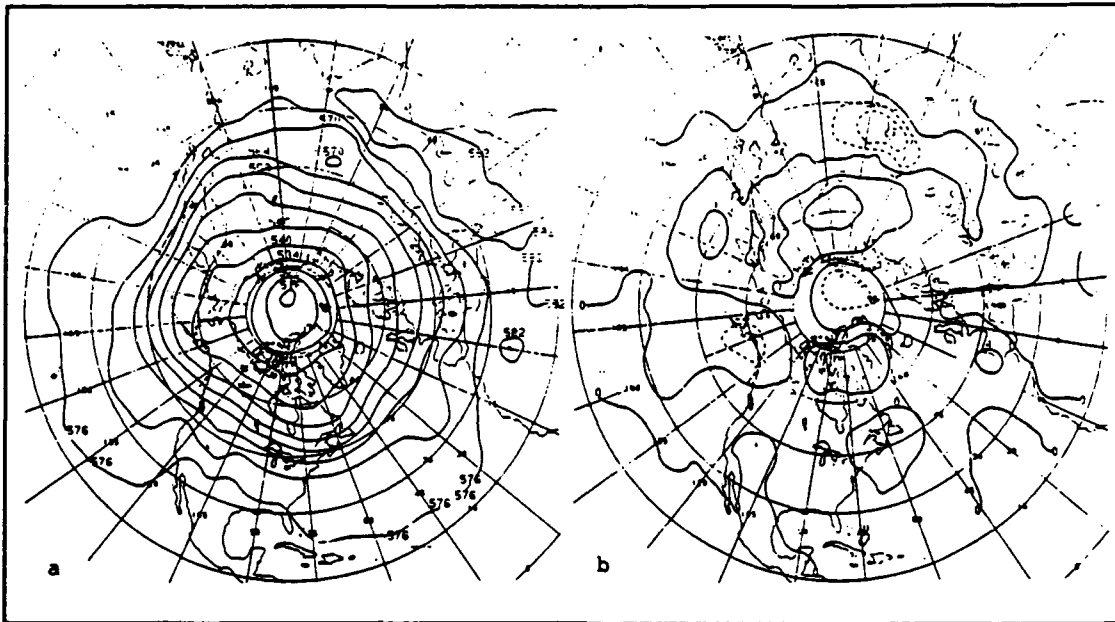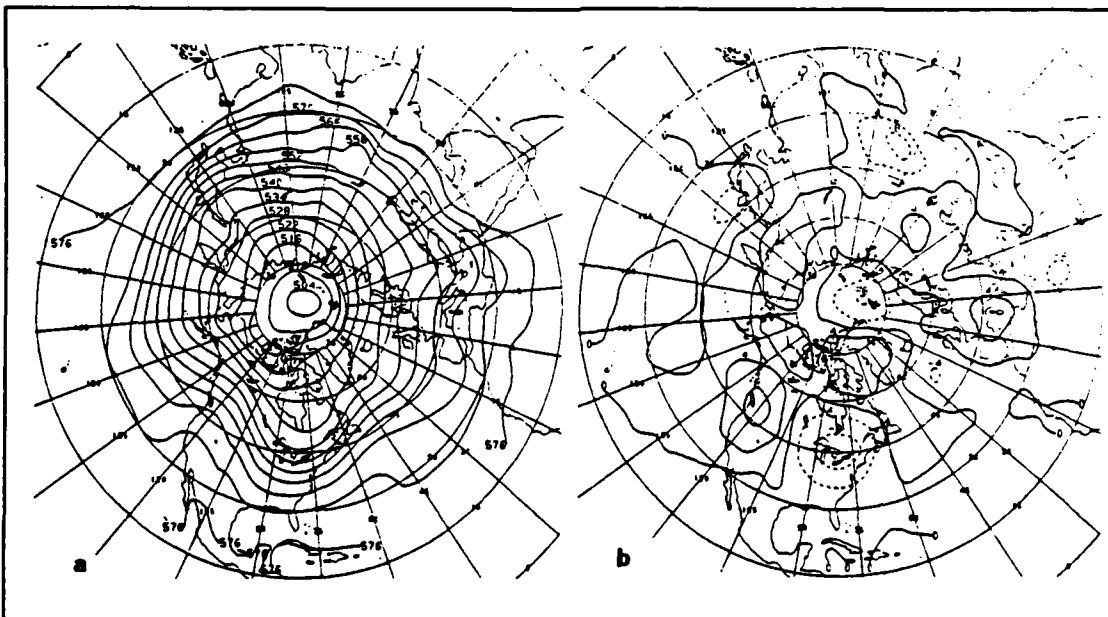

Fig. 24. a) Mean and b) anomaly 1000-500 mb thickness for October 1988 (Climate Analysis Center 1988b)

October has significantly more cyclone activity than September and is related to the stronger westerlies over the CEAREX area shown in the mean 500 mb geopotential heights chart (Fig. 23). In the beginning of October, troughing at 500 mb weakens over Svalbard and zonal flow commences. A low height center exists over the central Arctic basin with a weak short wave trough establishing over the east Greenland coast on the 6th. By the 8th, the trough deepens and moves east across Fram Strait. At the same time, the low height center over the central Arctic basin moves east north of 80°N between Greenland and Svalbard and deepens from 4969 meters to 4746 meters from 7 to 10 October. A short wave trough extends south from the low height center over Fram Strait through the Norwegian Sea. On the 10th, the height center begins to fill and move westward over northwest Greenland. By the afternoon of the 12th, a low height center forms north of Svalbard with troughing extending south from Svalbard to Norway. This event will be analyzed further in Chapter IV. The low height center moves east north of 80°N between Svalbard and Franz Joseph Land and remains with steady height values of 5901 meters early on the 13th. The low height center tracks east toward Franz Joseph Land and on the 14th begins to fill and move southeast toward northern U.S.S.R. Low heights resume over the central Arctic basin for the rest of the month.

At the lower levels satellite imagery on the 10th shows a developing mesoscale vortex forming over Spitzbergen and a second one over Northeast Land. A boundary layer front forms in Fram Strait which will be further studied in Chapter IV. The vertically stacked low pressure system that tracks into the Arctic basin and then tracks west, north of Greenland is visible in the NOAA satellite imagery on the 10th. By the afternoon of the 10th the vortex over Northeast Land moves north over the ice pack bringing southerly winds to the ship and low level warm air advection. The polar low over Spitzbergen dissipates. The northern portion of the boundary layer front is beginning to form a vortex which develops into a polar low in subsequent satellite images. Late on the 10th, DMSP imagery shows a well developed polar low in Fram Strait. Through 9 and 10 October the low pressure pattern is producing strong southerly flow in the vicinity of Svalbard. Satellite images over Svalbard on the 11th show multi-level cloudiness in strong cyclonic flow. By late evening on the 11th, a narrow band of clouds extends south from the Arctic Circle over Svalbard and extends into the northern portion of the Norwegian Sea. By the morning of the 12th, strong low level cyclonic turning is evident in Fram Strait by satellite imagery. Widespread multi-level cloudiness exists over Northeast Land and north through the eastern Arctic basin. Upper level

cloudiness through the 12th obscures the detection of the formation of the surface low pressure system. This development is the subject of a case study in Chapter IV. The morning of 13 October, the low pressure system is clearly visible as a well vertically developed cyclone. The cyclone moves east producing strong northwest winds behind the system in the vicinity of Svalbard. The vertically stacked low pressure system tracks east to Franz Joseph Land and begins to fill. Surface high pressure dominates Svalbard weather with light to moderate winds and variable directions. A low pressure system moves northeast from Iceland along the MIZ from 16 to 18 October but rapidly dissipates east of Svalbard over the advancing pack ice. Weak surface high pressure gradients dominate the weather the remainder of the month.

In October surface pressure at the ship (Fig. 25) decreases from 1008 mb to a low of 959 mb early on the 9th as a surface low pressure system rapidly tracks from Norway north-northeast, passing east of Kvitoya into the central Arctic basin. A second sharp pressure decrease occurs on the afternoon of the 12th and persists through the 13th. as a low forms over the ship and remains quasi-stationary for 24 hours, then tracks southeast to Novaya Zemlya. A more modest decrease in pressure on the 19th occurs when a low pressure trough extending south from a low over the central Arctic tracks eastward across Svalbard to Franz Joseph Land. The remainder of the month is dominated again by high pressure ranging from 1010 to 1020 mb. The wind direction is more variable this month from 6 to 20 October as the low pressure centers and the low pressure trough that pass through the region produce southerly winds in advance of the passage and then west-northwest winds after passage. Speeds above 10 ms^{-1} occur from 8 to 15 October with a period of 15 to 20 ms^{-1} on 12 and 13 October. After 20 October, winds are generally less than 10 ms^{-1} and from the northerly direction. Air temperatures are steady around −20°C until the 12th, when a sharp warming occurs (−24°C to −8.1°C) with a 16°C increase in temperature. The rest of the month air temperatures average −20°C with a general cooling trend to −25°C occurring near the end.
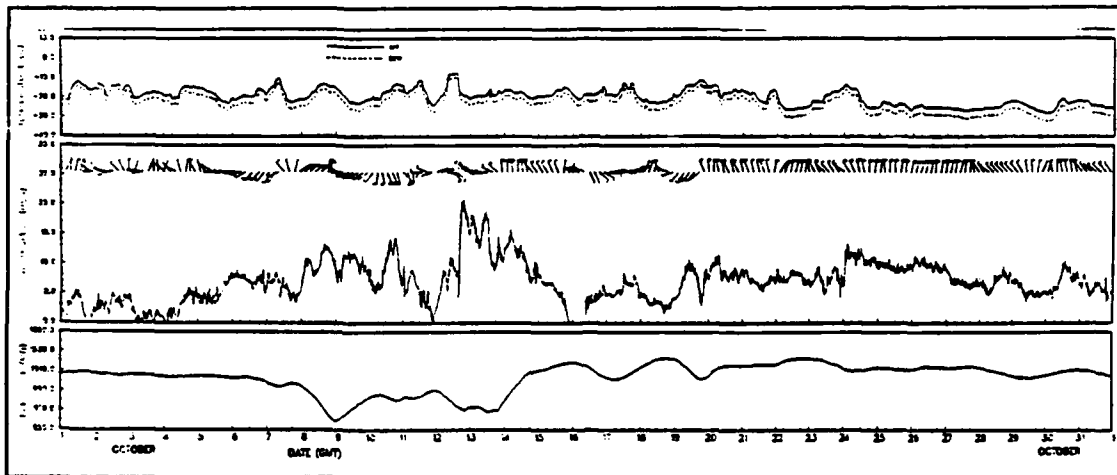
Fig. 25.   R/V Polarbjoern time series for October

3.   November 1988

The northern hemisphere mean sea level pressure pattern for November 1988
(Fig. 26 a) shows the dominance of low pressure over the Arctic basin from Svalbard
to Novaya Zemlya in the Barents Sea. The anomaly sea level pressure pattern (Fig. 26
b) reflects the tight gradient along 15°E as higher pressures than average exist over
Greenland Sea and lower pressures are over Novaya Zemlya producing a strong gradient
in the Barents Sea and Svalbard. The northern hemisphere 500 mb geopotential heights
(Fig. 27 a) shows two weak low height centers, one over Franz Joseph Land/Novaya
Zemlya, and one over the Canadian Archipelago. The anomaly 500 mb geopotential
height chart (Fig. 27 b) shows lower heights than average over Novaya Zemlya, Barents
Sea, and Svalbard and higher heights in the Greenland Sea. The 1000-500 mb thickness
chart (Fig. 28 a) reflects colder temperatures for November than October. A colder
pool of air than average over Svalbard and warmer temperatures exist over Greenland
is reflected in the anomaly thickness chart (Fig. 28b).

38

Fig. 26.   **a) Mean and b) anomaly sea level pressure for November 1988** (Climate
Analysis Center 1988c)

Fig. 27.   **a) Mean and b) anomaly 500 mb geopotential heights for November 1988**
(Climate Analysis Center 1988c)

Fig. 28. a) Mean and b) anomaly 1000-500 mb thickness for November 1988 (Climate Analysis Center 1988c)

November has very little significant cyclonic activity due to the strength of the circumpolar vortex as reflected in the anomaly thickness chart (Fig. 28b). The 500 mb NOGAPS analyses show a low height center over Severnaya Zemlya the first part of the month and a second low height center over the Canadian Archipelago. No significant troughing or low height center moves near Svalbard or Fram Strait.

At the surface, no significant weather features occur in November. The low pressure systems that do move into the region are weak. High pressure in the beginning of the month produce light and variable winds which gives way early in the month to a tight pressure gradient which produces strong northerly winds the remainder of the month. Strong northerly winds existed over the ship for almost the entire month of November as a result of the strong pressure pattern as seen in the mean sea level pressure pattern (Fig. 26a). Satellite imagery confirms the strong northerly flow off the ice sheet east of Svalbard and strong easterly and northerly winds in Fram Strait. One interesting satellite feature visible on NOAA imagery (Fig. 29) is a strong quasi-stationary Arctic front that is visible over Svalbard on the 14th along the MIZ. The Arctic front represents a sharp boundary between the cold pool of central Arctic air and the warmer air from the North Atlantic.

Fig. 29. NOAA-11 Satellite imagery on 140810Z November 1988

No significant weather features occurred at the ship in November as seen in the time series for that month (Fig. 30). Strong southerly winds (10 ms^{-1}) on 6 and 7 November occurred which caused temperatures to rise from $-30°C$ to a high of $-15.4°C$. Southerly winds sustained temperatures in the high teens through the 11th. Northerly

winds (5 to 12 ms^{-1}) brought a persistent cooling trend until the end of the month. No sharp pressure changes were noted for the entire month. Pressure ranged from 1010 to 1020 mb.
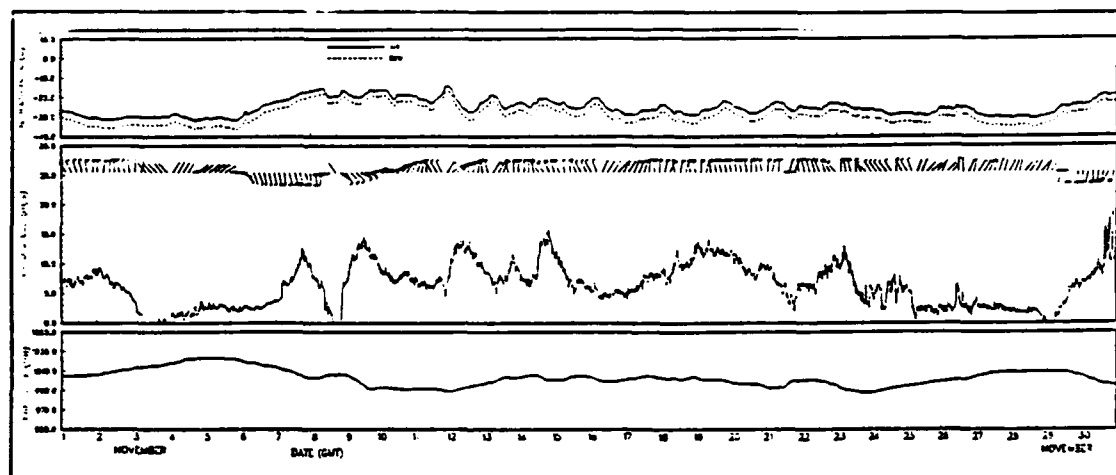
Fig. 30. R/V Polarbjoern time series for November

4. December 1988 to 7 January 1989

The northern hemisphere mean sea level pressure pattern for December 1988 (Fig. 31a) continues to show a low over the eastern Arctic basin between Svalbard and Severnaya Zemlya. The anomaly sea level chart (Fig. 31b) shows much lower than average pressures over the central Arctic, Barents, Greenland, and Norwegian Seas. The mean 500 mb geopotential height chart (Fig. 32a) shows a low height center between Svalbard and Severnaya Zemlya. The heights are significantly lower than average in the Arctic and Greenland Sea. The 1000-500 mb thickness anomaly chart (Fig. 33b) depicts a significantly colder pool of air than average from northeast Greenland to Novaya Zemlya. The colder air and lower heights than average increase the amount of cyclonic activity that occurs in December.
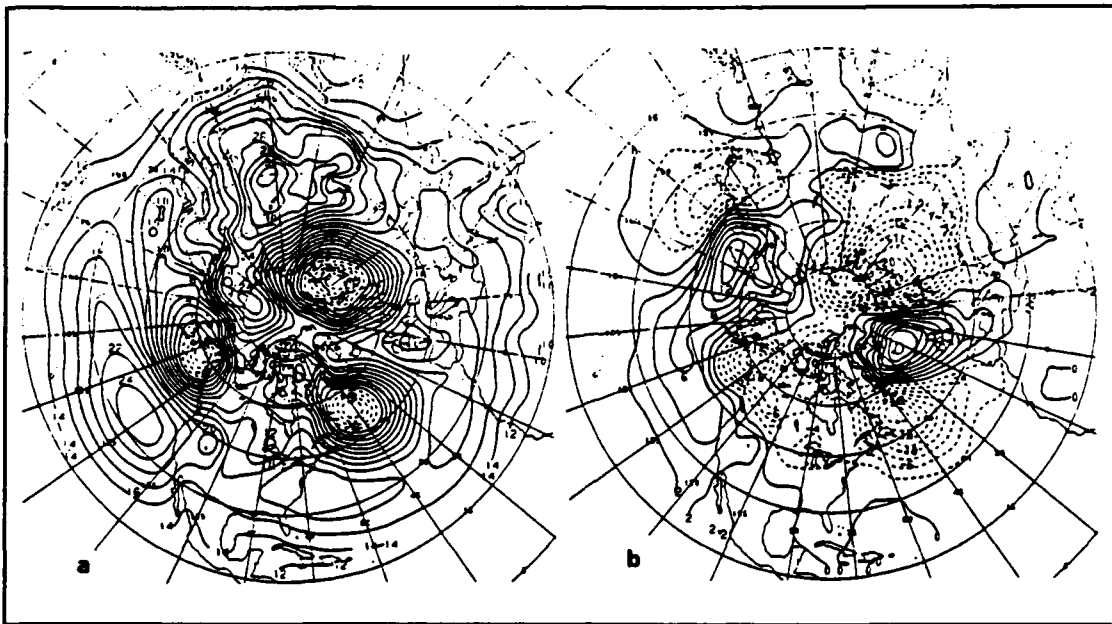
42
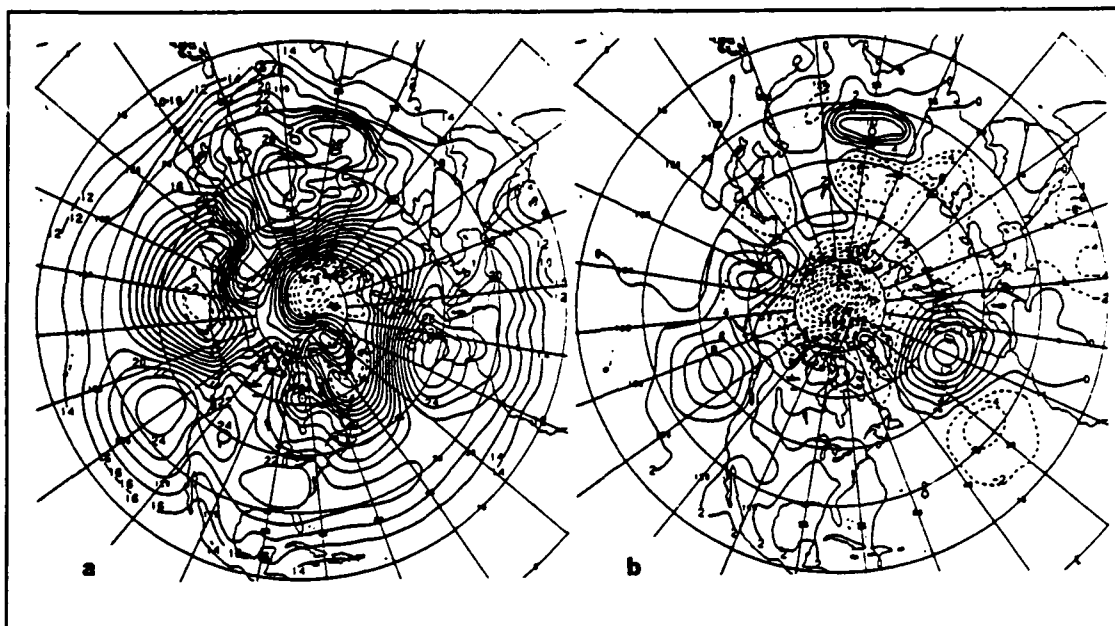
Fig. 31. a) Mean and b) anomaly sea level pressure for December 1988 (Climate Analysis Center 1988d)
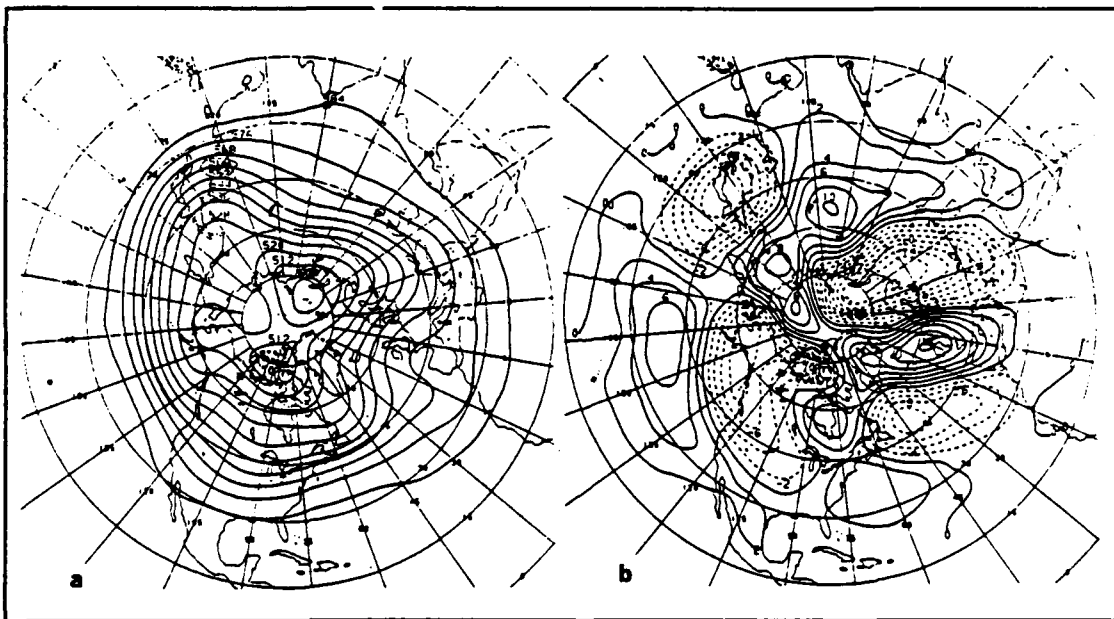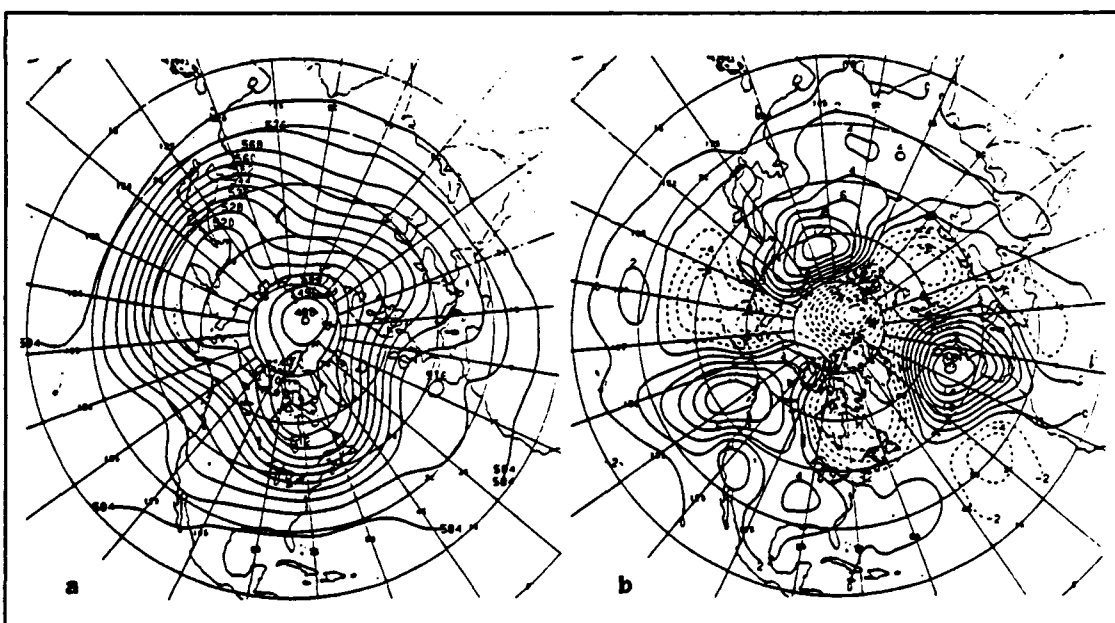

Fig. 32. a) Mean and b) anomaly 500 mb geopotential heights for December 1988 (Climate Analysis Center 1988d)
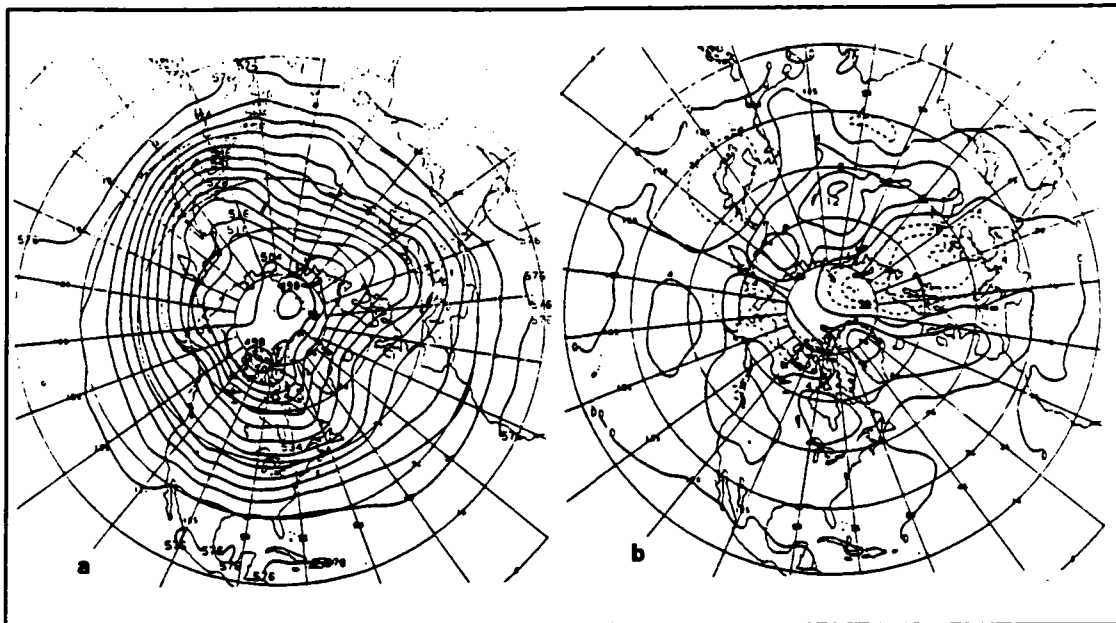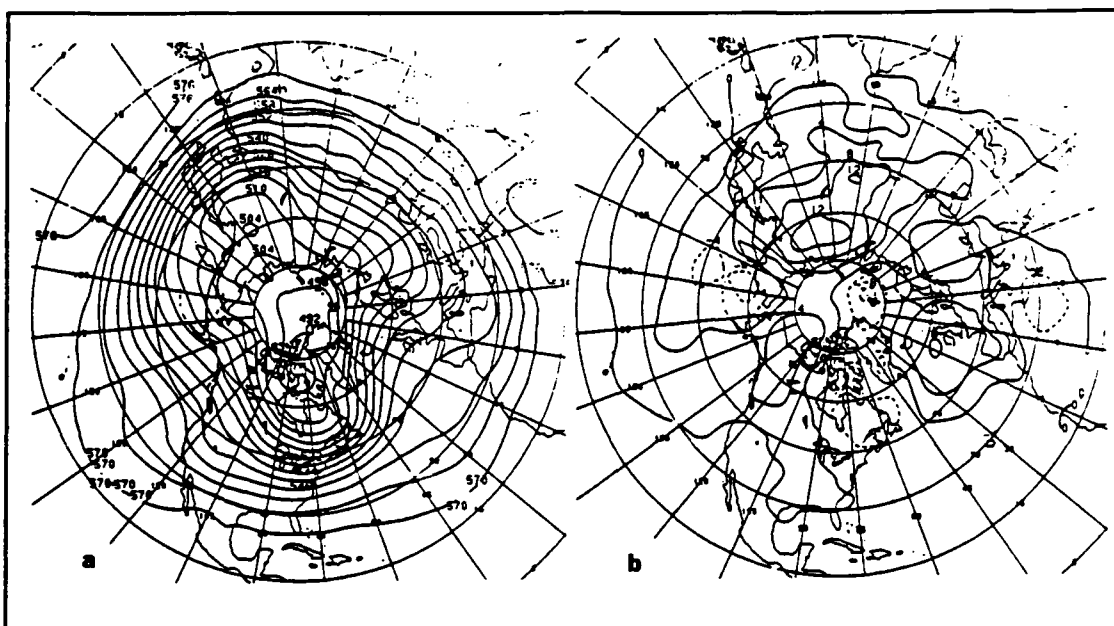
Fig. 33. a) Mean and b) anomaly 1000-500 mb thickness for December 1988 (Climate Analysis Center 1988d)

The average 500 mb statistics show a 500 mb low height center dominating the eastern Arctic basin. NOGAPS 500 mb height pattern the beginning of December depicts a short ridge in the Greenland Sea which moves east as a short wave enters the Greenland Sea on the 2nd. The short wave extends northwest to southeast across the Greenland Sea and Fram Strait. By the 3rd, the flow in the region becomes zonal and then ridging from northern Europe moves in east of Svalbard extending to the Arctic basin. On the 7th, the low height center over northern Greenland moves east-southeast into the Greenland Sea. This path is a secondary track according to the literature (Serreze and Barry 1988). The low height center continues to move east across Svalbard on the 8th deepening by 80 meters. The height center then moves north of 80°N, starts to fill, tracks slowly east, then north to the center of the Arctic circle where it stagnates. Ridging north from the North Atlantic moves over Greenland and Norwegian Seas and vicinity of Svalbard. A short wave trough digs south into Greenland and Norwegian Seas on the 16th and moves east. Weak troughing in the region persists until the 30th. Strong ridging north over east coast of Greenland moves slowly east over Svalbard. A deepening low height center moves east across Greenland into the Greenland Sea by 2 January. The low height center then tracks east across Svalbard on the 3rd. By the 4th

ridging over Norwegian and Greenland Seas from northern Europe resumes until the end of the period.

A review of surface pressure events indicates a low pressure center (1 December) located over the Greenland ice sheet deepens and tracks northeast entering the Greenland Sea early on the 2nd. The low remains steady and tracks east across Svalbard then northeast into the central Arctic basin where the low begins to slowly fill and move in erratic tracks. On the 4th a low pressure center over Iceland moves northeast into the Norwegian Sea and then tracks east south of Svalbard and along the east-west oriented MIZ and slowly fills. High pressure ridges north over Fram Strait and Svalbard commencing at 061200Z. A low pressure center over north Greenland begins to track east early on the 7th, deepens, and moves rapidly east across Greenland Sea to southern Svalbard by the 8th. The low continues to deepen and moves east along 80°N over Franz Joseph Land. High pressure ridging east across Greenland Sea, Fram Strait, and Svalbard behind the low pressure center occurs on the 10th. This ridging is replaced by ridging north from northern Europe. Weak low pressure begins to break down the northward ridging over Svalbard. High pressure center over north Greenland resumes its eastward ridging across Greenland Sea, Fram Strait, and Svalbard. Tight surface gradients produce strong northerly winds. On 1 January high pressure over northern Europe resumes it northward ridging over the region. A deepening low pressure system tracks from northeast Greenland east south of 80°N over Svalbard on the 2nd. The low then tracks east to Franz Joseph Land by the afternoon of the 3rd, then southeast to Novaya Zemlya. High pressure resumes over the region through the end of Phase I.

December brought many changes as evidenced in the ship's time series (Fig. 34). The passage of two cyclones on the 3rd and 9th brought significant changes in the weather pattern. December's average temperature was higher than expected due to the passage of the two cyclones which produced two sharp temperature increases which lasted from one to two days. On 30 November, southerly winds started a gradual warming near the ship where temperatures rose from $-30°C$ to $-3.3°C$ in three days. After the passage of the first cyclone, northerly winds resumed and the temperatures rapidly decreased to the high negative twenties. A minimum pressure of 957 mb occurred late afternoon on the second of December. The southerly winds ranged from 10 to 15 ms^{-1}. The northerly winds after storm passage were much stronger ranging from 12 to 17 ms^{-1} on the fourth of December. The wind changed direction again on the 7th to the southerly direction with the approach of the second cyclone with maximum speeds recorded at 16 ms^{-1}. Air temperatures again rose to $-3°C$ with a 24°C temperature in-

crease in less than 18 hours. Winds from the southerly direction maintained high temperatures through the 8th. Winds changed to northeast early on the 9th and temperatures decreased. Minimum pressure of 954 mb occurred on the morning of the eighth. From the 11th, winds were highly variable with averages of 6 ms^{-1} from 11 to 20 December and less than 5 ms^{-1} until the end of the month. Temperatures gradually dropped to −35°C in late December. No significant variations in pressure were observed during the later part of the month with a range of 990 to 1010 mb.

Early January brought another cyclone with minimum pressure recorded at the ship of 956 mb on the night of the 2nd. Light to moderate southerly winds brought a sharp temperature increase from −30°C to −1°C midday on the 2nd. Winds peaked at 14 ms^{-1} late on the afternoon of the 2nd from the south. Winds stayed from the southerly direction through the early evening of the third. At that time, strong (15 ms^{-1}) northeasterly winds commenced which cooled the air temperature to −25°C. Moderate northerly winds (8 to 12 ms^{-1}) persisted through the 7th when the ship began its transit to Tromso, Norway.
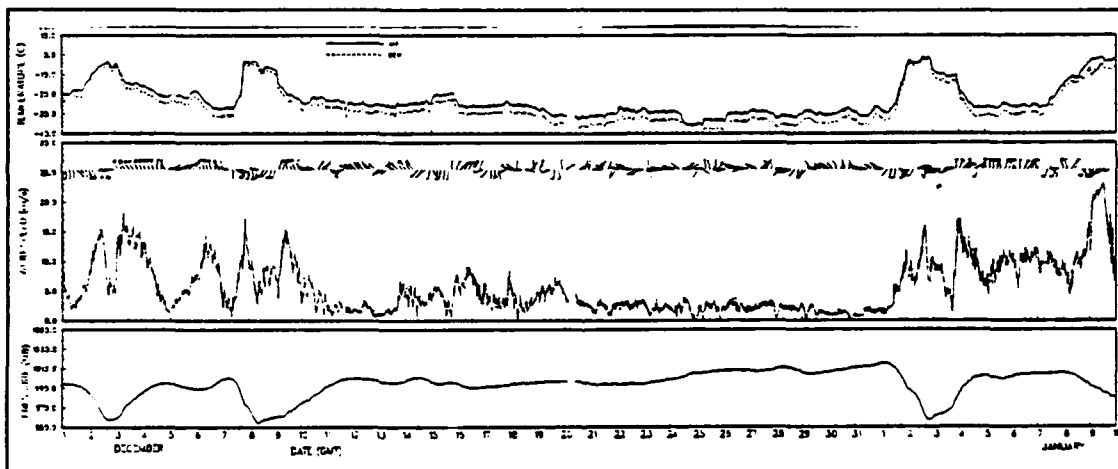
Fig. 34. R/V Polarbjoern time series from 1 December to 10 January

5. Summary

The wind speed at the ship was highly variable ranging from periods of calm to periods with winds as high as 20 ms^{-1}. The higher winds throughout the time period were associated with the passage of Arctic cyclones with moderate southerly winds ahead of the cyclone followed by strong persistent northwesterly winds after passage. The persistence of the north-northwest winds during Phase I steered the ship east of Svalbard. The strong cyclone activity to the east over Novaya Zemlya and ridging over

46

Greenland (illustrated in the ship's November pressure field) explain the ship and ice movement. Climatology suggested that northeast rather than northwest winds would dominate and the drift of the ship was to be southwest, west of Svalbard in Fram Strait.

The air temperatures ranged from 0°C to −35°C, with each month's average temperature decreasing 5 to 7 °C as winter approached. Dramatic temperature rises of 15 to 25°C occurred with the six major cyclone passages during the experiment.

The number of cyclones was significantly higher than what is expected for the climate of the region as evidenced by the 500 mb geopotential height and sea level pressure anomalies for October and December. Most of the significant weather features occurred in October, December, and early January. The storm that formed near the ship early on 12 October will be closely studied and contrasted with the storms that passed on 9 October, 2 and 8 December 1988, and 2 January 1989 along with other minor low pressure systems.

As Serreze and Barry (1988) noted in their climate study, cyclone tracks are subjective. The autumn and early winter period in this study represented a very large variability in both the number and direction of cyclones entering the Arctic basin. Most of the storms during Phase I of CEAREX, except for the cyclogenesis event on 12 October, represented the climatic principle and secondary cyclone tracks. The storms trajectories were very variable and followed the climate studies conducted by Gorshkov (1983) rather than Serreze and Barry (1988) as outlined in Chapter II. Gorshkov (1983) shows a large variability in cyclone trajectories for each month as well as from month to month which were corroborated in this study.

Each cyclones trajectory during the drift phase of CEAREX is illustrated in Fig. 35. All but one of September's cyclones tracked northeast along the west coast of Norway and then east across the southern Barents Sea. A low pressure system on the 20th migrated from the central Arctic basin south over Northeast Land and then southeast to Novaya Zemlya. This is an unusual trajectory for a cyclone. Gorshkov (1983) depicts a secondary cyclone track from north of Greenland within the Arctic basin to southeast Barents Sea in his January and February climatic cyclone charts (Fig. 10c and d). However, even these tracks do not show the cyclone as originating from the central Arctic basin like the 20 September cyclone.
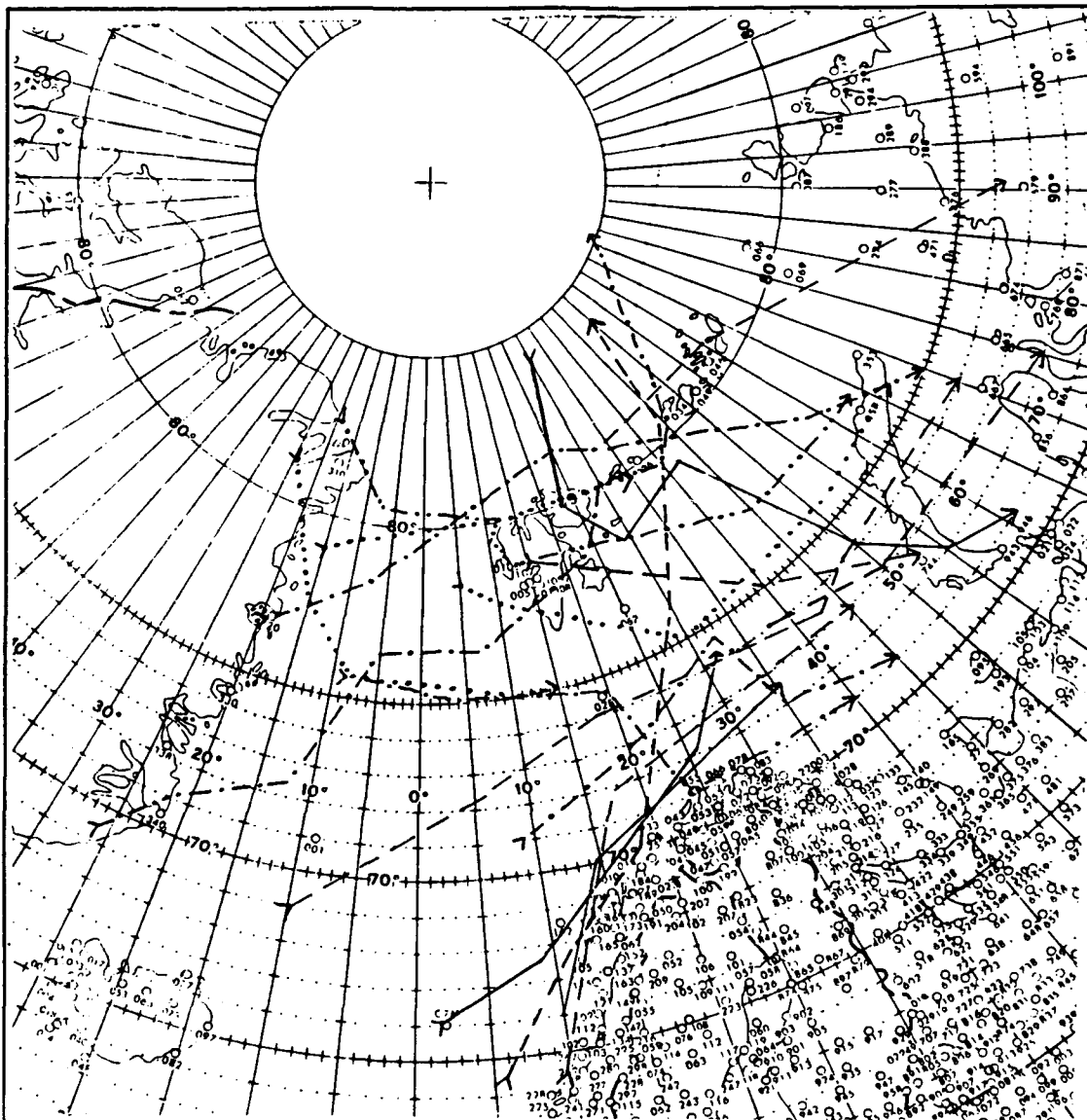
Fig. 35. **Cyclones Tracks for Phase I of CEAREX:** September (solid); October (dashed); November (dotted); December (dot-dash); and January (dot-dot-dash).

The cyclone that passed east of the *R/V Polarbjoern* on 9 October originated from the North Atlantic and moved northeast along the Norwegian coast, then tracked rapidly north-northeast through the Barents Sea and north over Kvitoya. The low pressure system then moved into the central Arctic basin where it slowly migrated in an erratic westward track to northwest Greenland and dissipated. This cyclone track for 9

48

October is typical of both the winter and summer cyclone track for this region from Serreze and Barry (1988) and is depicted in Gorshkov's (1983) September through January tracks as presented in Chapter II. Except for the cyclogenesis that occurred over the *R/V Polarbjoern* on the 12th, October's cyclones stayed south of 75°N. This correlates very well with climate studies which depict cyclones tracking northeast through the Norwegian Sea and then east through the southern Barents Sea. The strengthening circumpolar vortex during the fall to its winter maximum steers cyclones south of the central Arctic basin and south of 75°N.

The cyclone on 2 December tracked from northeast Greenland southeast across the Greenland Sea, Fram Strait, Svalbard, then southeast to Novaya Zemlya. This trajectory is very similar to The climatic cyclone track for January and February as depicted by Gorshkov (1983) in Fig. 10c and d. On 8 December, a cyclone originating from southeast Greenland tracked northeast into the Greenland Sea and then to Svalbard. From Svalbard, the cyclone moved into the Arctic basin where it stagnated and filled. This trajectory is well documented by Serreze and Barry (1988) and Gorshkov (1983) as being a major cyclone track. Similar to the cyclone on 2 December, the cyclone on 2 January 1989 tracked from northeast Greenland southeast over Svalbard and to Novaya Zemlya. This track mirrors the climate cyclone track for January and February depicted in Gorshkov (1983) Fig. 10c and d.

Only two of the five cyclones (9 October and 8 December) moved into the central Arctic basin as depicted in the Serreze and Barry climate study of the Arctic. Two of the storms (2 December and 2 January) entered the Arctic basin above 80°N but then tracked southeast to Novaya Zemlya. The cyclone on 12 October entered the Arctic basin for several days but then tracked southeast to Novaya Zemlya similar to the cyclones on 2 December and 2 January. One cyclone on 20 September tracked opposite of the other cyclones, out of the central Arctic basin and then southeast to Novaya Zemlya.

The synoptic patterns that occurred during Phase I correlate very well with the surface pressure patterns and cyclone trajectories described by Gorshkov (1983) and illustrated in Fig. 11a-c. These are Gorshkov's autumn-winter synoptic patterns that persist 40% of the time in the fall and early winter. Other patterns (Fig. 11d-f) did occur but less than 20% of the time in agreement with Gorshkov (1983).

C. TEMPERATURE INVERSIONS

Vertical profiles of potential temperature, potential dewpoint, and wind speed and direction were obtained from *R/V Polarbjoern* rawinsonde launches and were analyzed with regard to inversion properties. Inversions were identified in greater than 95% of the rawinsonde profiles. The temperature inversions were studied and compared to the climatology of the region. Results are summarized in Table 2 according to percent of inversion cases. An example of each inversion type during Phase I is illustrated in Fig. 36. The multiple inversion, mixed layer below inversion, and stable layer below inversion types represent upper level inversions. An interesting outcome of this data set is that the results differ significantly from those found by Vowinckel and Orvig (1970) which were described in Chapter II, Section A.4. Their findings for surface and upper level inversions are summarized in Table 3.

Table 2. INVERSION TYPE AND FREQUENCY DURING PHASE I

Month	Surface-based Inversions (%)	Multiple Inversions (%)	Mixed Layer Below Inversion (%)	Stable Layer Below Inversion (%)
September	20	30	40	10
October	24	25	56	4
November	22	7	53	15
December	21	21	31	16

Table 3. FREQUENCY OF INVERSIONS SUMMARIZED FROM VOWINCKEL AND ORVIG DATA

Month	Surface Inversion (%)	Upper Level Inversion (%)
September	38	42
October	55	40
November	78	17
December	72	25

The incident of surface-based inversions did not occur nearly as often in this study as reported by Vowinckel and Orvig (1970). An increase percentage of surface inversions toward winter did not occur as noted in their study. From October to December, the

SPECIFIC HUMIDITY G/KG
0 1 2 3 4

ALTITUDE M

10000
9000
8000
7000
6000
5000
4000
3000
2000
1000
0

-40 -30 -20 -10 0 10 20 30 40 50 60
POTENTIAL TEMPERATURE °C

5 NOV 1989 1100 GMT POLARBJOERN
LAT 80°47'N LONG 35°14'E **a**

SPECIFIC HUMIDITY G/KG
0 1 2 3 4

ALTITUDE M

10000
9000
8000
7000
6000
5000
4000
3000
2000
1000
0

-40 -30 -20 -10 0 10 20 30 40 50 60
POTENTIAL TEMPERATURE °C

1 DEC 1989 2240 GMT POLARBJOERN
LAT 79°53'N LONG 31°13'E **b**

SPECIFIC HUMIDITY G/KG
0 1 2 3 4

ALTITUDE M

10000
9000
8000
7000
6000
5000
4000
3000
2000
1000
0

-40 -30 -20 -10 0 10 20 30 40 50 60
POTENTIAL TEMPERATURE °C

14 DEC 1989 1055 GMT POLARBJOERN
LAT 78°47'N LONG 31°30'E **c**

SPECIFIC HUMIDITY G/KG
0 1 2 3 4

ALTITUDE M

10000
9000
8000
7000
6000
5000
4000
3000
2000
1000
0

-40 -30 -20 -10 0 10 20 30 40 50 60
POTENTIAL TEMPERATURE °C

23 NOV 1989 1040 GMT POLARBJOERN
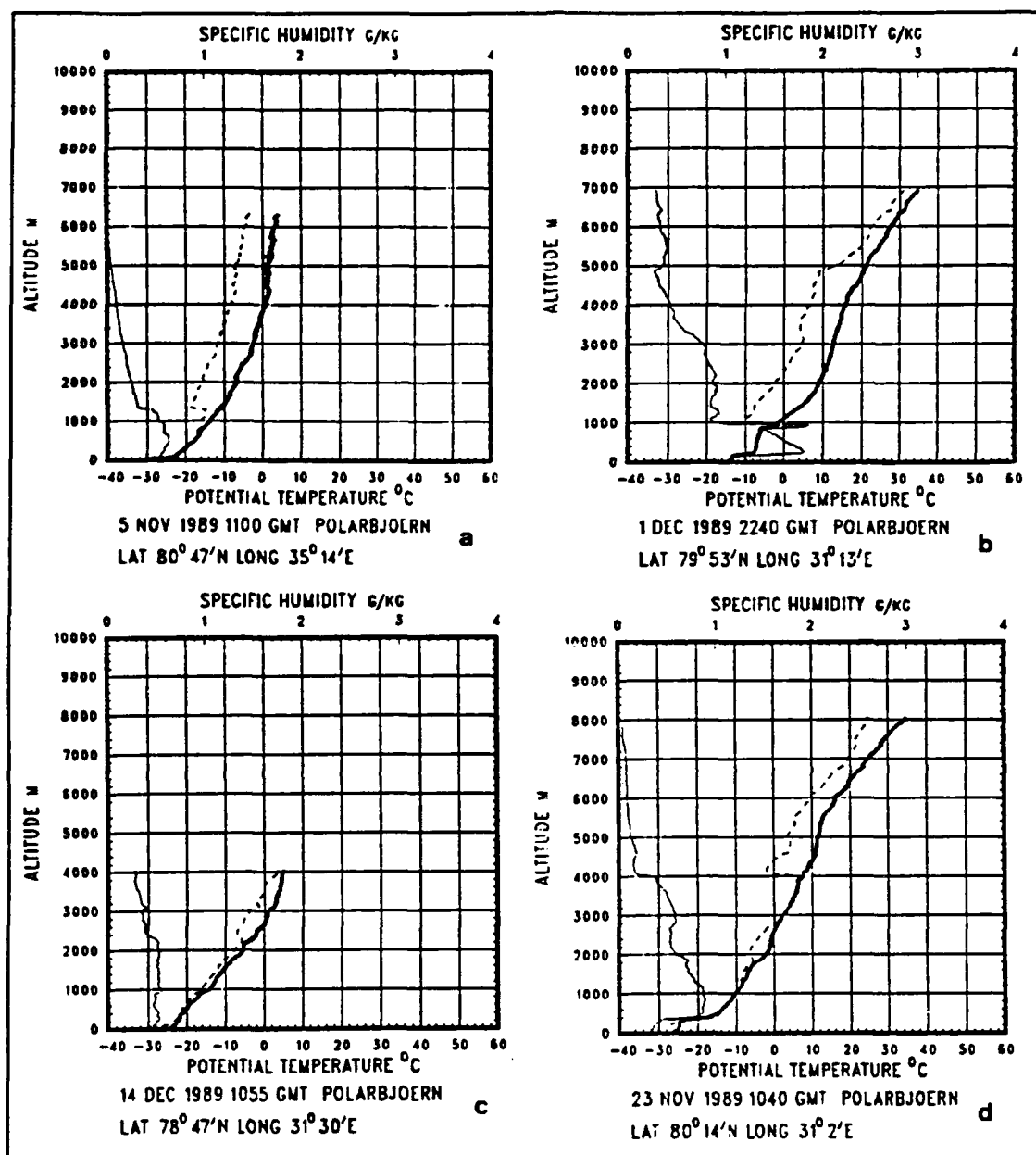LAT 80°14'N LONG 31°2'E **d**

Fig. 36. **Examples of Inversion Types during CEAREX:** (a) surface inversion; (b) multiple inversion; (c) stable layer below inversion; and (d) well mixed layer below inversion.

upper level inversions dominated surface inversions by a factor of four. This is in sharp contrast to Vowinckel and Orvig results which found that the percentage frequency of

51

surface and upper level inversion were nearly the same in October. Then the percentage frequency of surface inversions increase relatively during the fall until December when the percentage frequency of surface inversion is three times that of the upper level inversions.

November and December are the months most inconsistent with their study. This could be accounted for by several different factors. The *R/V Polarbjoern* was not located over the central Arctic basin as the study's results were. The *R/V Polarbjoern* was instead located on the eastern side of Svalbard on an ice flow that was moving south and in close proximity to the MIZ and the open ocean. The second factor is that two cyclones tracking through the region in December are an unusual occurrence for central pack ice and this could be an important factor in the small percentage of the surface-based inversion frequency for December. The strong winds and warm air advection could destroy surface-based inversions. Typically, a very large and stable pool of air sits over the central Arctic basin which accounts for the large number of surface-based inversions that should occur. East of Svalbard, a very strong surface temperature gradient is present as discussed in Chapter II and any moderate winds could easily advect warmer air into the region near the MIZ potentially destroying a surface inversion.

The next chapter will present two case studies. The first case study covers the intense storm that occurred over the *R/V Polarbjoern* on 12 October 1988. The second case study deals will a boundary layer front that formed in Fram Strait on 10 October 1988 and later evolved into a polar low.

IV.   CASE STUDIES

Results from analyses of two meteorological events are presented in this chapter. In the first case study, cyclogenesis over the R/V Polarbjoern on 12 October is compared with different cyclones tracks over the eastern Arctic ocean from September to January. Although there are only a small number of reporting land stations in the vicinity of the R/V Polarbjoern, the deployed drifting buoys and the available satellite imagery allowed the detection of cyclogenesis in the region. Cyclogenesis over the pack ice northeast of Svalbard is an unusual occurrence and not depicted in Arctic climate studies.

The second case study described a boundary layer front and polar low development and was selected to compare with studies conducted during MIZEX experiments and the Arctic Cyclone Expedition. Experiments were not being conducted in Fram Strait during the second case study, but satellite imagery available for the drift phase of CEAREX provided the necessary information for analyzing the boundary layer front and its evolution into a polar low on 10 October in Fram Strait. Fett (1990) assisted in the interpretation of cloud features and streamline analysis in the satellite imagery for both studies.

A.   CYCLOGENESIS EVENT OVER R/V POLARBJOERN (12 OCTOBER 1988)

Mesoscale analysis of the meteorological conditions will be presented for the region between Svalbard and Franz Joseph Land. Redrawn surface analyses were made using surface data from deployed buoys, observations from the R/V Polarbjoern, land and ship observations, satellite imagery, and NMC and NOGAPS global surface analyses. The times of the DMSP mosaics represent the swath closest to Svalbard.

1.   Cyclogenesis Event

The DMSP satellite mosaic for 112320 UTC October (Fig. 37) suggests a low level frontal zone extending south from the Arctic basin north of Svalbard then southwest over the Norwegian Sea. This surface frontal zone is also depicted on the NMC hand analyzed surface analysis for 120000 UTC. The NMC (not shown) surface analysis shows low level circulation north of Svalbard which is not evident on satellite imagery. Surface stations in the vicinity are reporting convective activity with rain and snow showers along the frontal zone. The NOGAPS 500 mb analysis for 120000 UTC (Fig. 38) shows a short wave trough extending south over Fram Strait and the Norwegian Sea.
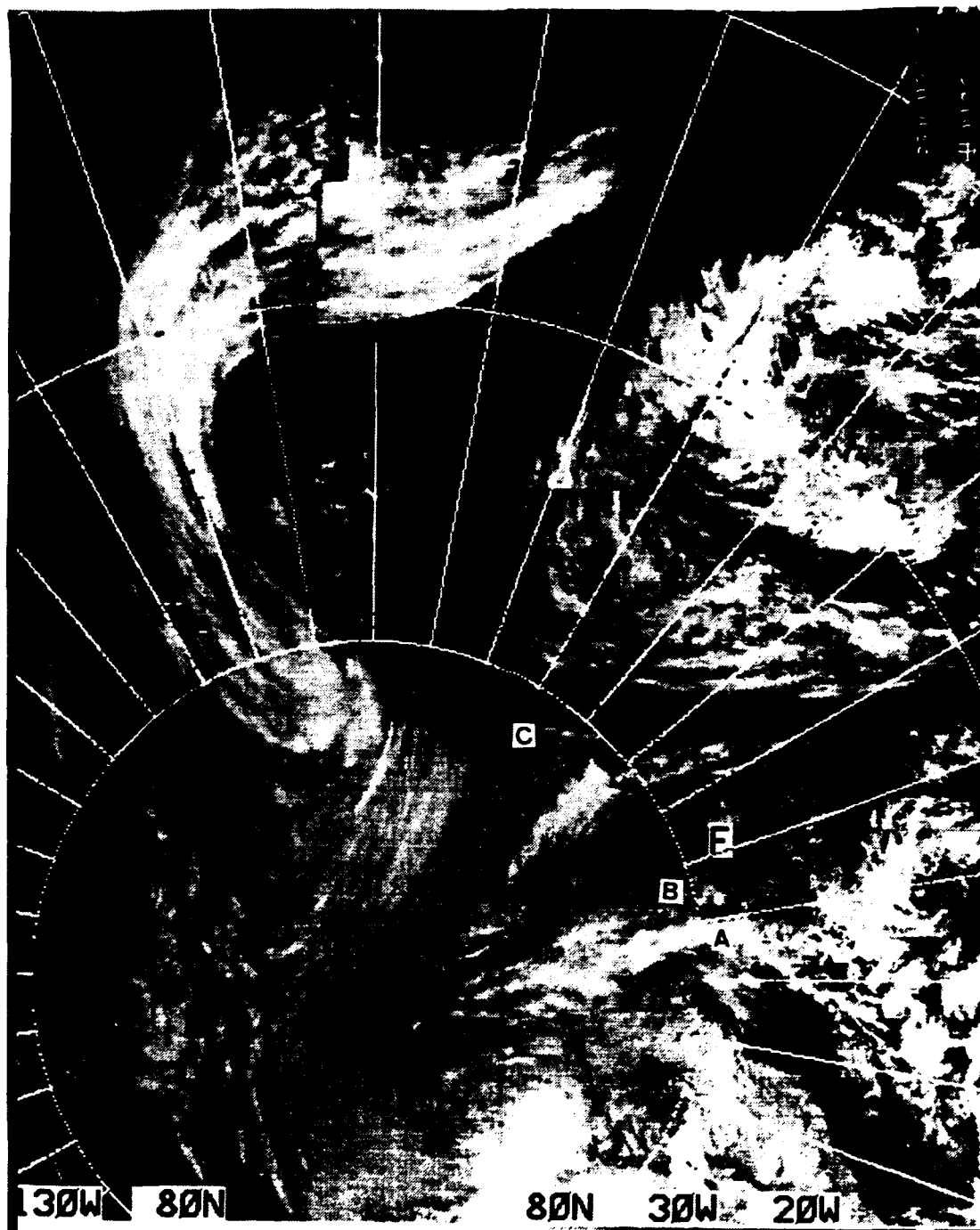
Fig. 37.   DMSP satellite mosaic for 112320 UTC October 1988:   A denotes the
location of Spitzbergen, B is Northeast Land and C is Franz Joseph Land.
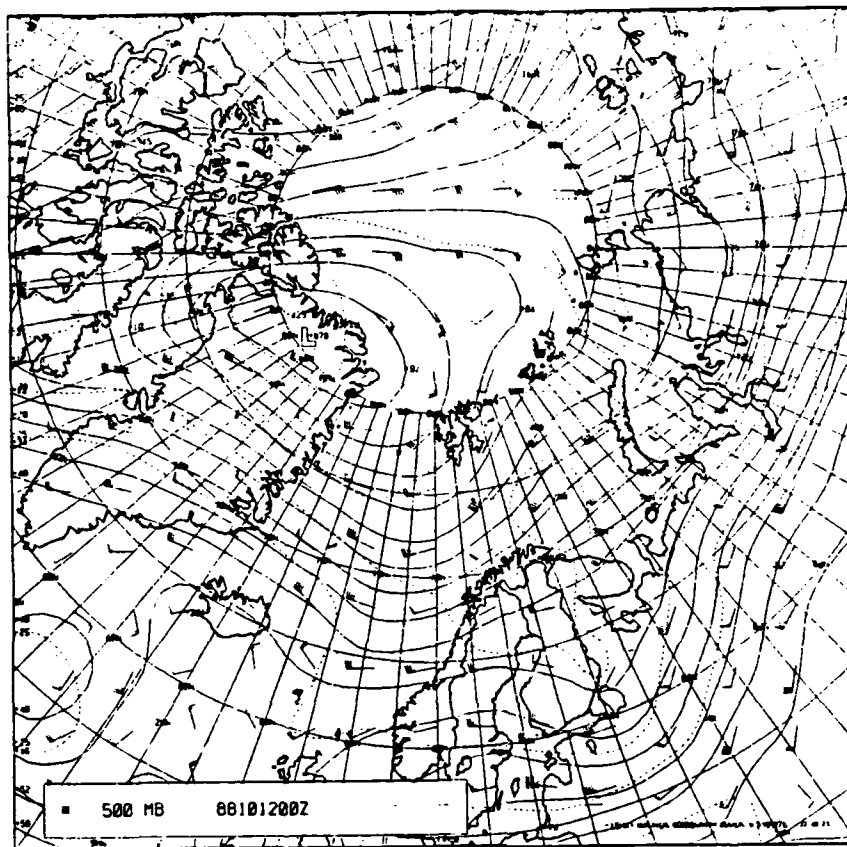
Fig. 38.   NOGAPS 500 mb analysis for 120000 UTC October 1988

On the DMSP satellite mosaic at 120828 UTC (Fig. 39) and NOAA-10 satellite image at 121012 UTC October (Fig. 40) the formation of a "baroclinic leaf" cloud pattern is evident north and east of Svalbard. The "leaf" is oriented north-south in the DMSP mosaic (Fig. 39) and located on the forward side of the 500 mb trough located in Fram Strait. Less than two hours later the "baroclinic leaf" cloud pattern (Fig. 40) has rotated slightly counterclockwise as described by Weldon (1979). The ragged edges at the northeast end are readily seen as well as the presence of low clouds at the tail end. Upper level cloudiness southeast of the 500 mb jet is present as was the case on the example of a "baroclinic leaf" in a high amplitude trough (Fig. 14) presented in Chapter II. Any low level development at this time is obscured by the high level clouds.

55

Fig. 39.   DMSP satellite mosaic at 120828 UTC October 1988
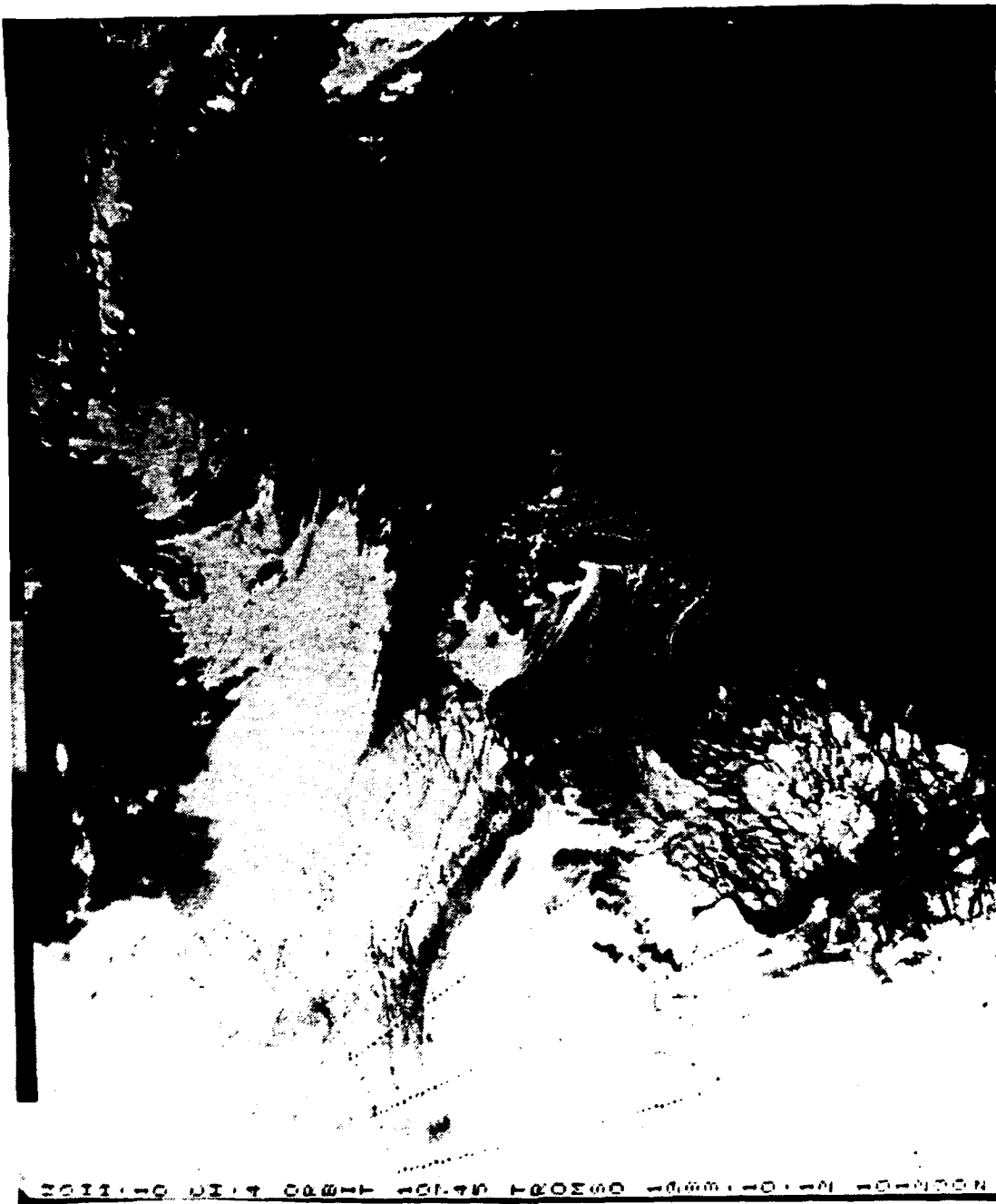
Fig. 40.   NOAA-10 satellite image for 121012 UTC October 1988

NOGAPS 500 mb analysis for 121200 UTC (Fig. 41 on page 58) depicts a low height center over northern Greenland with a troughing extending southeast then south over Fram Strait and the Norwegian Sea.   Maximum 500 mb winds lie upstream of the

57

"baroclinic leaf" in confluent flow. Decreasing winds in difluent flow are downstream of the cloud pattern (Fig. 41). NOGAP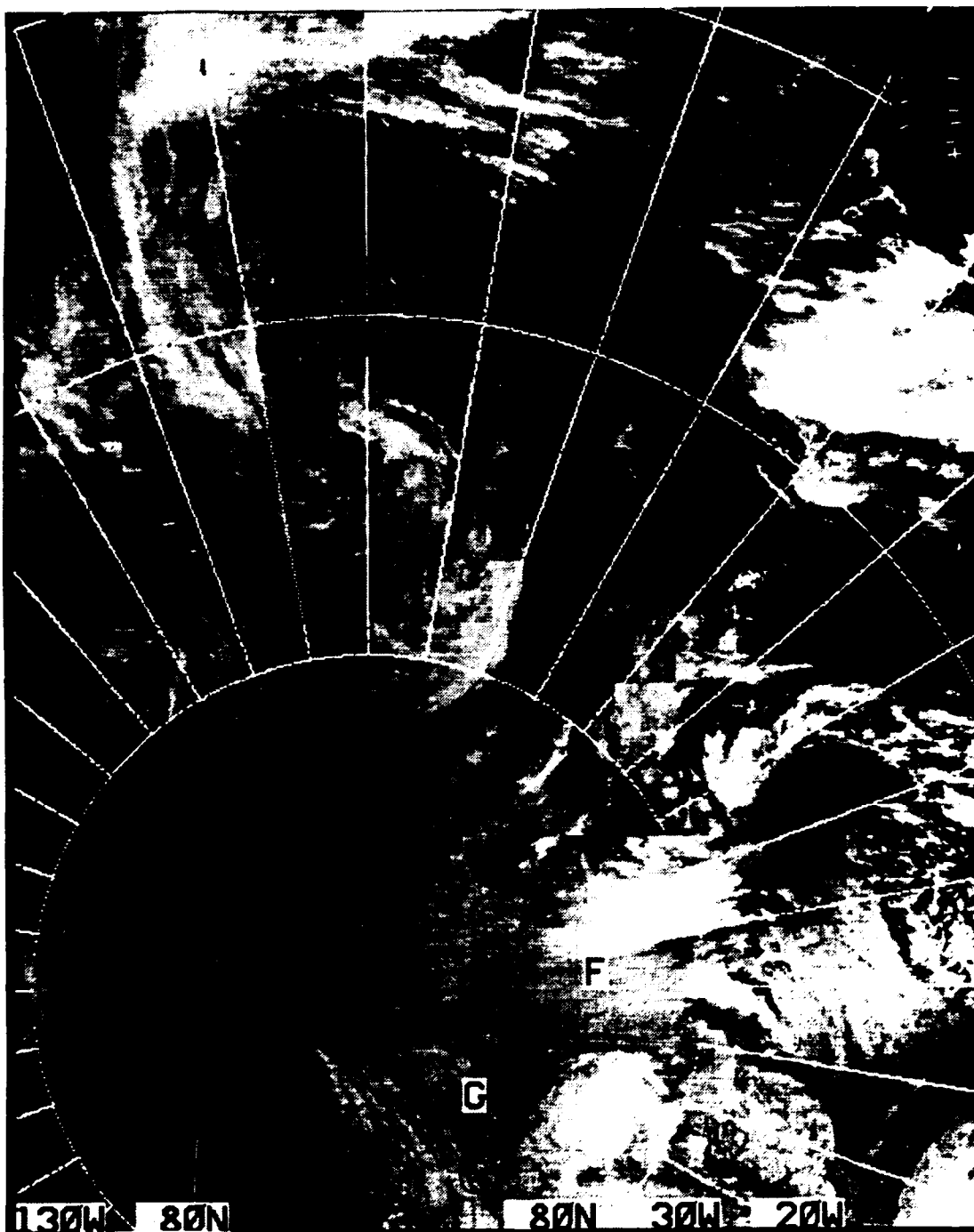S 850 mb analysis (not shown) shows moderate warm air advection at 111200 UTC with strong warm air advection occurring from 120000 UTC through 121200 UTC. Surface reports from 120000 UTC to 121200 UTC indicate continued convective activity along the surface frontal zone. Snow is falling at the R/V Polarbjoern which is located directly under the "leaf" system.
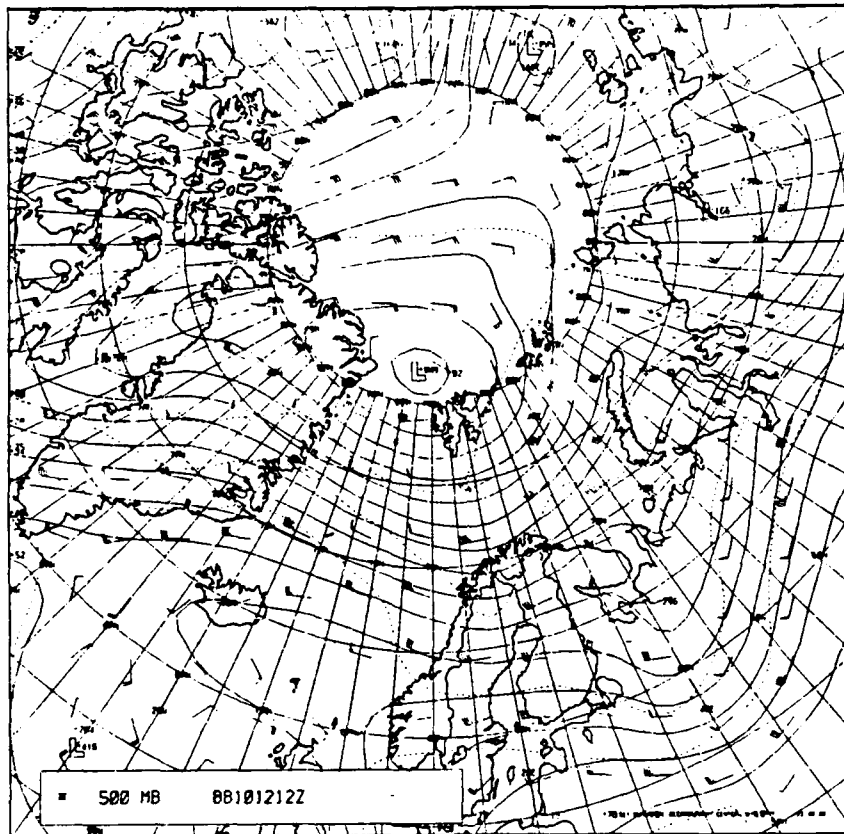
Fig. 41.   NOGAPS 500 mb analysis for 121200 UTC October 1988

The positions of the buoys and the R/V Polarbjoern for October 10th and 20th are shown in (Fig. 42). Time series of temperature and pressure for each buoy are presented in Fig. 43. Between 111800 UTC and 120000 UTC, the three southernmost drifting buoys (Fig. 43b) experience sharply rising temperatures which reach their peak between 06 UTC and 18 UTC on the 12th in the strong low level warm advection from the south. Buoy number four, located furthest west, showed a 10°C lower temperature minimum than the other buoys except for buoy number one which has a difference of 5°C. The three northernmost buoys (Fig. 43a) reached their temperature maximum at

a later time, between 1200 UTC and 1800 UTC on the 12th, except for buoy number one. This buoy, located farthest northwest over the ice pack, reached its maximum temperature at 06 UTC and was 5°C colder than all the buoys except for buoy number four, also located on the western side of the buoy array.
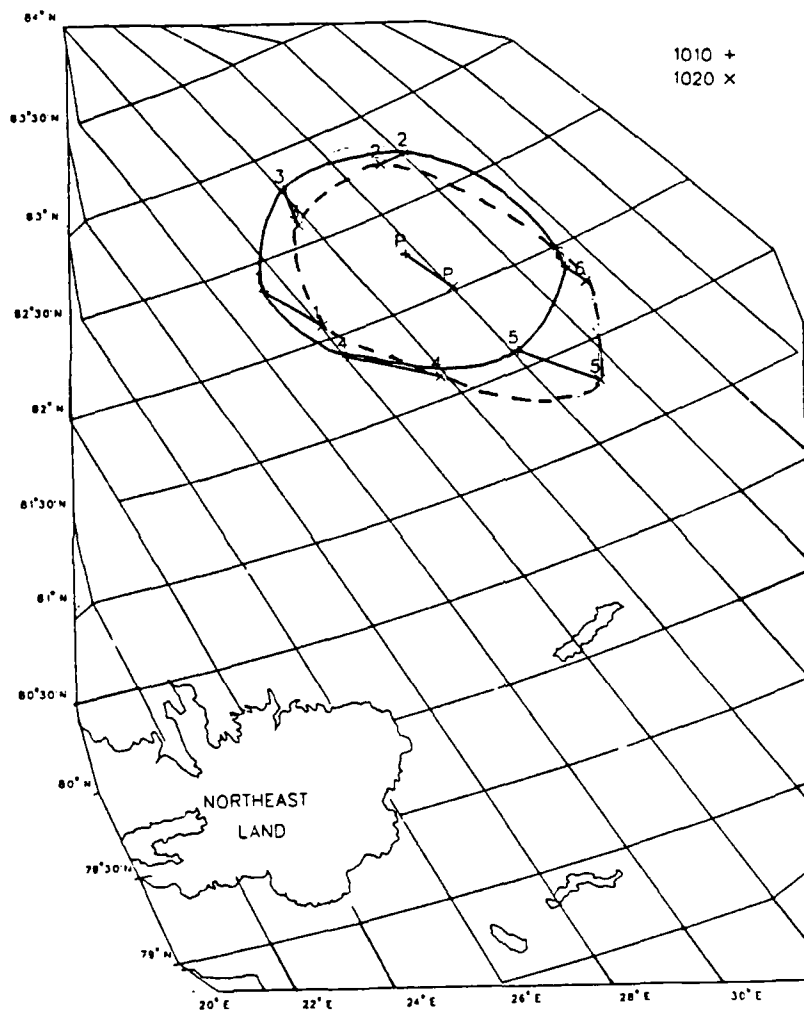
Fig. 42.   R/V Polarbjoern and buoy positions for October 1988

59
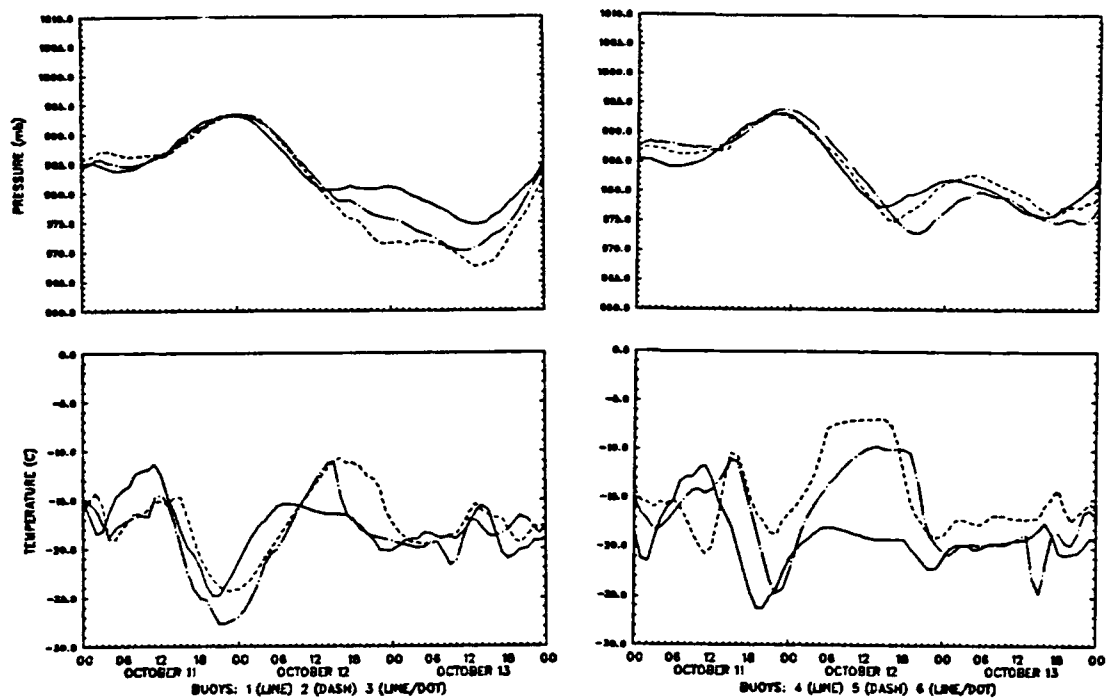
Fig. 43. Pressure and temperature time series for drifting buoys

Low level cyclonic circulation becomes evident on the 121200 UTC October redrawn surface analysis (Fig. 44). At 121500 UTC, surface pressures are still falling at the drifting buoy positions and at the ship. Winds at the ship indicate that the low pressure center is forming southwest of the ship. Temperatures at all buoy locations and at the ship are still increasing at this time.
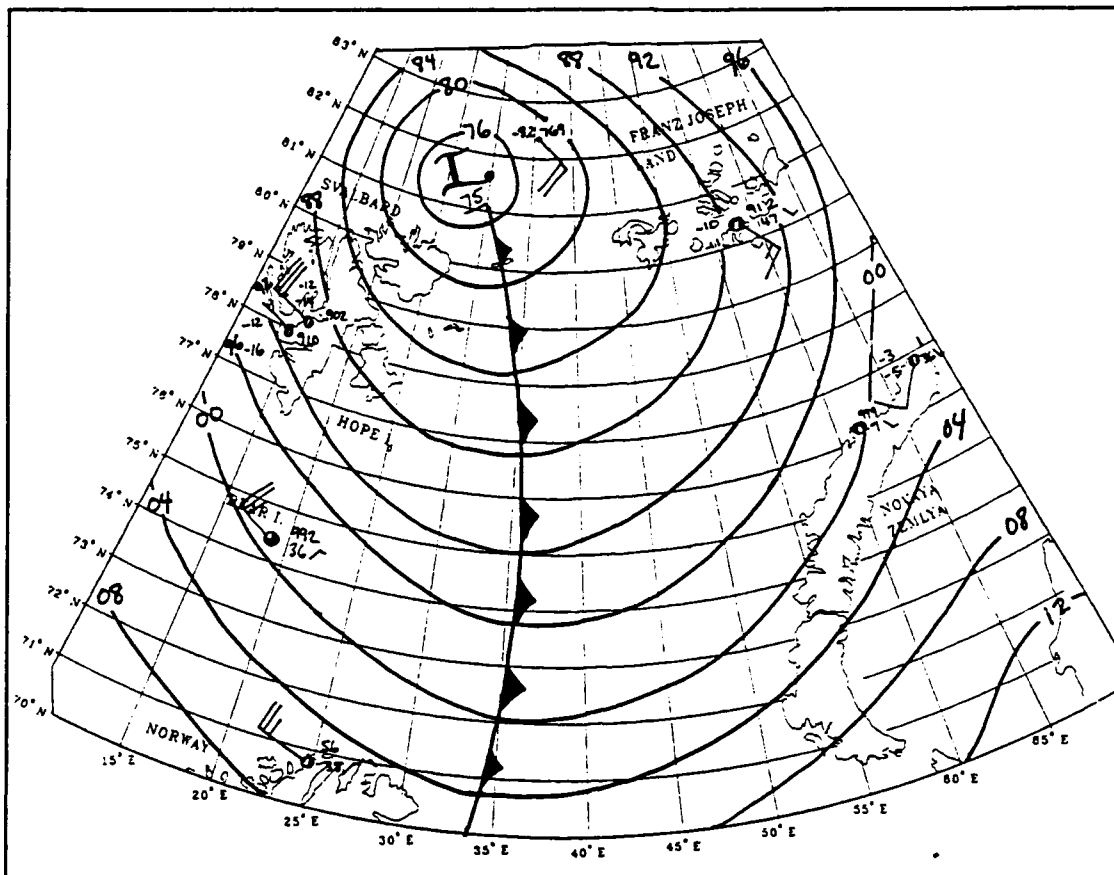
Fig. 44. Surface analysis for 121200 UTC October 1988

Winds at the *R/V Polarbjoern* back from southwest to northwest and increase from 8 to 20 *ms⁻¹* from 1500 UTC to 1800 UTC. The ship's time series plot from 10 to 17 October (Fig. 45) illustrate this sharp wind shift, both in direction and speed. Temperatures at the ship and the buoy locations begin to sharply decrease in the low level cold air advection from strong northwesterly winds. The cyclone deepens from 975 mb to 967mb from 121200 UTC to 121800 UTC. The surface analysis at 121800 UTC (Fig. 46) shows the cyclone position northeast of the ship and the resulting surface wind field. Snow is falling heavily at the ship and convective activity continues to occur in the frontal zone. The surface low pressure system is not discernable on the DMSP satellite mosaic at 122310 UTC due to the presence of the high level cloudiness.

61
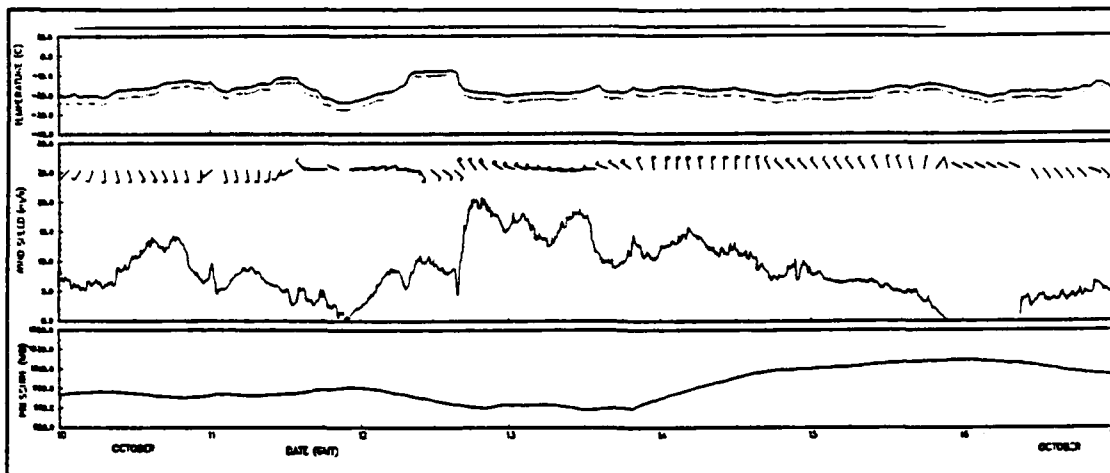
Fig. 45.   Time series of observations for R/V Polarbjoern (10-17 October) (from Lackman et al. 1989)
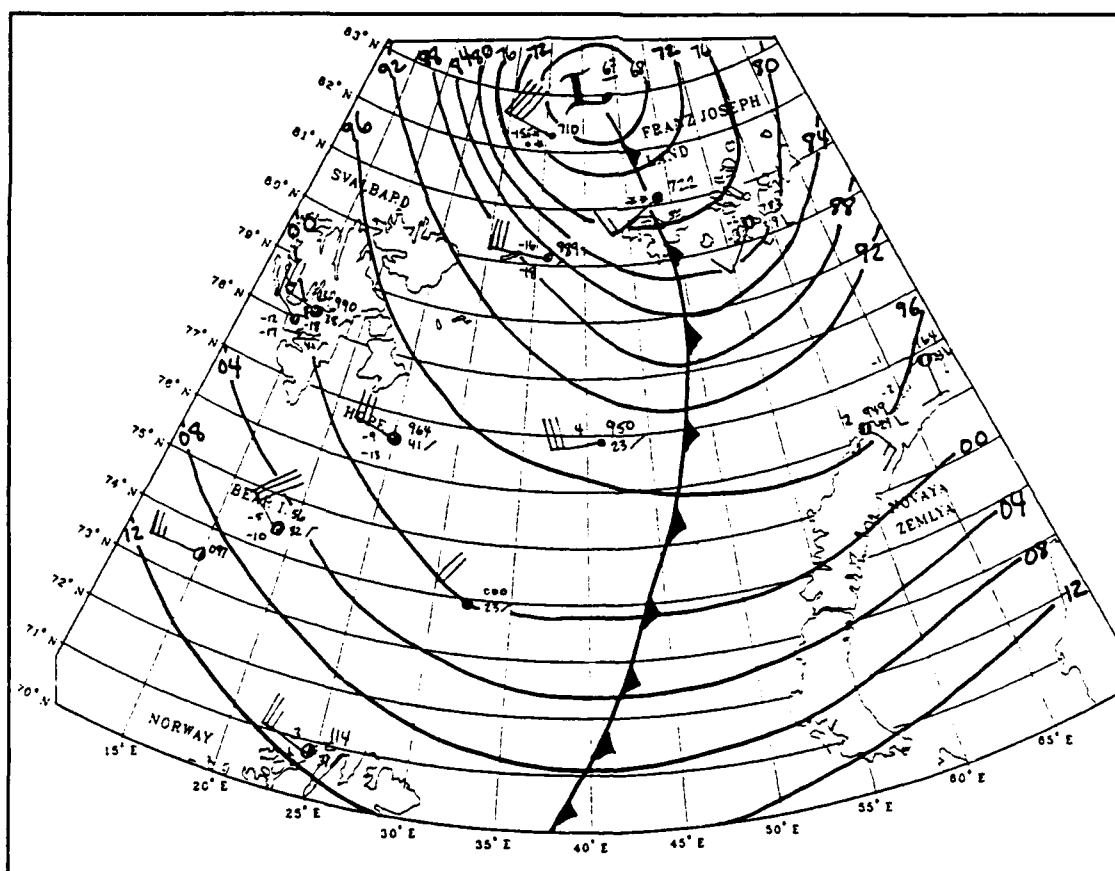
Fig. 46.   Surface analysis for 121800 UTC October 1988

NOGAPS 500 mb analysis at 130000 UTC October shows a 5903 m low height center north of 80°N between Svalbard and Franz Joseph Land (Fig. 47). At this time NOGAPS analyses at 500, 700, and 850 mb, and the surface indicate that the cyclone is now fully vertically-developed. The redrawn surface analysis at 130000 UTC October (Fig. 48) positions the cyclone north of the NOGAPS surface analysis.
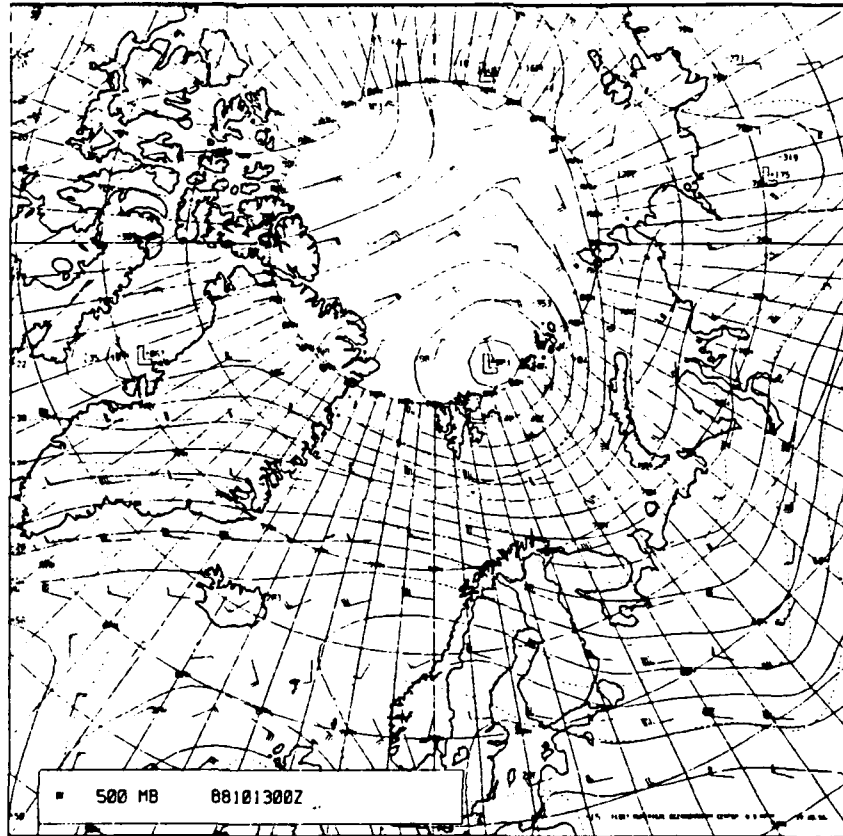
Fig. 47.   NOGAPS 500 mb analysis at 130000 UTC October 1988
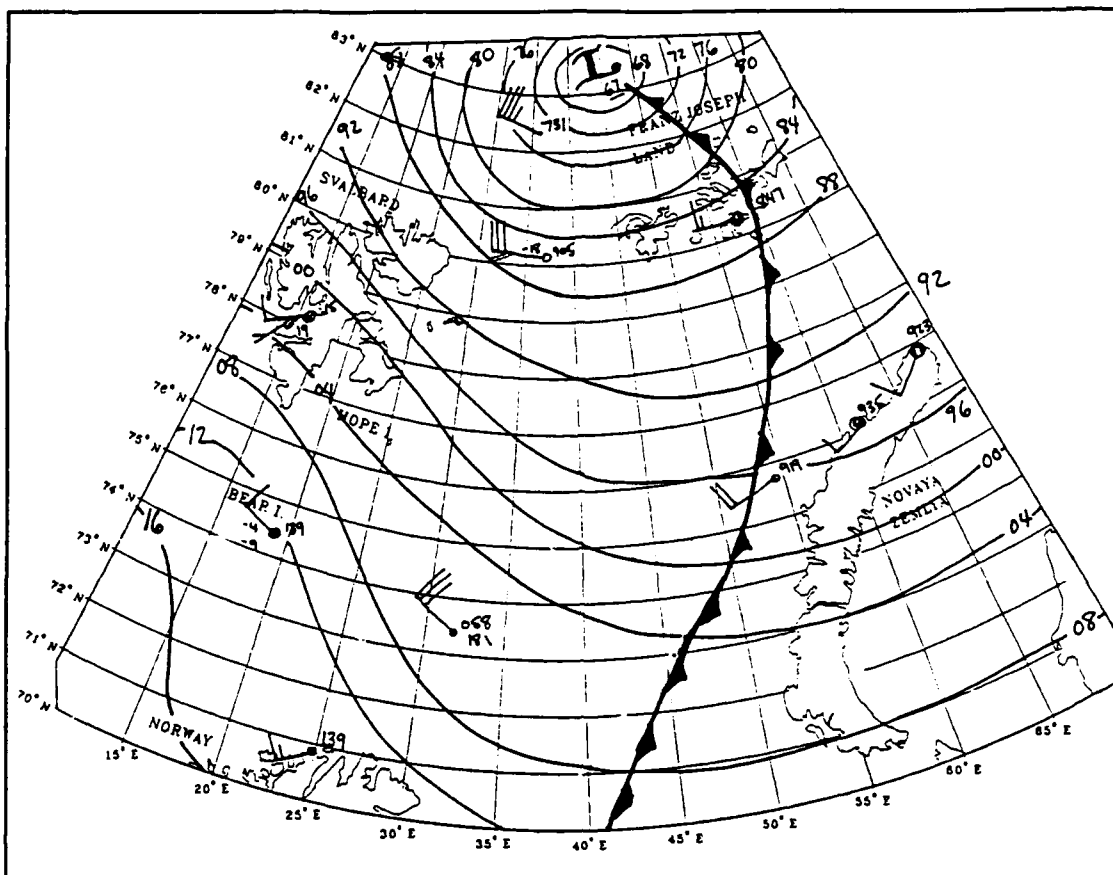
Fig. 48.   Surface analysis at 130000 UTC October 1988

The low pressure system remains steady at 967 mb and quasi-stationary north-east of the *R/V Polarbjoern* from 121800 UTC to 131200 UTC. By 131800, the cyclone drifts slowly south, east-northeast of the ship and the central pressure begins to rise as depicted on the 131800 UTC surface analysis (Fig. 49). The pressure at the ship was considered too low and was disregarded. The ship's surface pressure was consistently lower than the array of buoys throughout the experiment. At this time, the surface buoys were reporting surface pressures of 974 to 978 mb. NOAA-10 satellite image at 130950 UTC (Fig. 50) shows a well developed comma shaped cloud pattern located northeast of Northeast Land. A clear cold dry slot of air is beginning to wrap around the vertically developed low pressure system.
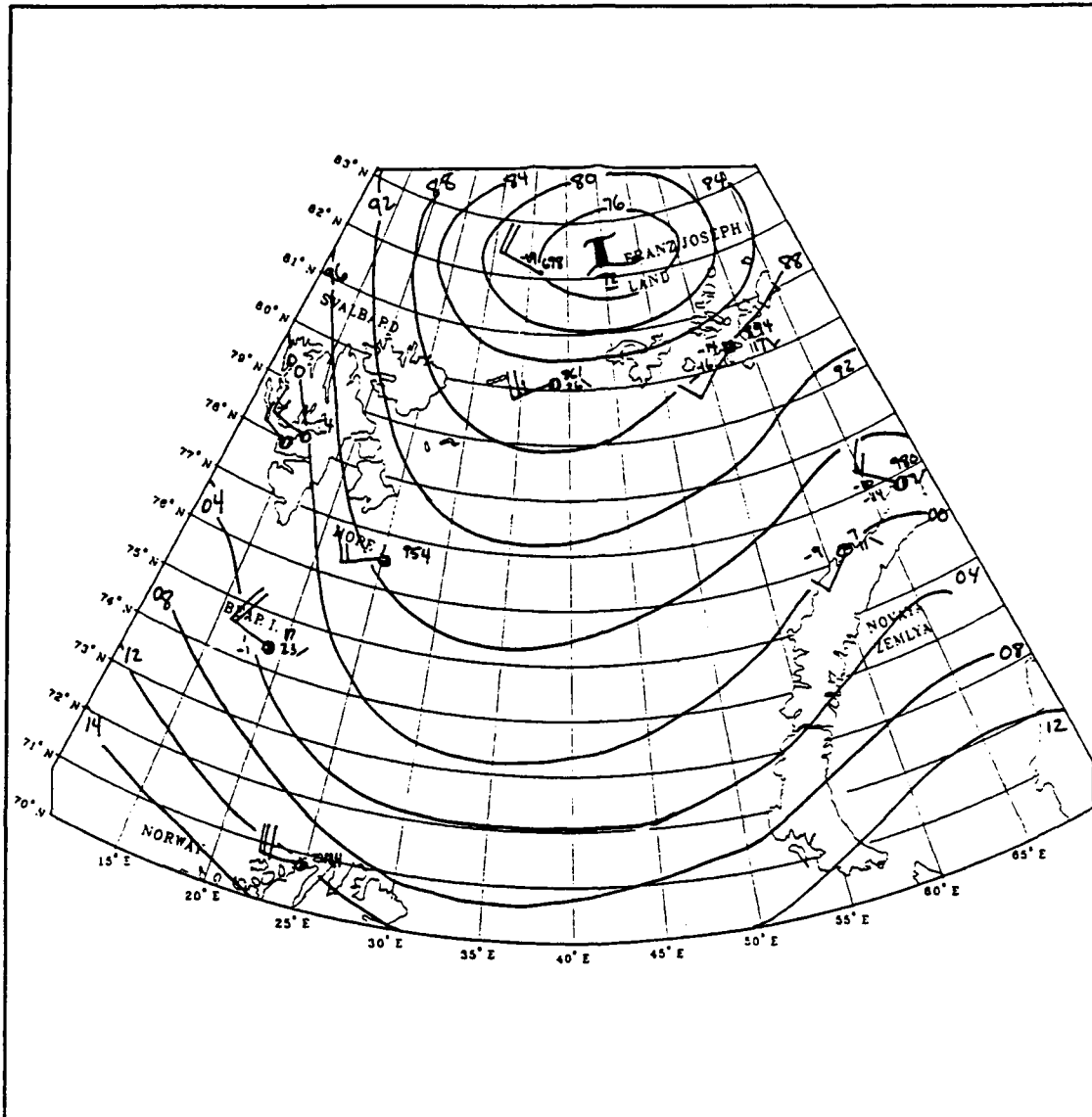
Fig. 49. Surface analysis for 131800 UTC October 1988

Fig. 50.   NOAA-10 satellite image at 130950 UTC October 1988

NOGAPS 500 mb analysis shows a low height center over Franz Joseph Land at 131200 UTC (Fig. 51). The low height center remains quasi-stationary and slowly starts to fill as indicated by rising surface pressures from 131800 UTC to 140000 UTC (not shown).

DMSP satellite mosaic at 132240 UTC (Fig. 52) shows cloud bands beginning to weaken and become disorganized as the cold air is being entrained into the center of the low pressure system. By 140749 UTC, DMSP mosaic (Fig. 53) suggest that the cold dry air that is being wrapped around the core of the low pressure system. The cyclone has tracked slowly east and is still filling. Winds at the ship decreased to below 10 ms^{-1} by 141800 UTC and precipitation ceased.
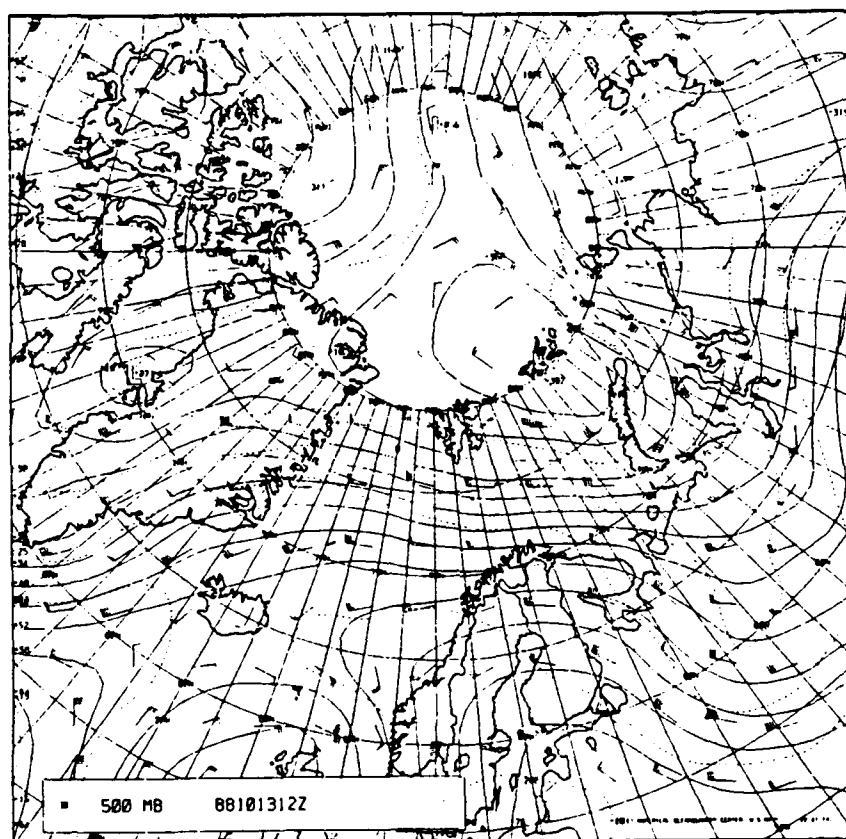
Fig. 51.   NOGAPS 500 mb analysis for 131200 UTC October 1988

Fig. 52.   DMSP satellite mosaic at 132240 UTC October 1988
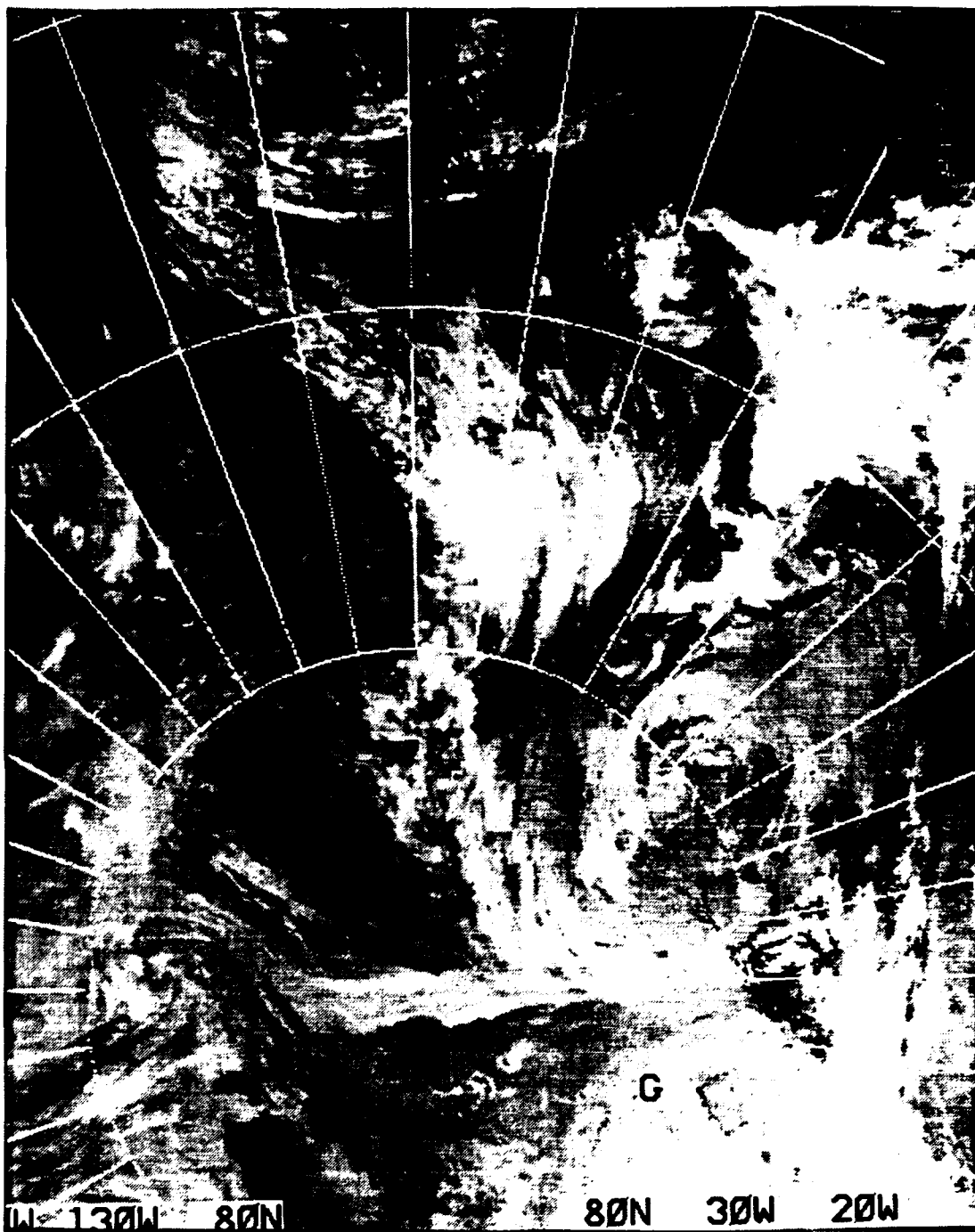
Fig. 53. DMSP satellite mosaic at 140749 UTC October 1988

69

2. Summary and Conclusions

The development of the cyclone on 12 October in a "baroclinic leaf" cloud system was detected through satellite imagery. Cyclogenesis over the Arctic ice pack is not evident in most of the Arctic climate studies (Serreze and Barry 1988; Sater et al 1971; and Sechrist et al. 1989). This is undoubtably associated with lack of data. Only Gorshkov (1983) shows a cyclogenesis region over the Barents Sea in February which may or may not be ice covered. The track from this cyclogenesis region is southeast, which is the track the 12 October cyclone takes on the 14th and 15th of October to north U.S.S.R. Gorshkov also depicts cyclogenesis near the North Pole, over central pack ice with the cyclone then moving east as did the 13 October cyclone.

The significant difference is October is that an anticyclone did not persist over the northern Arctic basin near the U.S.S.R. This accounts for the lower anomalous sea level pressures and low heights correlated for the month of October in that region. The 500 mb geopotential heights and 1000-500 mb thickness charts illustrate the lower heights and colder temperatures than average for October. The lower heights and colder temperatures over the central Arctic and the higher heights over Greenland set up a stronger temperature and pressure pattern gradient in the vicinity of Svalbard, Norwegian and Barents Seas for October which led to higher than average cyclone activity. The significantly lower heights north of 80°N. between Svalbard and Franz Joseph Land, in combination with the weaker circumpolar vortex set up a strong baroclinic zone in the Barents Sea that supported vigorous cyclogenesis. The "baroclinic leaf" represents an area where a baroclinic zone is forming or intensifying. This correlates well with the sharp temperature gradients in the vicinity of Svalbard where cyclogenesis occurred.

Although the 12 October cyclone developed over the Arctic ice pack, the strong southerly winds in advance of the upper level trough over Fram Strait brought warm moist air to the vicinity of the ship. The warm moist air being advected into the region in combination with the cold pool of air moving south towards the ship over the pack ice, created a strong baroclinic zone formation as indicated by the presence of the "baroclinic leaf". A "baroclinic leaf" does not always evolve into a well vertically developed low pressure system and the resultant classic comma cloud (Weldon 1979). It is proposed that the availability of warm moist air from open water in the Barents Sea had the most influence on the rate of surface cyclogenesis. Although no rawinsondes were launched during the cyclogenesis event, temperature increases of 15 to 20 °C at the buoy and at the ship over a relatively short time period indicates the presence of a warm

maritime air mass which did not modify or lose much of it's moisture as it moved north over the ice pack. The 500 mb winds upstream were extremely strong. A strong low level front also existed with convective activity along its frontal position. The "leaf" formed in a 500 mb trough moving slowly east across Greenland Sea and Fram Strait bring positive vorticity advection. Strong warm air advection from the surface to 850 mb played a crucial role in stretching the column of air over the region producing upward motion and increased vorticity. Strong convective activity, which is unusual for the Arctic is occurring in the vicinity.

Although the cyclogenesis on 12 October was an infrequent event, cloud patterns like the "baroclinic leaf" can be indicative of much more dynamic conditions occuring than indicated by surface reports and global analyses. Especially in the Arctic, where data is sparse and the input to the models is much less abundant than at mid latitudes, cloud patterns must be closely studied.

B. BOUNDARY LAYER FRONT AND POLAR LOW DEVELOPMENT

1. Overview

This section describes the formation on 10 October 1988 of what has interpreted to be a boundary layer front on which a polar low formed. The analysis is based primarily on satellite imagery and NOGAPS upper level pressure, wind, and temperature fields. There are few land reporting stations on Svalbard and the northeast coast of Greenland, however, they are not sufficiently close to the formation location of the front for significant contribution. The front was clearly visible on DMSP and NOAA satellite imagery.

NOGAPS 500 mb analysis at 100000 UTC October shows a 5775 meter low height center north of 80°N between Greenland and Svalbard. A deep trough extends southward over Fram Strait and into southern Norway. The low height center remains under constant pressure and moves westward, north of Greenland by 110000 UTC. A weaker upper level trough then becomes established over the east coast of Greenland. At 850 mb, warm air is being advected into Fram Strait from southwest winds over the Norwegian Sea. West-northwest flow from Greenland ice sheet and the Arctic ice pack is maintaining cold air flow into the Greenland Sea.

2. Satellite Imagery and Streamline Analysis

NOAA 10 satellite image at 100915 UTC (Fig. 54) shows a well defined line of convective activity in the Greenland Sea, east of the MIZ. Northerly flow turns anticyclonically in the northern portion of the neutral point then sharply cyclonic

around the northern edge of the boundary layer front. Winds from east Greenland are converging into the front and producing multiple vortices. A broad area of stratocumulus clouds are pre. ~?t in Fram Strait. Svalbard is reporting moderate southerly winds and lowering pressure as a small vortex is seen forming over Spitzbergen.

Fig. 54.   NOAA 10 Satellite Image at 100915 UTC October 1988

73

NOAA 10 satellite image at 101056 UTC (Fig. 55) shows an enlarged view of the boundary layer front region. The sharp anticyclonic turning of the winds over Fram Strait is evident in the cloud streets in the image. The winds then become cyclonic converging with the cold dry winds from east Greenland. Streamline analysis depicts a broad area of stratocumulus clouds present under strong divergent flow.

By 101307 UTC (Fig. 56), NOAA satellite image shows the ice edge boundary layer front north and east of its previous position. Low level cumuliform clouds are turning cyclonically at the northern edge of the layer front. Converging streamlines are analyzed along the thin band of convective clouds as seen in (Fig. 56). Stratocumulus clouds are maintained between Spitzbergen and the boundary layer front under divergent flow. Spitzbergen reported 10 ms^{-1} of westerly wind at 1200 UTC as the northerly winds west of Spitzbergen turn sharply cyclonic around Svalbard. Winds along the east coast of Greenland are reported as west or southwest during this time.

Fig. 55.   NOAA 10 satellite image at 101056 UTC October 1988

Fig. 56.   NOAA 10 satellite image at 101307 UTC October 1988

The next available satellite mosaic was at 102350 UTC (Fig. 57), ten hours later to the previous, shows a polar low west of Spitzbergen at the northern end of the boundary layer front. The low clouds become tightly banded into the center of the vortex. The thin band of convective activity along the front is now oriented to the southeast and extends south of Spitzbergen. Spitzbergen is reporting southerly winds at 27 knots and lowering pressure in approach of the polar low and the boundary layer front. Strong northwest winds are indicated by the clouds streets in east Greenland Sea behind the front and polar low. At 110853 UTC (not shown) satellite imagery shows that the polar low and boundary layer front have dissipated. The entire event lasted less than 24 hours.
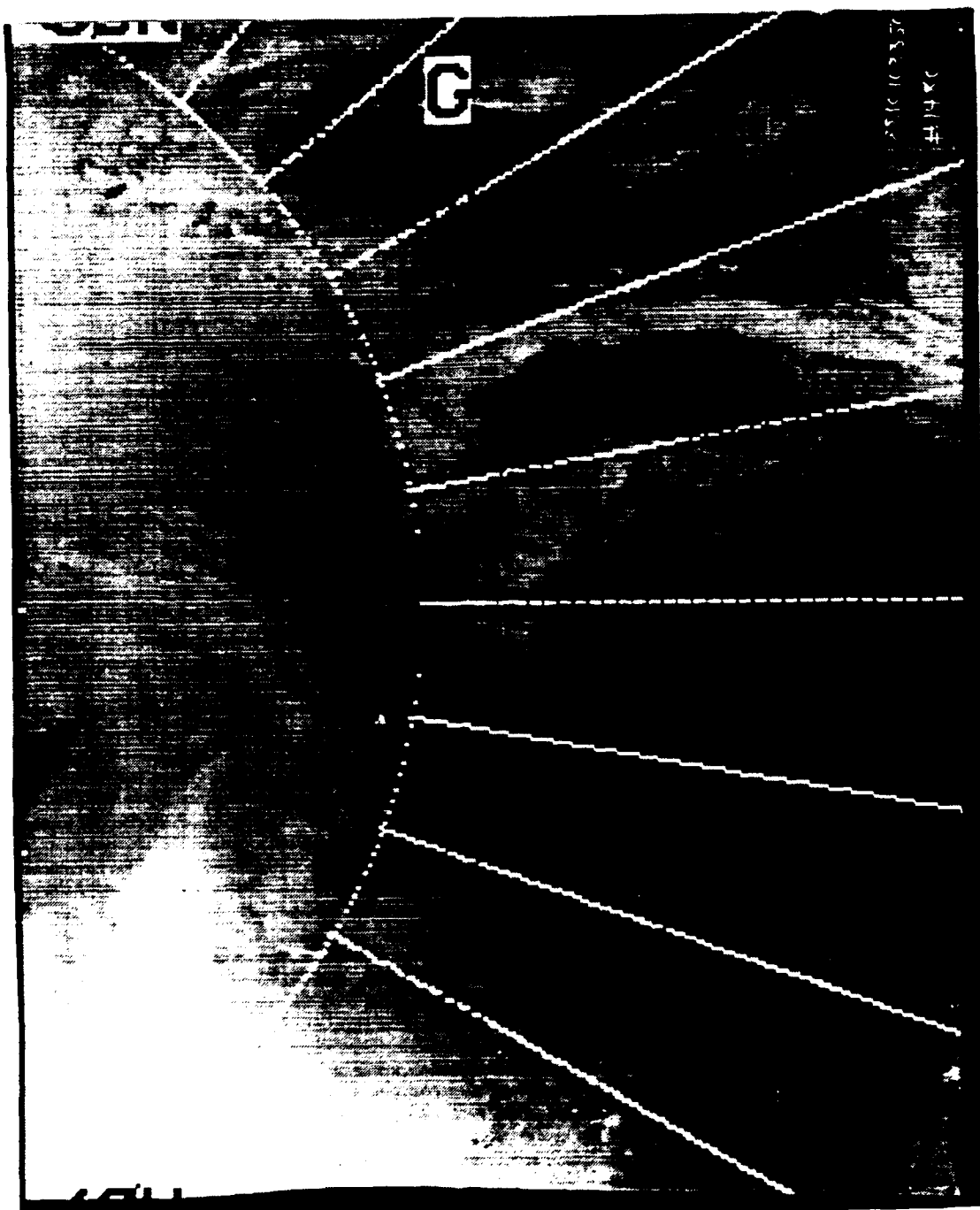
Fig. 57.   DMSP satellite image at 102318 UTC October 1988

3. Comparison with Other Studies

This ice-edge boundary layer front formation differs from previously described studies of boundary layer fronts. Fett (1989b) study of a boundary layer front formed with colder air to the east and warmer modified air to the west. In this case, colder air was to the west and warmer air was to the east. The boundary layer front formed with the outbreak of cold air from the ice pack that flowed southward over Fram Strait. The warm tongue of water in Fram Strait, a branch of the Norway Current, modified the cold air from off the ice regions. This modified relatively warm and moist air meets the unmodified cold air flowing east from the Greenland ice sheet. This front was found farther north than previous case studies and in a different season. Shapiro and Fedor (1989) and Fett (1989b) observed boundary layer fronts in the winter, from December through March, rather than the fall.

The major difference between this front and the boundary layer front described by Fett (1989b) and Shultz (1987) is that this front formed under a low-level trough that moved northeast with this upper level flow. Maximum vorticity occurred at the northern boundary of the front as evidenced by the multiple large vortices visible along the northern portion of the front on satellite imagery. The large amount of vorticity concentrated at the northern boundary of the front accounts for the subsequent formation of a polar low at that location. Fett (1989b) and Shultz (1987) case study involved the formation of boundary layer front that propagated westward in an easterly wave. The vorticity in this inverted trough was centered at the southern end of the boundary layer front as evidenced by the presence of strong vortices shown in satellite imagery. Although a polar low did not form from this boundary layer front in an easterly wave, other cases by Fett (1989b) involved polar low development on the southern portion of boundary layer fronts.

A polar low formed with this ice-edge boundary layer front. Fett (1989b) proposes that boundary layer fronts can evolve into polar lows only if cold air aloft and a 500 mb trough or low height center are present. As presented in the overview of this section, NOGAPS 500 and 850 mb analyses depict a deep upper level trough and cold advection into the East Greenland Sea. This upper level support and strong baroclinic zone at the surface together with the ice-edge boundary layer front provided for the development of a polar low.

V. SUMMARY AND RECOMMENDATIONS

A. SUMMARY

The drift phase of CEAREX was dominated by short periods of frequent cyclone activity followed by long periods of high pressure ridging over the Eastern Arctic from Greenland or northern Europe. Winds were predominately from the north-northwest which steered the ship east of Spitzbergen and Kvitoya as it drifted within the southward advancing Arctic pack ice.

On 12 October 1988, strong cyclogenesis occurred over the drift ship. This is an infrequent event over Arctic ice due to the presence of a layer of very stable, cold, and dry air over the surface and the absence of any strong baroclinicity. The ship's position was close the MIZ and was under the influence of warm air advection from the surface to 850 mb coming from the warm waters of the Norwegian Sea. This warm moist air being advected in the region in combination with an upper level trough provided a strong baroclinic zone which was evident in a "baroclinic leaf" that was observed in satellite imagery. The "leaf's" subsequent vertical development and intense cyclogenesis at the surface was tracked by surface observations. Data from the research ship and the six drifting buoys proved invaluable to the reconstruction and analysis of this cyclogenesis event.

On 10 October 1988, a boundary layer front was observed in the east Greenland Sea by satellite imagery. The front formed between a cold dry air mass flowing east from the Greenland continent and affixed ice sheet, and a relatively warm moist air mass to the east that was initially cold air flowing south from the Arctic ice pack which became modified over the warm waters of Fram Strait, west of Spitzbergen. Vortices on the northern end of the boundary layer front subsequently developed into a polar low that was seen on satellite imagery several hours later. The polar low formed in Fram Strait and then moved east-southeast toward Spitzbergen where it dissipated. The boundary layer front in this study is quite different than those noted by Shultz (1987), Fett (1989b), and Shapiro and Fedor (1989). A major difference noted that this front was moving eastward, not stationary or moving westward as noted by the previous cases. In addition, the polar low formed at the northern rather than the southern end of the front. The use of satellite imagery proved crucial to this analysis as no ship or buoys were reporting in this area.

Other than these two events, the synoptic conditions during the drift phase are well represented in the climate study presented by Gorshkov (1983). Gorshkov's frequency of occurrence of cyclonic activity in the Eastern Arctic is much higher than Serreze and Barry (1988) and coincided with this study's findings.

B. RECOMMENDATIONS

The detection of the cyclogenesis over pack ice was possible because of the research ship and the array of drifting buoys. A permanent and widespread array of drifting buoys are required to monitor the meteorological conditions in the Arctic.

A more detailed understanding of the formation of boundary layer fronts and their subsequent development into polar lows require surface and upper air observations in the area in addition to satellite imagery. Further studies of the phenomena described require in situ measurements. The use of drifting buoys and additional ship and aircraft measurements are necessary to further document and understand these phenomena.

Satellite imagery still remains the forecaster's primary tool for detecting rapid developing Arctic storms and observing mesoscale features like boundary layer fronts and polar lows. Any gap of satellite imagery can cause an incorrect analysis or omission of a meteorological event. Training on interpreting satellite imagery is essential to exploiting the full potential of satellite images in the Arctic. The forecaster must have a basic knowledge of cloud patterns and associated meteorological features in the atmosphere. A thorough knowledge of the physical processes indigenous to the Arctic is the key to successful analyses in this unique area of the world.

LIST OF REFERENCES

Bader, M.J., K.A. Browning, G.S. Forbes, V.J. Oliver, and T.W. Schlatter, 1988: Towards improved subjective interpretation of satellite and radar imagery in weather forecasting: results of a workshop. *Bull. Amer. Met. Soc.*, **69**, 764-769.

Businger, S., and R. J. Reed, 1989: Polar Lows. In *Polar and Arctic Lows*, P.F. Twitchell, E.A. Rasmussen, and K.L. Davidson (Eds), A. Deepak Publishing, Hampton, VA, 3-45.

Climate Analysis Center, 1988a: Climate Diagnostics Bulletic, September 1988, near real-time analyses, ocean/atmosphere, No. 88/9. Prepared by U.S. Department of Commerce, Washington, D.C., 37 pp.

_____, 1988b: Climate Diagnostics Bulletic, October 1988, near real-time analyses, ocean/atmosphere, No. 88/10. Prepared by U.S. Department of Commerce, Washington, D.C., 38 pp.

_____, 1988c: Climate Diagnostics Bulletic, November 1988, near real-time analyses, ocean/atmosphere, No. 88/11. Prepared by U.S. Department of Commerce, Washington, D.C., 48 pp.

_____, 1988d: Climate Diagnostics Bulletic, December 1988, near real-time analyses, ocean/atmosphere, No. 88/12. Prepared by U.S. Department of Commerce, Washington, D.C., 43 pp.

_____, 1989: Climate Diagnostics Bulletic, January 1988, near real-time analyses, ocean/atmosphere, No. 89/1. Prepared by U.S. Department of Commerce, Washington, D.C., 48 pp.

Ebert, E.E., 1989: Analysis of polar clouds from satellite imagery using pattern recognition and a statistical cloud analysis scheme. *J. Appl. Met.*, **28**, 382-399.

Fett, R.W., 1989a: Navy Tactical Appl. Guide, Vol. 8, *Arctic Weather Analysis and Forecast Applications,* NEPRF Technical Report 89-07, Naval Environmental Prediction Research Facility, Monterey, CA, 364 pp.

_____, 1989b: Polar development associated with boundary layer fronts in the Greenland, Norwedian, and Barents Sea. In *Polar and Arctic Lows,* P.F. Twitchell, E.A. Rasmussen, and K.L. Davidson (Eds), A. Deepak Publishing, Hampton, VA, 313-332.

_____, 1990: Personal Communication.

Gorshkov, S.G., 1983: *World Ocean Atlas Vol. 3 Arctic Ocean.* Pergamon Press, 184 pp.

Lackman, G. M., P. S. Guest, K. L. Davidson, R. J. Link and J. Gonzalex, 1989: *CEAREX¡Polarbjorn Meteorological Atlas.* Naval Postgraduate School, Monterey, CA, 545 pp.

Lystad, M. (Ed.), 1986: *Polar Lows in the Norwegian, Greenland and Barents Sea.* Final Rep., Polar Lows Project, The Norwegian Meteorological Institute, Oslo, Norway, 196 pp.

National Science Foundation, 1987: *Arctic Research of the United States, Volume 1.* Prepared by the Interagency Arctic Research Policy Committee, Washington, DC, 121 pp.

_____, 1988: *Arctic Research of the United States, Volume 2.* Prepared by the Interagency Arctic Research Policy Committee, Washington, DC, 102 pp.

Phegley, L.D., 1985: *Synoptic/Mesoscale Meteorology Features in the Marginal Ice Zone.* M.S. Thesis, Naval Postgraduate School, Monterey, CA, 92 pp.

Rao, P.K., S.J. Holmes, R.K. Anderson, J.S. Winston, and P.E. Lehr, 1990: *Weather Satellites: systems, data, and environmental applications.* American Meteorological Society, Boston, MA, 503 pp.

Rasmussen, E.A., 1989: A comparative study of tropical cyclones and polar lows. In *Polar and Arctic Lows*, P.F. Twitchell, E.A. Rasmussen, and K.L. Davidson (Eds), A. Deepak Publishing, Hampton, VA, 47-80.

Sater, J.E., A.G. Ronhovde, And L.C. van Allen, 1971: *Arctic Environment and Resources*. Arctic Institute for North America, Washington, DC, 310 pp.

Schultz, R.R., 1987: *Meteorological Features During the Marginal Ice Zone Experiment from 20 March to 10 April 1987*. M.S. Thesis, Naval Postgraduate School, Monterey, CA, 85 pp.

Sechrist, F. S., R. W. Fett and D. C. Perryman, 1989: *Forecasters Handbook for the Arctic*. Draft Rep., T.R. 89-10. Naval Environmental Prediction Research Facility, Monterey, CA, 346 pp.

Serreze, M.C., and R.G. Barry, 1988: Synoptic activity in the arctic basin, 1979-85. *J. Climate*, 1, 1276-1295.

Shapiro, M.A., and L.S. Fedor, 1989: A case study of an ice-edge boundary layer front and polar low development over the Norwegian and and Barents Seas. In *Polar and Arctic Lows*, P.F. Twitchell, E.A. Rasmussen, and K.L. Davidson (Eds), A. Deepak Publishing, Hampton, VA, 257-277.

Stringer, W.J., D.G. Barnett, R.H. Godin, 1984: *Handbook for Sea Ice Analysis and Forecasting*, CR 84-03. Naval Environmental Prediction Research Facility, Monterey, CA.

Tchernia, P., 1980: *Descriptive Regional Oceanography*. Pergamon Press, Oxford, England, 253 pp.

Vowinckel, E., and S. Orvig, 1970: The climate of the North Polar basin, In: *World Survey of Climatology: Volume 14, Climates of the Polar Regions*. Amsterdam, Elsevier, 129-252.

Walsh, J.E. and W.L. Chapman, 1990: Short-term climatic variability of the Arctic. *J. Climate*, **3**, 237-250.

Weldon, R. 1979: Satellite Training Course Notes, Part IV, *Cloud Patterns and the Upper Air Wind Field*. Applications Division, National Environmental Satellite Service, NOAA, Washinton, DC, 79 pp.

_____, 1986a: An oceanic cyclogenesis - its cloud pattern interpretation. In *Meteorological Monographs: satellite imagery interpretation for forecasters, Vol. I, general interpretation synoptic analysis*, P. S. Parke (Ed.), The National Weather Association, Temple Hills, MD, 2-G-1 to 2-G-11.

_____, 1986b: Synoptic scale cloud systems. In *Meteorological Monographs: satellite imagery interpretation for forecasters, Vol. I, general interpretation synoptic analysis*, P. S. Parke (Ed.), The National Weather Association, Temple Hills, MD, 2-A-1 to 2-A-35.

Zumberge, J.H., 1986: Introduction. *Oceanus*, **29**, 2-8.

INITIAL DISTRIBUTION LIST

		No. Copies
1.	Defense Technical Information Center Cameron Station Alexandria, VA 22304-6145	2
2.	Library, Code 52 Naval Postgraduate School Monterey, CA 93943-5002	2
3.	Chairman (Code MR/Hy) Department of Meteorology Naval Postgraduate School Monterey. CA 93943-5000	1
4.	Professor Kenneth L. Davidson (Code MR/Ds) Department of Meteorology Naval Postgraduate School Monterey, CA 93943-5000	1
5.	Professor Carlyle H. Wash (Code MR/Wx) Department of Meteorology Naval Postgraduate School Monterey, CA 93943-5000	1
6.	LT Stephanie W. Hamilton, USN Officer in Charge Naval Oceanography Command Detachment Adak AK FPO Seattle, WA 98791-2943	1
7.	Commander Naval Oceanography Command Stennis Space Center MS 39529-5000	1
8.	Director Naval Oceanographic and Atmospheric Research Laboratory Monterey, CA 93943-5006	1

86

9. Mr. Robert W. Fett   1
    Naval Oceanographic and Atmospheric
    Research Laboratory
    Monterey, CA 93943-5006

10. Chief of Naval Research   1
    800 North Quincy Street
    Arlington, VA 22217

11. Dr. Tom Curtin (Code 1125AR)   1
    Office of Naval Research
    800 North Quincy Street
    Arlington, VA 22217-5000

12. Dr. J. E. Overland   1
    Pacific Marine Environmental Laboratory
    National Oceanic and Atmospheric
    Administration
    7600 Sandpoint Way, NE
    Seattle, WA 98115

13. Commanding Officer   1
    Naval Polar Oceanography Center
    Suitland
    Washington, DC 20373